Finite Elements in Analysis and Design 141 (2018) 96–118

Contents lists available at ScienceDirect

Finite Elements in Analysis and Design

journal homepage: www.elsevier.com/locate/finel

Fast and accurate two-field reduced basis approximation for parametrized thermoelasticity problems

Khac Chi Hoang [a], Tae-Yeon Kim [b], Jeong-Hoon Song [a,*]

[a] Department of Civil, Environmental and Architectural Engineering, University of Colorado at Boulder, Boulder, CO, 80309, USA
[b] Civil Infrastructure and Environmental Engineering, Khalifa University of Science and Technology, 127788, Abu Dhabi, United Arab Emirates

ARTICLE INFO

Keywords:
Model order reduction
Parametrized one-way coupled thermoelasticity
Constitutive relation error
Posteriori error estimation
Effective coefficient of thermal expansion

ABSTRACT

This paper concerns a two-field reduced basis algorithm for the metamodelling of parametrized one-way coupled thermoelasticity problems based on the constitutive relation error (CRE) estimation. The coupled system consists of parametrized thermal diffusion and elastostatic equations which are explicitly coupled in a one-way manner. The former can be solved in advance independently and the latter can be solved afterwards using the solution of the former. For the fast and accurate analysis of the coupled system, we developed an algorithm that can choose adaptively the number of reduced basis functions of the temperature field to approximate the CRE equality of the mechanical field. We compute *approximately* the upper bound for the true errors of displacement and stress fields in energy norms. To enable this, a two-field greedy sampling strategy is adopted to construct the displacement and stress fields in an efficient manner. The computational efficiency of the proposed approach is demonstrated with computing the effective coefficient of thermal expansion of heterogeneous materials.

1. Introduction

Coupled systems exist in many engineering applications such as fluid-structure interaction, thermo-mechanical, electro-mechanical, electro-magnetic, and so on. The coupling is caused by the interaction between different subsystems describing different physical quantities such as temperature, displacement, velocity, pressure, etc. After discretizing coupled systems with certain traditional numerical methods such as finite-element and finite-volume methods, their resulting algebraic systems are often complex and very large. Such a complex and large algebraic system entails difficulties for the real-time computation which is vital for tailoring responses of the complex system via computational system design approach. To circumvent such difficulties, the purpose of this work is to develop a two-field model order reduction (MOR) technique that can enable metamodelling of the coupled system for the fast and accurate computation.

In the following, we provide a brief literature review on the use of MOR techniques for coupled problems, as a more exhaustive overview on this topic can be found in Refs. [1,2]. The first MOR technique to deal with coupled systems is the component mode synthesis method proposed for structural dynamics problems [3–5]. After that, different MOR techniques have been proposed and can be categorized into several types. For examples, MOR techniques based on systems and control theory such as balanced truncation [6,7], MOR techniques based on approximation theory such as moment-matching [8,9], MOR techniques such as the reduced basis (RB) method [10,11], proper orthogonal decomposition (POD) method [12,13] and proper generalized decomposition method [14] have been successfully applied to coupled systems, and have shown significant efficiency for various multi-physics problems.

In this work, we focus on the application of a reduced order model (ROM) for the class of one-way coupled thermoelasticity problems. In particular, a one-way coupled thermoelasticity problem shall include one thermal elliptic partial differential equation (PDE) and one elastic elliptic PDE, where the former can be solved *in advance* independently and the latter is solved *afterwards* using the solution of the former [15,16]. Due to this special property, the application of the ROM for the thermal PDE is straightforward and simple: any available ROM with associated error estimation technique (e.g., a snapshot-proper orthogonal decomposition method [17–20], a hyper-reduction technique [21,22], a proper generalized decomposition method [23], reduced basis with a successive constraint method [24,25], or a recent two-field reduced basis method (TF-RBM) [26]) will work well for such thermal problem. However, *a posteriori* error estimation for the

* Corresponding author.
E-mail address: JH.Song@colorado.edu (J.-H. Song).

https://doi.org/10.1016/j.finel.2017.12.004
Received 20 June 2017; Received in revised form 4 December 2017; Accepted 4 December 2017
Available online 22 December 2017

ROM of the elastic PDE is complicated because of the passing of the approximated ROM temperature field from the thermal PDE to the elastic one. To the best of our knowledge, there is no work in literature to evaluate such an error of the elastic PDE in this context. As references, the application of ROM techniques for the class of coupled thermoelasticity problems can be found in, for example, [7,27]. These works belong to the class of either balance truncation or moment-matching methods which were described briefly in the previous paragraph.

In this paper, we pursue the RB methodology with a CRE estimation to handle such parametrized coupled thermoelasticity problems. In particular, we use the TF-RBM with the CRE estimation technique [26] to approximate *certifiably* both thermal and elastic PDEs. As mentioned in the previous paragraph, while such an approach to handle the thermal PDE is straightforward, that to handle the elastic PDE is not trivial and requires some special modifications. This is due to the appearance of expansion terms which depend on the true error of the RB temperature field, besides the usual true errors of the RB displacement and stress fields in the CRE equality.

Therefore, the first purpose of this paper is to propose an algorithm to choose *adaptively* the number of RB basis functions of the temperature field in such a way that these expansion terms are eliminated — thus recovers *approximately* the CRE equality. In other words, we recover the upper boundedness of the CRE estimator for true errors of RB displacement and stress fields [26]. In turn, this CRE estimator is used in a two-field greedy sampling algorithm to build the corresponding reduced spaces of these displacement and stress fields. The second purpose of this paper is to extend the CRE upper error bound to goal-oriented error bounds for several quantities of interest (QoIs), where these QoIs are linear functionals of the displacement field. (Note that the QoIs of the thermal PDE are addressed in the RB approximation of the thermal PDE *in advance*.) Based on these goal-oriented error bounds, the final objective is to compute the *certified* ROM approximations of the effective coefficient of thermal expansion (CTE) for parametrized coupled thermoelasticity problems.

The remainder of the paper is organized as follows. In section 2, we state the exact parametrized coupled thermoelasticity problem and its finite-element discretization. In section 3, we describe our ROM approximations for the thermal equation in section 3.1 and the elastic equation in section 3.2. While section 3.1 repeats briefly the work in Ref. [26], section 3.2 and section 4 present all the novel proposed theory of this paper. In particular, section 3.2 is devoted to the CRE estimator, the proposed algorithm to select appropriately the number of RB basis vectors for the temperature field, and the two-field greedy sampling algorithm. Goal-oriented error bounds and the extension to compute the effective CTE are presented in section 4. In section 5, the performance of all the proposed algorithms is investigated for a 2D material homogenization problem. Finally, we provide some concluding remarks in section 6.

2. Parametrized explicitly coupled thermoelasticity equations

2.1. Exact formulation

2.1.1. Strong form

We consider the problem of determining the displacement field $u(x)$ and the (excess) temperature field $\theta(x)$[1] within a static thermoelastic body occupying the physically spatial domain $\Omega \in \mathbb{R}^d$ $(d = 2, 3)$. The displacement field $u \in \mathcal{U}(\Omega) = \left(H^1(\Omega)\right)^d$ and the temperature field $\theta \in \Theta(\Omega) = H^1(\Omega)$ satisfy the nonhomogeneous Dirichlet boundary conditions $u = w$ and $\theta = \vartheta$ on the parts Γ^u and Γ^θ of the boundary Γ, respectively. Here, $H^1(\Omega) = \left\{v \in L^2(\Omega) \mid \nabla v \in (L^2(\Omega))^d\right\}$ is a Hilbert space and $L^2(\Omega)$ is the space of square integrable functions over Ω. The body may also be subjected to prescribed tractions t, body forces b, prescribed flux h and heat source f on the boundary parts Γ^t, Ω, Γ^h and Ω, respectively.

We define a set of input parameters $D \subset \mathbb{R}^P$, a typical point of which is denoted by $\mu \equiv (\mu_1, \ldots, \mu_P)$. In particular, the force densities b, t; the heat densities h, f; the Dirichlet boundary conditions w, ϑ and the material properties of the structure may be functions of parameter μ. We assume that Ω, Γ^u and Γ^θ do not undergo any parametric changes.

For a given parameter μ, the strong formulation is stated as: obtain $(\theta(\mu), u(\mu))$ by solving the following one-way coupled system

$$\text{Heat equation} \begin{cases} -k(\mu)\nabla^2\theta(\mu) = f(\mu) & \text{on } \Omega, \\ \theta = \vartheta & \text{on } \Gamma^\theta, \\ q(\mu) = k(\mu)\cdot\nabla\theta(\mu) & \text{on } \Omega, \end{cases} \tag{1}$$

$$\text{Elastic equation} \begin{cases} -div\left(\sigma(u(\mu))\right) = b(\mu) & \text{on } \Omega, \\ u = w & \text{on } \Gamma^u, \\ \sigma(u(\mu)) = D(\mu) : \epsilon(u(\mu)) - D(\mu) : \epsilon_0(\theta(\mu)) & \text{on } \Omega. \end{cases} \tag{2}$$

Here, $q(\mu)$ is the flux field and $k(\mu)$ is the heat conductivity tensor for the heat equation. For the elastic equation, $\epsilon(v) = \frac{1}{2}\left(\nabla v + \nabla v^T\right)$ is the strain field, $\sigma(\mu)$ is the Cauchy stress field, $D(\mu)$ is the fourth-order Hooke's elasticity tensor which depends on the two Lamé constants $\lambda(\mu)$ and $G(\mu)$, $\epsilon_0(\theta(\mu))$ is the thermal strain which depends on the temperature field $\theta(\mu)$ that was solved from Eq. (1) (see for instance Eq. (1.9) in Ref. [28] or Eq. (8.23) in Ref. [29]). System (1) and (2) is thus one-way coupled in this sense. (Interested readers can refer to the full coupled thermomechanical system, for instance, arising in shear band modelling application [30,31].)

2.1.2. Weak form

For a given parameter μ, the corresponding weak form is described by

$$-\int_\Omega q(\mu)\cdot\nabla v_1\, d\Omega + \int_\Omega f(\mu)\cdot v_1\, d\Omega + \int_{\Gamma^h} h(\mu)\cdot v_1\, d\Gamma = 0, \quad \forall v_1 \in \Theta^{\mathrm{Ad},0}(\Omega), \tag{3a}$$

$$-\int_\Omega \sigma(\mu) : \epsilon(v_2)\, d\Omega + \int_\Omega b(\mu)\cdot v_2\, d\Omega + \int_{\Gamma^t} t(\mu)\cdot v_2\, d\Gamma = 0, \quad \forall v_2 \in \mathcal{U}^{\mathrm{Ad},0}(\Omega). \tag{3b}$$

Here, $\Theta^{\mathrm{Ad}}(\Omega;\mu) = \{v \in \Theta(\Omega) \mid v_{|\Gamma^\theta} = \vartheta(\mu)\}$ and $\Theta^{\mathrm{Ad},0}(\Omega) = \{v \in \Theta(\Omega) \mid v_{|\Gamma^\theta} = 0\}$ are the spaces which contain the full and homogeneous temperature fields; $\mathcal{U}^{\mathrm{Ad}}(\Omega;\mu) = \left\{v \in \mathcal{U}(\Omega) \mid v_{|\Gamma^u} = w(\mu)\right\}$ and $\mathcal{U}^{\mathrm{Ad},0}(\Omega) = \left\{v \in \mathcal{U}(\Omega) \mid v_{|\Gamma^u} = 0\right\}$ are the spaces which contain the full and homogeneous displacement fields. The solution to the parametrized heat conduction problem (3a) is an admissible pair $(\theta(\mu), q(\mu)) \in \Theta^{\mathrm{Ad}}(\Omega;\mu) \times \mathcal{Q}^{\mathrm{Ad}}(\Omega;\mu)$ that verifies the isotropic linear constitutive law

$$q(\mu) = k(\mu)\cdot\nabla\theta(\mu). \tag{4}$$

Similarly, the solution to the parametrized problem of elasticity is an admissible pair $(u(\mu), \sigma(\mu)) \in \mathcal{U}^{\mathrm{Ad}}(\Omega;\mu) \times \mathcal{S}^{\mathrm{Ad}}(\Omega;\mu)$ that verifies the isotropic linear constitutive law

$$\sigma(\mu) = D(\mu) : \epsilon(u(\mu)) - D(\mu) : \epsilon_0(\theta(\mu)). \tag{5}$$

By substituting (4) into (3a) and (5) into (3b), the parametric problem of thermoelasticity can be written in the following primal variational form: for any $\mu \in \mathcal{D}$, find $\theta(\mu) \in \Theta^{\mathrm{Ad}}(\Omega;\mu)$ and $u(\mu) \in \mathcal{U}^{\mathrm{Ad}}(\Omega;\mu)$ such that

[1] $\theta^{\mathrm{tot}}(x) = \theta^{\mathrm{ref}} + \theta(x)$ where $\theta^{\mathrm{tot}}(x)$ is the total (absolute) temperature and θ^{ref} is the reference temperature corresponding to the zero thermal strains state, which motivates the notion *excess* temperature for θ.

$$a^{\theta\theta}\left(\theta(\mu), v_1; \mu\right) = f^{\theta}\left(v_1; \mu\right), \quad \forall v_1 \in \Theta^{\mathrm{Ad},0}(\Omega), \tag{6a}$$

$$a^{uu}\left(u(\mu), v_2; \mu\right) = f^{u}\left(v_2; \mu\right) + a^{u\theta}\left(\theta(\mu), v_2; \mu\right), \quad \forall v_2 \in \mathcal{U}^{\mathrm{Ad},0}(\Omega) \tag{6b}$$

where

$$a^{\theta\theta}\left(\theta, v_1; \mu\right) = \int_{\Omega} k(\mu)\nabla\theta\nabla v_1 \, d\Omega, \tag{7a}$$

$$f^{\theta}\left(v_1; \mu\right) = \int_{\Omega} f(\mu)\cdot v_1 \, d\Omega + \int_{\Gamma^h} h(\mu)\cdot v_1 \, d\Gamma, \tag{7b}$$

$$a^{uu}\left(u, v_2; \mu\right) = \int_{\Omega} \epsilon(u) : D(\mu) : \epsilon(v_2) \, d\Omega, \tag{7c}$$

$$f^{u}\left(v_2; \mu\right) = \int_{\Omega} b(\mu)\cdot v_2 \, d\Omega + \int_{\Gamma^t} t(\mu)\cdot v_2 \, d\Gamma, \tag{7d}$$

$$a^{u\theta}\left(\theta, v_2; \mu\right) = \int_{\Omega} \epsilon_0(\theta) : D(\mu) : \epsilon(v_2) \, d\Omega, \tag{7e}$$

respectively. We recall that $a^{\theta\theta} : \Theta^{\mathrm{Ad}}(\Omega)\times\Theta^{\mathrm{Ad},0}(\Omega)\times\mathcal{D}$, $a^{uu} : \mathcal{U}^{\mathrm{Ad}}(\Omega)\times\mathcal{U}^{\mathrm{Ad},0}(\Omega)\times\mathcal{D}$ are symmetric, continuous and coercive parametrized bilinear forms. We assume that $f^{\theta} : \Theta^{\mathrm{Ad},0}(\Omega)\times\mathcal{D}$, $f^{u} : \mathcal{U}^{\mathrm{Ad},0}(\Omega)\times\mathcal{D}$ are continuous, bounded linear forms, and that the bilinear form $a^{u\theta} : \Theta^{\mathrm{Ad}}(\Omega)\times\mathcal{U}^{\mathrm{Ad},0}(\Omega)\times\mathcal{D}$ is sufficiently regular. Under these conditions, there exists unique "weak" solutions $\theta(\mu)\in\Theta(\Omega)$ to (6a) and $u(\mu)\in\mathcal{U}(\Omega)$ to (6b).

Multiple QoIs can be extracted from $u(\mu)$ and $\theta(\mu)$ as

$$Q_i(\mu) = Q_i^u(\mu) + Q_i^{\theta}(\mu) = \ell_i^u\left(u(\mu)\right) + \ell_i^{\theta}\left(\theta(\mu)\right), \quad 1\le i\le n^{\mathrm{Q}} \tag{8}$$

with $\ell_i^{\theta} : \Theta^{\mathrm{Ad}}(\Omega)\times\mathcal{D}$ and $\ell_i^{u} : \mathcal{U}^{\mathrm{Ad}}(\Omega)\times\mathcal{D}$ being continuous and bounded linear forms. Outputs $\ell_i^{\theta,u}$ may be compliant or noncompliant linear functionals. Notice that system (6) (or (3)) is explicitly coupled in a staggered manner, i.e., one-way coupled. In other words, for given any input parameter $\mu\in\mathcal{D}$, (6a) (respectively (3a)) is solved independently *first* to obtain the temperature field $\theta(\mu)$. This resulting $\theta(\mu)$ is then substituted to (7e) to solve the elastic Eq. (6b) (respectively (3b)) to get the corresponding displacement field $u(\mu)$. Finally, the QoIs are computed from (8).

A crucial assumption to efficiently deal with parametrized problems is the *affine decomposition* property of the operators that governs our problem. In particular, $\forall\theta\in\Theta^{\mathrm{Ad}}(\Omega), v_1\in\Theta^{\mathrm{Ad},0}(\Omega)$, $\forall u\in\mathcal{U}^{\mathrm{Ad}}(\Omega), v_2\in\mathcal{U}^{\mathrm{Ad},0}(\Omega)$, $\mu\in\mathcal{D}$, we require that

$$a^{\theta\theta}\left(\theta, v_1; \mu\right) = \sum_{q=1}^{Q^{\theta\theta}} \varrho_q^{\theta\theta}(\mu)\, a_q^{\theta\theta}(\theta, v_1), \tag{9a}$$

$$f^{\theta}\left(v_1; \mu\right) = \sum_{q=1}^{Q^{\theta}} \varrho_q^{\theta}(\mu) f_q^{\theta}(v_1), \tag{9b}$$

$$\ell_i^{\theta}\left(v_1; \mu\right) = \sum_{q=1}^{Q^{\ell_i^{\theta}}} \varrho_q^{\ell_i^{\theta}}(\mu)\, \ell_{i,q}^{\theta}(v_1), \quad 1\le i\le n^{\mathrm{Q}}, \tag{9c}$$

$$a^{uu}\left(u, v_2; \mu\right) = \sum_{q=1}^{Q^{uu}} \varrho_q^{uu}(\mu)\, a_q^{uu}(u, v_2), \tag{9d}$$

$$f^{u}\left(v_2; \mu\right) = \sum_{q=1}^{Q^{u}} \varrho_q^{u}(\mu) f_q^{u}(v_2), \tag{9e}$$

$$\ell_i^{u}\left(v_2; \mu\right) = \sum_{q=1}^{Q^{\ell_i^{u}}} \varrho_q^{\ell_i^{u}}(\mu)\, \ell_{i,q}^{u}(v_2), \quad 1\le i\le n^{\mathrm{Q}}, \tag{9f}$$

for some (preferably) small integers $Q^{\theta\theta}, Q^{\theta}, Q^{\ell_i^{\theta}}, Q^{uu}, Q^{u}$ and $Q^{\ell_i^{u}}$. Here, the smooth functions $\varrho_q^{\bullet} : \mathcal{D}\to\mathbb{R}$ depend on μ but all the bilinear and linear forms $a_q^{\bullet}, f_q^{\bullet}$ and $\ell_{i,q}^{\bullet}$ do *not* depend on the parameter. In practice, such an *affine decomposition* is at hand if the parametrized data are originally given in the form of separate variables; namely

$$k(x,\mu) = \sum_{i=1}^{n^{\mathrm{k}}} \gamma_i^{\mathrm{k}}(\mu)\overline{k}_i(x), \quad \forall\mu\in\mathcal{D}, x\in\Omega; \tag{10a}$$

$$h(x,\mu) = \sum_{i=1}^{n^{\mathrm{h}}} \gamma_i^{\mathrm{h}}(\mu)\overline{h}_i(x), \quad \forall\mu\in\mathcal{D}, x\in\Gamma^h, \tag{10b}$$

$$f(x,\mu) = \sum_{i=1}^{n^{\mathrm{f}}} \gamma_i^{\mathrm{f}}(\mu)\overline{f}_i(x), \quad \forall\mu\in\mathcal{D}, x\in\Omega, \tag{10c}$$

$$\vartheta(x,\mu) = \sum_{i=1}^{n^{\theta,\mathrm{w}}} \gamma_i^{\theta,\mathrm{w}}(\mu)\overline{\vartheta}_i(x), \quad \forall\mu\in\mathcal{D}, x\in\Gamma^{\theta}; \tag{10d}$$

$$D(x,\mu) = \sum_{i=1}^{n^{\mathrm{D}}} \gamma_i^{\mathrm{D}}(\mu)\overline{D}_i(x), \quad \forall\mu\in\mathcal{D}, x\in\Omega; \tag{10e}$$

$$t(x,\mu) = \sum_{i=1}^{n^{\mathrm{t}}} \gamma_i^{\mathrm{t}}(\mu)\overline{t}_i(x), \quad \forall\mu\in\mathcal{D}, x\in\Gamma^{\mathrm{t}}, \tag{10f}$$

$$b(x,\mu) = \sum_{i=1}^{n^{\mathrm{b}}} \gamma_i^{\mathrm{b}}(\mu)\overline{b}_i(x), \quad \forall\mu\in\mathcal{D}, x\in\Omega, \tag{10g}$$

$$w(x,\mu) = \sum_{i=1}^{n^{u,\mathrm{w}}} \gamma_i^{u,\mathrm{w}}(\mu)\overline{w}_i(x), \quad \forall\mu\in\mathcal{D}, x\in\Gamma^{u}. \tag{10h}$$

Here all the $\gamma_i^{\bullet}(\mu) : \mathcal{D}\to\mathbb{R}$ are explicitly known functions of the parameter μ, while $\overline{k}_i(x)$, $\overline{h}_i(x)$, $\overline{f}_i(x)$, $\overline{\vartheta}_i(x)$, $\overline{D}_i(x)$, $\overline{t}_i(x)$, $\overline{b}_i(x)$ and $\overline{w}_i(x)$ are operators/functions that do *not* depend on μ.

Lastly, by inserting (10) into (7) we can easily infer all the bilinear and linear forms in (9). For example, insert equation (10a) into (7a), we can see in (9a) that $\varrho_q^{\theta\theta}(\mu) = \gamma_q^{\mathrm{k}}(\mu)$, $a_q^{\theta\theta}(\theta, v_1) = \int_{\Omega}\overline{k}_q(x)\nabla\theta\nabla v_1$, $1\le q\le Q^{\theta\theta}$ and $Q^{\theta\theta} = n^{\mathrm{k}}$. We do not provide the definitions of all bilinear and linear forms in (9) here but they can be inferred easily by the same way as described above.

2.2. Finite-element discretization

We approximate the solutions of the coupled system (6) using the finite-element method (FEM). The finite-element (FE) solution spaces are defined as

$$\Theta^{\mathrm{h}}(\Omega) = \left\{ w\in\Theta(\Omega) \,|\, w\in\mathrm{span}\left\{\widehat{N}_i, 1\le i\le n_{\mathrm{n}}\right\}\right\}, \tag{11a}$$

$$\mathcal{U}^{\mathrm{h}}(\Omega) = \left\{ v\in\mathcal{U}(\Omega) \,|\, \forall j\in\{1,\dots,d\}, v_j\in\mathrm{span}\left\{\widehat{N}_i, 1\le i\le n_{\mathrm{n}}\right\}\right\}, \tag{11b}$$

where v_j denotes the jth component of the vector field v and $\widehat{N}_i$'s are compactly supported FE shape functions. Here, n_{n} is the number of nodes in the FE mesh and $\mathcal{N}^{\theta}$ and $\mathcal{N}^{u}$ represent the dimensions of the FE spaces $\Theta^{\mathrm{h},0}(\Omega)$ and $\mathcal{U}^{\mathrm{h},0}(\Omega)$ (defined in the following paragraphs), respectively.

Let $\Theta^{\mathrm{h},0}(\Omega) = \Theta^{\mathrm{h}}(\Omega)\cap\Theta^{\mathrm{Ad},0}(\Omega)$ be the space of FE temperature fields that vanish on Γ^{θ} and $\theta^{\mathrm{p}}(\mu)$ be a particular field of $\Theta^{\mathrm{Ad}}(\Omega;\mu)$, for any $\mu\in\mathcal{D}$. The FE approximation $\theta^{\mathrm{h}}(\mu)$ of $\theta(\mu)$ is the solution to the following variational problem [32]: find $\theta^{\mathrm{h}}(\mu)\in\Theta^{\mathrm{h},0}(\Omega) + \{\theta^{\mathrm{p}}(\mu)\}$ such that

$$a^{\theta\theta}\left(\theta^{\mathrm{h}}(\mu), v_1; \mu\right) = f^{\theta}\left(v_1; \mu\right), \quad \forall v_1\in\Theta^{\mathrm{h},0}(\Omega). \tag{12}$$

We assume that the parametrized Dirichlet boundary conditions conform to the FE space, meaning that $\Theta^{\mathrm{h}}(\Omega)\cap\Theta^{\mathrm{Ad}}(\Omega;\mu)\neq\{\}$. In this context, $\theta^{\mathrm{p}}(\mu)$ can always be chosen in the FE space $\Theta^{\mathrm{h}}(\Omega)$. The variational problem (12) can be recast in the form

$$a^{\theta\theta}\left(\theta^{\mathrm{h},0}(\mu),v_1;\mu\right)=f^{\theta}\left(v_1;\mu\right)-a^{\theta\theta}\left(\theta^{\mathrm{p}}(\mu),v_1;\mu\right),\quad \forall v_1\in\Theta^{\mathrm{h},0}(\Omega). \tag{13}$$

As $\theta^{\mathrm{p}}(\mu)$ is known, we denote $\widehat{f}^{\theta}\left(v_1;\mu\right)=f^{\theta}\left(v_1;\mu\right)-a^{\theta\theta}\left(\theta^{\mathrm{p}}(\mu),v_1;\mu\right)$. Then, the final variational form is: for a given $\mu\in\mathcal{D}$, find $\theta^{\mathrm{h},0}(\mu)\in\Theta^{\mathrm{h},0}(\Omega)$ such that

$$a^{\theta\theta}\left(\theta^{\mathrm{h},0}(\mu),v_1;\mu\right)=\widehat{f}^{\theta}\left(v_1;\mu\right),\quad \forall v_1\in\Theta^{\mathrm{h},0}(\Omega). \tag{14}$$

The FE solution is obtained by using the lifting identity $\theta^{\mathrm{h}}(\mu)=\theta^{\mathrm{h},0}(\mu)+\theta^{\mathrm{p}}(\mu)$. Under standard assumptions, the linear system (14) possesses a unique solution.

Following a completely similar treatment, the final variational form for the elastic Eq. (6b) is: for a given $\mu\in\mathcal{D}$, find $u^{\mathrm{h},0}(\mu)\in\mathcal{U}^{\mathrm{h},0}(\Omega)$ such that

$$a^{uu}\left(u^{\mathrm{h},0}(\mu),v_2;\mu\right)=\widehat{f}^{u}\left(v_2;\mu\right),\quad \forall v_2\in\mathcal{U}^{\mathrm{h},0}(\Omega), \tag{15}$$

where $\widehat{f}^{u}\left(v_2;\mu\right)=f^{u}\left(v_2;\mu\right)-a^{uu}\left(u^{\mathrm{p}}(\mu),v_2;\mu\right)+a^{u\theta}\left(\theta^{\mathrm{h}}(\mu),v_2;\mu\right)$. Here, $\mathcal{U}^{\mathrm{h},0}(\Omega)=\mathcal{U}^{\mathrm{h}}(\Omega)\cap\mathcal{U}^{\mathrm{Ad},0}(\Omega)$ is the space of FE displacement fields that vanish on Γ^u and $u^{\mathrm{p}}(\mu)$ is a particular displacement field of $\mathcal{U}^{\mathrm{Ad}}(\Omega;\mu)$, for any $\mu\in\mathcal{D}$. The FE displacement solution is then obtained by using the lifting identity $u^{\mathrm{h}}(\mu)=u^{\mathrm{h},0}(\mu)+u^{\mathrm{p}}(\mu)$. Similar to (14), the linear system (15) also possesses a unique solution (which depends on the FE temperature field $\theta^{\mathrm{h}}(\mu)$).

The FE QoIs can then be evaluated as

$$Q_i^{\mathrm{h}}(\mu)=Q_i^{\mathrm{h},u}(\mu)+Q_i^{\mathrm{h},\theta}(\mu)=\ell_i^{u}\left(u^{\mathrm{h}}(\mu)\right)+\ell_i^{\theta}\left(\theta^{\mathrm{h}}(\mu)\right),\quad 1\le i\le n^{\mathrm{Q}}. \tag{16}$$

In the following, we assume that the FE spaces are sufficiently fine so that any relevant measure of the FE errors $e_{\theta}^{\mathrm{h}}(\mu)=\theta(\mu)-\theta^{\mathrm{h}}(\mu)$ and $e_{u}^{\mathrm{h}}(\mu)=u(\mu)-u^{\mathrm{h}}(\mu)$ are very small for all $\mu\in\mathcal{D}$. In this context, the source of error will come from using the metamodelling technique described in the next sections.

3. Reduced basis approximations

The basic idea of projection-based reduced order modelling relies on the fact that the solutions of the parametrized boundary value problem reside on a smooth and low-dimensional parametrically induced manifold. The governing equations can then be projected onto this manifold, leading to a reduced system of equations that can be solved inexpensively for any parameter set.

In this work, we propose to use the TF-RBM approach [26,33] to build the ROM models for the explicitly coupled thermoelasticity problem and assess the approximated quality of these ROM models using the CRE bounding technique [23,26]. With this spirit, the heat Eq. (14) is approximated using one TF-RBM approach with corresponding CRE bounds, while the elastic Eq. (15) is approximated by another TF-RBM with other CRE bounds. All these contents are presented in this section. However, due to the length limit of the paper, we only present the necessary equations with the new proposed techniques (section 3.2), and refer readers to [26] for full details of standard/repeated equations and algorithms (section 3.1).

3.1. Two-field reduced basis approximations for the heat diffusion equation

3.1.1. Reduced order model for the temperature field

To apply the reduced basis method for general nonhomogeneous Dirichlet boundary condition problems, we perform a lifting of the FE solution over the parameter domain

$$\theta^{\mathrm{h}}(\mu)=\theta^{\mathrm{h},0}(\mu)+\theta^{\mathrm{h},\mathrm{p}}(\mu),\quad \forall\mu\in\mathcal{D}. \tag{17}$$

Here, $\theta^{\mathrm{h},0}(\mu)\in\Theta^{\mathrm{h},0}(\Omega)$, i.e., $\theta^{\mathrm{h},0}(\mu)=0$ on Γ^{θ} for any $\mu\in\mathcal{D}$, while $\theta^{\mathrm{h},\mathrm{p}}(\mu)\in\Theta^{\mathrm{h}}(\Omega)$ satisfies *exactly* the nonhomogeneous Dirichlet boundary conditions. This equation is to be understood as follows: for given a valid lifting $\theta^{\mathrm{h},\mathrm{p}}(\mu)$, the complementary part $\theta^{\mathrm{h},0}(\mu)$ can be formally calculated from the knowledge of $\theta^{\mathrm{h}}(\mu)$. We approximate $\theta^{\mathrm{h},0}(\mu)$ by its projection in a reduced vector space, while the lifting $\theta^{\mathrm{h},\mathrm{p}}(\mu)$ is an explicit function of the parameters. The computation of $\theta^{\mathrm{h},\mathrm{p}}(\mu)$ is standard in literature and thus is not repeated here. Readers can refer to [26] (section 3.1.2) or [33] for the detailed computation.

Using a global lifting technique and with the assumption of the affine form for prescribed temperatures, the FE lifting $\theta^{\mathrm{h},\mathrm{p}}(\mu)$ can be defined by the following affine expansion

$$\theta^{\mathrm{h},\mathrm{p}}(\mu)=\sum_{i=1}^{n^{\theta,\mathrm{w}}}\gamma_i^{\theta,\mathrm{w}}(\mu)\psi_i^{\theta},\quad \forall\mu\in\mathcal{D} \tag{18}$$

where ψ_i^{θ} is a set of $n^{\theta,\mathrm{w}}$ of temperature fields that can be obtained by solving $n^{\theta,\mathrm{w}}$ standard FE problems with nonhomogeneous boundary conditions, i.e.,

$$\begin{cases} a^{\theta\theta}\left(\psi_i^{\theta},v;\mu_0\right)=0, & \forall v\in\Theta^{\mathrm{h},0}(\Omega),\\ \psi_i^{\theta}(x)=\vartheta_i(x), & \forall x\in\Gamma^{\theta}, \end{cases}\qquad \forall\mu_0\in\mathcal{D}.$$

We assume the availability of nested parameter sets $S_{N^{\theta}}^{\theta}=\{\mu_1^{\theta}\in\mathcal{D},\dots,\mu_{N^{\theta}}^{\theta}\in\mathcal{D}\}, 1\le N^{\theta}\le N_{\max}^{\theta}$, and associated nested Lagrange RB spaces $\Theta_{N^{\theta}}^{\mathrm{r},0}(\Omega)=\mathrm{span}\left\{\phi_n^{\theta},1\le n\le N^{\theta}\right\}, 1\le N^{\theta}\le N_{\max}^{\theta}$, where $\phi_n^{\theta}\in\Theta_{N^{\theta}}^{\mathrm{r},0}(\Omega), 1\le n\le N_{\max}^{\theta}$ are mutually orthonormal RB basis functions with respect to a particular norm using a Gram–Schmidt process. The procedure to construct efficiently the sets $S_{N^{\theta}}^{\theta}$ and $\Theta_{N^{\theta}}^{\mathrm{r},0}(\Omega)$ is discussed in (3.1.5).

For any $\mu\in\mathcal{D}$, we find an approximation $\theta^{\mathrm{r}}(\mu)$ to $\theta^{\mathrm{h}}(\mu)$ in the form

$$\theta^{\mathrm{h}}(\mu)\approx\theta^{\mathrm{r}}(\mu)=\theta^{\mathrm{r},0}(\mu)+\theta^{\mathrm{h},\mathrm{p}}(\mu),\quad \text{where}\quad \theta^{\mathrm{r},0}(\mu)=\sum_{n=1}^{N^{\theta}}\alpha_n^{\theta}(\mu)\phi_n^{\theta}, \tag{19}$$

and $\alpha_n^{\theta}(\mu)$'s are interpolation weights, called "reduced variables". The RB approximation $\theta^{\mathrm{r},0}(\mu)$ to $\theta^{\mathrm{h},0}(\mu)$ is optimally (in the sense of the energy norm, see Céa Lemma) obtained by a standard Galerkin projection: for given $\mu\in\mathcal{D}$, find $\theta^{\mathrm{r},0}(\mu)$ that satisfies

$$\begin{aligned} a^{\theta\theta}(\theta^{\mathrm{r},0}(\mu),v_1;\mu)&=\widehat{f}^{\theta}(v_1;\mu),\\ &=f^{\theta}\left(v_1;\mu\right)-a^{\theta\theta}\left(\theta^{\mathrm{h},\mathrm{p}}(\mu),v_1;\mu\right)\quad \forall v_1\in\Theta_{N^{\theta}}^{\mathrm{r},0}(\Omega),\mu\in\mathcal{D}. \end{aligned} \tag{20}$$

This typically very small system of linear equations can be solved on demand, for any parameter set of interest. The RB QoIs can then be evaluated from the reduced solution as

$$Q_i^{\mathrm{r},\theta}(\mu)=\ell_i^{\theta}\left(\theta^{\mathrm{r}}(\mu)\right),\quad 1\le i\le n^{\mathrm{Q}}. \tag{21}$$

We note that systems (20) and (21) accept the very efficient offline-online computational procedures [25,34] which include an expensive μ-independent Offline stage performed only *once* and *many* cheap Online computations for any input parameter value $\mu\in\mathcal{D}$. In particular, in the Offline stage the affine terms $\{\psi_i^{\theta},1\le i\le n^{\theta,\mathrm{w}}\}$ (18), the RB basis functions $\{\phi_n^{\theta},1\le n\le N^{\theta}\le N_{\max}^{\theta}\}$ (19) and all the *parameter-independent* terms (in (20) and (21)) are computed and stored. In the Online stage, for any given μ, all the *parameter-dependent* functions (in (20) and (21)) are evaluated, the reduced system (39) is assembled and solved to find the RB coefficients $\alpha_n^{\theta}(\mu), 1\le n\le N^{\theta}$, and the RB QoIs are obtained through the simple scalar product (21). The Offline cost depends on $\mathcal{N}^{\theta}$ and thus expensive, while the Online cost is completely independent of $\mathcal{N}^{\theta}$. The detailed computation of these procedures are standard in MOR community and hence will not be repeated here. An elaborated description is referred to as [26,35].

3.1.2. Reduced order model for the heat flux field

The principles underlying the construction of the heat flux surrogate are parallel to those employed for the construction of the temperature surrogate [26,33]. We first recall that the "exact" FE flux field $q^{\mathrm{h}}(\mu) = k(\mu) \cdot \nabla\theta^{\mathrm{h}}(\mu)$ satisfies the equilibrium in the FE sense, namely, it verifies

$$-\int_\Omega q^{\mathrm{h}}(\mu) \cdot \nabla v_1 \, d\Omega + \int_\Omega f(\mu) \cdot v_1 \, d\Omega + \int_{\Gamma^h} h(\mu) \cdot v_1 \, d\Gamma = 0, \quad \forall v_1 \in \Theta^{\mathrm{h},0}(\Omega). \tag{22}$$

We denote by $\mathcal{Q}^{\mathrm{h,Ad}}(\Omega;\mu)$ the space of fluxes satisfying the parametrized equilibrium in the FE sense (22). The construction of the flux surrogate relies on the separation of the FE flux field into two parts:

$$q^{\mathrm{h}}(\mu) = q^{\mathrm{h},0}(\mu) + q^{\mathrm{h,p}}(\mu), \quad \forall \mu \in \mathcal{D}. \tag{23}$$

The first part $q^{\mathrm{h},0}(\mu)$ belongs to the space $\mathcal{Q}^{\mathrm{h},0}(\Omega)$ of flux fields satisfying the following homogeneous equilibrium condition

$$\int_\Omega q^{\mathrm{h},0}(\mu) \cdot v_1 \, d\Omega = 0, \quad \forall v_1 \in \Theta^{\mathrm{h},0}(\Omega), \mu \in \mathcal{D}, \tag{24}$$

while the second part belongs to $\mathcal{Q}^{\mathrm{h,Ad}}(\Omega;\mu)$ and therefore satisfies the equation

$$-\int_\Omega q^{\mathrm{h,p}}(\mu) \cdot v_1 \, d\Omega + \int_\Omega f(\mu) \cdot v_1 \, d\Omega + \int_{\Gamma^h} h(\mu) \cdot v_1 \, d\Gamma = 0, \quad \forall v_1 \in \Theta^{\mathrm{h},0}(\Omega). \tag{25}$$

Here, (23) is to be understood as follows: given a valid equilibrated flux $q^{\mathrm{h,p}}(\mu)$, then the complementary part $q^{\mathrm{h},0}(\mu)$ can be formally calculated from the knowledge of the exact FE flux $q^{\mathrm{h}}(\mu)$.

The flux field $q^{\mathrm{h,p}}(\mu) \in \mathcal{Q}^{\mathrm{h,Ad}}(\Omega;\mu)$ will be explicitly defined as a function of the parametrized heat source and prescribed flux, while the complementary part $q^{\mathrm{h},0}(\mu)$ will be approximated by its projection in a reduced vector space.

Using a standard technique as described in section 3.2.2 of [26] and with the assumption of affine forms for heat source $f(\mu)$ and prescribed flux $h(\mu)$, the particular flux field $q^{\mathrm{h,p}}(\mu)$ can have the following affine forms

$$q^{\mathrm{h,p}}(\mu) = \sum_{i=1}^{\widetilde{n}^{q,\mathrm{p}}} \widetilde{\gamma}_i^{q,\mathrm{p}}(\mu) q_i^{\mathrm{p}}, \quad \forall \mu \in \mathcal{D}. \tag{26}$$

We now introduce the nested parameter sets $S_{N^q}^q = \left\{\mu_1^q \in \mathcal{D}, \ldots, \mu_{N^q}^q \in \mathcal{D}\right\}, 1 \le N^q \le N_{\max}^q$, and associated nested Lagrange RB spaces $\mathcal{Q}_{N^q}^{\mathrm{r},0}(\Omega) = \mathrm{span}\left\{\phi_m^q, 1 \le m \le N^q\right\}, 1 \le N^q \le N_{\max}^q$, where $\phi_m^q \in \mathcal{Q}_{N^q}^{\mathrm{r},0}(\Omega), 1 \le m \le N_{\max}^q$ are mutually orthonormal RB basis functions with respect to a particular norm using a Gram–Schmidt process. Details on how to construct efficiently the sets $S_{N^q}^q$ and $\mathcal{Q}_{N^q}^{\mathrm{r},0}(\Omega)$ are discussed in (3.1.5).

As mentioned above, we construct the surrogate flux field $\widehat{q}(\mu)$ as

$$q^{\mathrm{h}}(\mu) \approx \widehat{q}(\mu) = q^{\mathrm{r},0}(\mu) + q^{\mathrm{h,p}}(\mu), \ \ \forall \mu \in \mathcal{D}, \quad \text{where} \quad q^{\mathrm{r},0}(\mu) = \sum_{i=1}^{N^q} \alpha_i^q(\mu) \phi_i^q, \tag{27}$$

where $\alpha^q(\mu) \in \mathbb{R}^{N^q}$ are (unknown) generalized coefficients to be obtained by the projection.

The generalized coefficients are required to satisfy the optimum property

$$\widehat{q}(\mu) = \arg \min_{q^\star \in \mathcal{Q}^{\mathrm{r}}(\Omega;\mu)} \left\| q^\star - q^{\mathrm{h}}(\mu) \right\|_{k^{-1}(\mu)}, \tag{28}$$

where the admissible space for reduced flux field is defined by $\mathcal{Q}^{\mathrm{r}}(\Omega;\mu) = \{q^\star \in \mathcal{Q}(\Omega) \mid q^\star = \sum_{i=1}^{N^q} \alpha_i^\star \phi_i^q + q^{\mathrm{h,p}}(\mu), \forall \alpha^\star \in \mathbb{R}^{N^q}\}$; $\|\cdot\|_{k^{-1}(\mu)}$ is the so-called energy norm for the flux fields and is defined in (3.1).

Using the constitutive relation (4), the optimization problem (28) can be recast in the following variational form: find $\widehat{q}(\mu) \in \mathcal{Q}^{\mathrm{r}}(\Omega;\mu)$ such that

$$-\int_\Omega \widehat{q}(\mu) \cdot k^{-1}(\mu) \cdot q^\star \, d\Omega + \int_\Omega \nabla\theta^{\mathrm{h}}(\mu) \cdot q^\star \, d\Omega = 0, \quad \forall q^\star \in \mathcal{Q}^{\mathrm{r},0}(\Omega), \tag{29}$$

where $\mathcal{Q}^{\mathrm{r},0}(\Omega) = \{q^\star \in \mathcal{Q}(\Omega) \mid q^\star = \sum_{i=1}^{N^q} \alpha_i^\star \phi_i^q, \forall \alpha^\star \in \mathbb{R}^{N^q}\}$.

Now, substituting (27) and (19) into (29) and noting (24), we obtain the variational form that we will use to compute the flux field $q^{\mathrm{r},0}(\mu)$:

$$\int_\Omega q^{\mathrm{r},0}(\mu) \cdot k^{-1}(\mu) \cdot q^\star \, d\Omega = \int_\Omega \nabla\theta^{\mathrm{h,p}}(\mu) \cdot q^\star \, d\Omega - \int_\Omega q^{\mathrm{h,p}}(\mu) \cdot k^{-1}(\mu) \cdot q^\star \, d\Omega, \quad \forall q^\star \in \mathcal{Q}^{\mathrm{r},0}(\Omega). \tag{30}$$

From (18) and (26), and assuming that $k^{-1}(\mu)$ has the affine decomposition form, (30) also accepts the very efficient offline-online computational procedures which include an expensive μ-independent Offline stage performed only *once* and *many* cheap Online computations for any input parameter value $\mu \in \mathcal{D}$. In particular, in the Offline stage the affine terms $q_i^{\mathrm{p}}, 1 \le i \le \widetilde{n}^{q,\mathrm{p}}$ (26), the RB basis functions $\{\phi_n^q, 1 \le n \le N^q \le N_{\max}^q\}$ (27) and all the *parameter-independent* terms (in (30)) are computed and stored. In the Online stage, for any given μ, all the *parameter-dependent* functions (in (30)) are evaluated and (30) is assembled and solved to find the RB coefficients $\alpha_n^q(\mu), 1 \le n \le N^q$. The system matrix is very small, with a size $(N^q \times N^q)$ completely independent of the FE space dimension $\mathcal{N}^q$. Again, the detailed computation of these procedures is standard and hence is not repeated here. Readers are referred to [26,35] for an elaborated description.

3.1.3. Constitutive relation error for the heat diffusion equation

We recall briefly here the CRE equality for heat equation, and refer to [26,33] for its full presentation.

Proposition 3.1. *Let $e_\theta(\mu) = \theta^{\mathrm{h}}(\mu) - \theta^{\mathrm{r}}(\mu)$ and $e_q(\mu) = q^{\mathrm{h}}(\mu) - \widehat{q}(\mu)$ be the RB errors for the temperature and flux fields, respectively; $\|q^\star\|_{k^{-1}(\mu)} = \left(\int_\Omega q^\star \cdot k^{-1}(\mu) \cdot q^\star \, d\Omega\right)^{1/2}$ be the energy norm associated to an arbitrary flux field $q^\star \in \mathcal{Q}(\Omega)$ and $\|v\|_{k(\mu)} = \left(\int_\Omega \nabla v \cdot k(\mu) \cdot \nabla v \, d\Omega\right)^{1/2}$ be the energy norm associated to an arbitrary temperature field $v \in \Theta^{\mathrm{h},0}(\Omega)$.*

Then, the square of the distance $\Delta_\theta^{\mathrm{CRE}}(\mu)$ between the RB flux field $q^{\mathrm{r}}(\mu) \in \mathcal{Q}(\Omega)$ and the surrogate flux field $\widehat{q}(\mu) \in \mathcal{Q}^{\mathrm{h,Ad}}(\Omega;\mu)$, measured in energy norm, will be equal exactly to the sum of square of energy norms of the RB errors of the temperature and flux fields as follows

$$\Delta_\theta^{\mathrm{CRE}}(\mu)^2 := \left\|q^{\mathrm{r}}(\mu) - \widehat{q}(\mu)\right\|_{k^{-1}(\mu)}^2 = \left\|e_\theta(\mu)\right\|_{k(\mu)}^2 + \left\|e_q(\mu)\right\|_{k^{-1}(\mu)}^2. \tag{31}$$

The proof is standard and can be found in Appendix A of [26] (Note that $q^{\mathrm{r}}(\mu) = k(\mu) \cdot \nabla\theta^{\mathrm{r}}(\mu)$ in (31) above.). It is important to understand from (31) that the RB errors $\left\|e_\theta(\mu)\right\|_{k(\mu)}$ and $\left\|e_q(\mu)\right\|_{k^{-1}(\mu)}$ are individually uncomputable, but the sum of their squares is computable in an *a posteriori* manner. It was shown in Ref. [26] that the computation of $\Delta_\theta^{\mathrm{CRE}}(\mu)$ is very efficient which can be decomposed into Offline–Online computational procedures. The key point to note is that the cost to compute $\Delta_\theta^{\mathrm{CRE}}(\mu)$ (in the Online stage) is completely independent of $\mathcal{N}^\theta$, $\mathcal{N}^q$, and is only dependent on N^θ, N^q. The effectivities of the CRE bound for both temperature and flux fields are defined as

$$\eta_\theta^{\mathrm{CRE}}(\mu) = \frac{\Delta_\theta^{\mathrm{CRE}}(\mu)}{\|\theta^{\mathrm{h}}(\mu) - \theta^{\mathrm{r}}(\mu)\|_{k(\mu)}}, \quad \text{and} \quad \eta_q^{\mathrm{CRE}}(\mu) = \frac{\Delta_\theta^{\mathrm{CRE}}(\mu)}{\|q^{\mathrm{h}}(\mu) - \widehat{q}(\mu)\|_{k^{-1}(\mu)}}, \tag{32}$$

respectively.

3.1.4. Goal-oriented error bound for the heat diffusion equation

Duality technique is a standard tool to bound engineering QoIs for linear problems [36,37]. Readers that are familiar with this topic should only scan through this section to identify the notations used throughout the remainder of this paper.

For each one of the QoIs, we define the FE dual (or adjoint) problem

$$a^{\theta\theta}\left(\zeta_i^{\mathrm{h},0}(\mu), v_1; \mu\right) = \ell_i^{\theta}\left(v_1; \mu\right), \quad \forall v_1 \in \Theta^{\mathrm{h},0}(\Omega), \quad 1 \le i \le n_{\mathrm{Q}}, \tag{33}$$

where $\zeta_i^{\mathrm{h},0}(\mu) \in \Theta^{\mathrm{h},0}$ is the FE dual temperature field corresponding to the output functional ℓ_i^{θ}, which is required to satisfy homogeneous Dirichlet boundary conditions.

We solve this problem approximately by the projection-based ROM obtained by the reduced Galerkin formulation: find $\zeta_i^{\mathrm{r},0}(\mu) \in \Theta^{\mathrm{h},0}(\Omega)$ such that

$$a^{\theta\theta}\left(\zeta_i^{\mathrm{r},0}(\mu), v_1; \mu\right) = \ell_i^{\theta}\left(v_1; \mu\right), \quad \forall v_1 \in \Theta_{\zeta,i}^{\mathrm{r},0}(\Omega), \quad 1 \le i \le n_{\mathrm{Q}}, \tag{34}$$

where $\Theta_{\zeta,i}^{\mathrm{r},0}(\Omega) \subset \Theta^{\mathrm{h},0}(\Omega)$ is the reduced basis space for the dual temperature field associated with the output functional ℓ_i^{θ}; and generally $\Theta_{\zeta,i}^{\mathrm{r},0}(\Omega) \neq \Theta_{N^{\theta}}^{\mathrm{r},0}(\Omega)$. For consistency, for the $i-$th QoI, we also define the sets of RB basis functions $\{\phi_n^{\zeta,i}, 1 \le n \le N^{\zeta,i}\}$ for dual temperature and $\{\phi_m^{\xi,i}, 1 \le m \le N^{\xi,i}, 1 \le i \le n_{\mathrm{Q}}\}$ for dual fluxes, respectively.

Using the classical technique as described in Refs. [26,36], we obtain the following inequality

$$Q_i^{\mathrm{r},\theta,\mathrm{low}}(\mu) \le Q_i^{\mathrm{h},\theta}(\mu) \le Q_i^{\mathrm{r},\theta,\mathrm{up}}(\mu), \tag{35}$$

where

$$\begin{cases} Q_i^{\mathrm{r},\theta,\mathrm{low}}(\mu) = Q_i^{\mathrm{r},\theta}(\mu) + R^{\theta}\left(\zeta_i^{\mathrm{r},0}(\mu); \mu\right) - \Delta_{\theta}^{\mathrm{CRE}}(\mu)\Delta_{\zeta,i}^{\mathrm{CRE}}(\mu) \\ Q_i^{\mathrm{r},\theta,\mathrm{up}}(\mu) = Q_i^{\mathrm{r},\theta}(\mu) + R^{\theta}\left(\zeta_i^{\mathrm{r},0}(\mu); \mu\right) + \Delta_{\theta}^{\mathrm{CRE}}(\mu)\Delta_{\zeta,i}^{\mathrm{CRE}}(\mu) \end{cases}, \quad 1 \le i \le n_{\mathrm{Q}}.$$

In the above expression, $R^{\theta} : \Theta^{\mathrm{h},0}(\Omega) \times \mathcal{D} \to \mathbb{R}$ is the residual form of (20) defined as

$$R^{\theta}(v_1; \mu) = \widehat{f}^{\theta}(v_1; \mu) - a^{\theta\theta}(\theta^{\mathrm{r},0}(\mu), v_1; \mu), \quad \forall v_1 \in \Theta^{\mathrm{h},0}(\Omega), \ \forall \mu \in \mathcal{D}. \tag{36}$$

The inequality (35) is fundamental to our Greedy sampling strategy. It provides an interval in which the FE output, which is not computable, is guaranteed to be found. We call this interval "uncertainty gap", and our aim is to control and minimize its length through our Greedy sampling algorithm. In fact, we use a relative measure of this gap defined as

$$\mathtt{gap}_i(\mu) = \frac{\left|Q_i^{\mathrm{r},\theta,\mathrm{up}}(\mu) - Q_i^{\mathrm{r},\theta,\mathrm{low}}(\mu)\right|}{1/2\left(|Q_i^{\mathrm{r},\theta,\mathrm{up}}(\mu)| + |Q_i^{\mathrm{r},\theta,\mathrm{low}}(\mu)|\right)}, \quad \forall \mu \in \mathcal{D}, \quad 1 \le i \le n_{\mathrm{Q}}, \tag{37}$$

for the i-th QoI.

3.1.5. Goal-oriented greedy sampling for the heat equation

Several authors have shown the advantage of devising goal-oriented sampling strategies to construct the projection spaces used in reduced order modelling [38–40]. Instead of aiming at minimizing the maximum over the parameter domain of an arbitrary measure of the error, one aims at minimizing the error in the quantity or quantities of interest. This type of approach has been shown to lead to faster convergence rates of the greedy algorithm in terms of input-output maps.

In this study, (37) shows that the output accuracy is controlled by the primal/dual temperatures and fluxes ROMs through the CRE (37). Therefore, it is natural to set the minimization of the maximum uncertainty gap (35) over the parameter domain as our target for the construction of the projection spaces.

Of course, such a minimization problem is not directly solvable, and we will make use of a greedy algorithm, as proposed in the original RB method. The method proceeds iteratively by assuming the existence of projection subspaces for primal/dual temperature and flux and performing a rank-one correction in such a way that the maximum of the uncertainty gap over the parameter domain is approximately minimized. The algorithm can be stopped whenever the uncertainty gap is sufficiently low over the entire parameter domain.

The rank-one update is performed as follows. First, we identify the point of the parameter domain where the uncertainty gap is at its largest. Then, we enrich one, and only one of the bases, temperature/flux of the primal or temperature/flux of one of the adjoint problems, by its corresponding FE solution (after orthonormalization) to the corresponding existing reduced basis. The choice of the field to enrich is simply based on testing which one of the enrichments would result in largest decrease in the gap at this particular point of the parameter domain. A more detailed full algorithm description is referred to as section 5.2 in Ref. [26].

3.2. Two-field reduced basis approximations for the elastostatic equation

3.2.1. Reduced order model for the displacement field

Similar to the heat equation, we use a global lifting technique to handle general nonhomogeneous Dirichlet boundary condition problem

$$u^{\mathrm{h}}(\mu) = u^{\mathrm{h},0}(\mu) + u^{\mathrm{h},\mathrm{p}}(\mu), \quad \forall \mu \in \mathcal{D}. \tag{38}$$

Here, $u^{\mathrm{h},0}(\mu) \in \mathcal{U}^{\mathrm{h},0}(\Omega)$, which means that $u^{\mathrm{h},0}(\mu)$ vanishes on Γ^u for any $\mu \in \mathcal{D}$, while $u^{\mathrm{h},\mathrm{p}}(\mu) \in \mathcal{U}^{\mathrm{h}}(\Omega)$ satisfies *exactly* the nonhomogeneous Dirichlet boundary conditions. This equation is to be understood as follows: given a valid lifting $u^{\mathrm{h},\mathrm{p}}(\mu)$, the complementary part $u^{\mathrm{h},0}(\mu)$ can be formally calculated from the knowledge of $u^{\mathrm{h}}(\mu)$. We approximate $u^{\mathrm{h},0}(\mu)$ by its projection in a reduced vector space, while $u^{\mathrm{h},\mathrm{p}}(\mu)$ is an explicit function of the parameters. Again, the computation of $u^{\mathrm{h},\mathrm{p}}(\mu)$ is standard in literature, and thus is not repeated here. Readers can refer to [26] (section 3.1.2) or [33] for the detailed computation.

Using a global lifting technique and with the assumption of the affine form for the prescribed displacement, $u^{\mathrm{h},\mathrm{p}}(\mu)$ can be defined by the following expansion

$$u^{\mathrm{h},\mathrm{p}}(\mu) = \sum_{i=1}^{n^{u,\mathrm{w}}} \gamma_i^{u,\mathrm{w}}(\mu)\psi_i^u, \quad \forall \mu \in \mathcal{D} \tag{39}$$

where ψ_i^u is a set of $n^{u,\mathrm{w}}$ of displacement fields that can be obtained by solving $n^{u,\mathrm{w}}$ standard FE problems with nonhomogeneous boundary conditions (see section 3.1.2 in Ref. [26]).

We assume the availability of nested parameter sets $S_{N^u}^u = \left\{\mu_1^u \in \mathcal{D}, \ldots, \mu_{N^u}^u \in \mathcal{D}, 1 \le N^u \le N_{\max}^u\right\}$, and associated nested Lagrange RB spaces $\mathcal{U}_{N^u}^{\mathrm{r},0}(\Omega) = \mathrm{span}\left\{\phi_n^u, 1 \le n \le N^u, 1 \le N^u \le N_{\max}^u\right\}$, where $\phi_n^u \in \mathcal{U}_{N^u}^{\mathrm{r},0}(\Omega), 1 \le n \le N_{\max}^u$ are mutually orthonormal RB basis functions with respect to a particular norm using a Gram–Schmidt process. The procedure to construct efficiently the sets $S_{N^u}^u$ and $\mathcal{U}_{N^u}^{\mathrm{r},0}(\Omega)$ is discussed in (3.2.5).

For any $\mu \in \mathcal{D}$, we find an approximation $u^{\mathrm{r}}(\mu)$ of $u^{\mathrm{h}}(\mu)$ in the form

$$u^{\mathrm{h}}(\mu) \approx u^{\mathrm{r}}(\mu) = u^{\mathrm{r},0}(\mu) + u^{\mathrm{h},\mathrm{p}}(\mu), \quad \text{where} \quad u^{\mathrm{r},0}(\mu) = \sum_{n=1}^{N^u} \alpha_n^u(\mu)\phi_n^u, \tag{40}$$

and $\alpha_n^u(\mu)$'s are interpolation weights, called "reduced variables". The RB approximation $u^{\mathrm{r},0}(\mu)$ to $u^{\mathrm{h},0}(\mu)$ is optimally (in the sense of the energy norm) obtained by a standard Galerkin projection: given $\mu \in \mathcal{D}$, find $u^{\mathrm{r},0}(\mu)$ such that

$$\begin{aligned} a^{uu}(u^{\mathrm{r},0}(\mu), v_2; \mu) &= \widehat{f}^{u}(v_2; \mu), \\ &= f^{u}\left(v_2; \mu\right) - a^{uu}\left(u^{\mathrm{h},\mathrm{p}}(\mu), v_2; \mu\right) + a^{u\theta}\left(\theta^{\mathrm{r}}(\mu), v_2; \mu\right) \\ &\forall v_2 \in \mathcal{U}_{N^u}^{\mathrm{r},0}(\Omega), \ \mu \in \mathcal{D}. \end{aligned} \tag{41}$$

The key point to note here is that we use the RB temperature field $\theta^{\mathrm{r}}(\mu)$ in (41) rather than the original FE temperature field $\theta^{\mathrm{h}}(\mu)$ in (15). If we use $\theta^{\mathrm{h}}(\mu)$ in (41), its ROM efficiency would be lost as we need to solve a full FE heat problem (14) for every input parameter μ.

This typically very small system of linear equations can be solved on demand, for any parameter set of interest. The RB QoIs can then be evaluated from the reduced solution as

$$Q_i^{\mathrm{r},u}(\mu) = \ell_i^u\left(u^{\mathrm{r}}(\mu)\right), \quad 1 \le i \le n^{\mathrm{Q}}. \tag{42}$$

Offline-Online computational procedures for the reduced variables In this subsection, we recall briefly the usual offline-online computational procedures for the Galerkin ROM, which is necessary in order to fully exploit the dimensional reduction of problem [25,34,35,41].

Using (40) and $v = \phi_n^u, 1 \le n \le N^u$, then invoking the affine decomposition (9), (10) and using the expanded expression of the RB temperature field $\theta^{\mathrm{r}}(\mu) = \sum_{i=1}^{N^\theta} \alpha_i^\theta(\mu)\phi_i^\theta + \sum_{i=1}^{n^{\theta,\mathrm{w}}} \gamma_i^{\theta,\mathrm{w}}(\mu)\psi_i^\theta$ from (18), (19), Eqs. (41) and (42) can be expressed explicitly as

$$\begin{aligned}
&\sum_{m=1}^{N^u}\left(\sum_{q=1}^{Q^{uu}} o_q^{uu}(\mu)\boldsymbol{a}_{\boldsymbol{q}}^{\boldsymbol{uu}}\left(\boldsymbol{\phi}_{\boldsymbol{m}}^{\boldsymbol{u}},\boldsymbol{\phi}_{\boldsymbol{n}}^{\boldsymbol{u}}\right)\right)\alpha_m^u(\mu)\\
&\quad = \sum_{q=1}^{Q^u} o_q^u(\mu)\boldsymbol{f}_{\boldsymbol{q}}^{\boldsymbol{u}}\left(\boldsymbol{\phi}_{\boldsymbol{n}}^{\boldsymbol{u}}\right) - \sum_{q=1}^{Q^{uu}}\sum_{i=1}^{n^{u,\mathrm{w}}} o_q^{uu}(\mu)\gamma_i^{u,\mathrm{w}}(\mu)\boldsymbol{a}_{\boldsymbol{q}}^{\boldsymbol{uu}}\left(\boldsymbol{\psi}_{\boldsymbol{i}}^{\boldsymbol{u}},\boldsymbol{\phi}_{\boldsymbol{n}}^{\boldsymbol{u}}\right)\\
&\qquad + \sum_{i=1}^{N^\theta}\alpha_i^\theta(\mu)\boldsymbol{a}^{\boldsymbol{u\theta}}\left(\boldsymbol{\phi}_{\boldsymbol{i}}^{\boldsymbol{\theta}},\boldsymbol{\phi}_{\boldsymbol{n}}^{\boldsymbol{u}}\right) + \sum_{i=1}^{n^{\theta,\mathrm{w}}}\gamma_i^{\theta,\mathrm{w}}(\mu)\boldsymbol{a}^{\boldsymbol{u\theta}}\left(\boldsymbol{\psi}_{\boldsymbol{i}}^{\boldsymbol{\theta}},\boldsymbol{\phi}_{\boldsymbol{n}}^{\boldsymbol{u}}\right), \quad 1 \le n \le N^u,
\end{aligned} \tag{43}$$

and

$$\begin{aligned}
Q_i^{\mathrm{r},u}(\mu) &= \sum_{n=1}^{N^u}\sum_{q=1}^{Q_i^{\ell^u}} o_q^{\ell_i^u}(\mu)\alpha_n^u(\mu)\boldsymbol{\ell}_{\boldsymbol{i,q}}^{\boldsymbol{u}}\left(\boldsymbol{\phi}_{\boldsymbol{n}}^{\boldsymbol{u}}\right)\\
&\quad + \sum_{j=1}^{n^{u,\mathrm{w}}}\sum_{q=1}^{Q_i^{\ell^u}}\gamma_j^{u,\mathrm{w}}(\mu)o_q^{\ell_i^u}(\mu)\boldsymbol{\ell}_{\boldsymbol{i,q}}^{\boldsymbol{u}}\left(\boldsymbol{\psi}_{\boldsymbol{j}}^{\boldsymbol{u}}\right), \quad 1 \le i \le n^{\mathrm{Q}}.
\end{aligned} \tag{44}$$

From the above decompositions, the computational procedures are now clear: an expensive μ-independent Offline stage performed only *once* and *many* cheap Online computations for any input parameter value $\mu \in \mathcal{D}$. In the Offline stage, the terms $\{\psi_i^\theta, 1 \le i \le n^{\theta,\mathrm{w}}\}$ (18), $\{\psi_i^u, 1 \le i \le n^{u,\mathrm{w}}\}$ (39), the RB basis functions $\left\{\phi_n^\theta, 1 \le n \le N_{\max}^\theta\right\}$ (19), $\left\{\phi_n^u, 1 \le n \le N_{\max}^u\right\}$ (40) and all the *parameter-independent* terms (bold typeface in (43), (44)) will be computed and stored. In the Online stage, for any given μ, all the *parameter-dependent* functions (normal typeface in (43), (44)) are evaluated, the reduced system (43) is assembled and solved to find the RB coefficients $\alpha_n^u(\mu), 1 \le n \le N^u$ and the RB QoI are obtained through the simple scalar product (44). The Offline cost will be expensive as it depends on $\mathcal{N}^u$ (the dimension of the FE space). The Online operation count is $O\left(Q^{uu}N^{u2}\right)$ to assemble the system and $O\left(N^{u3}\right)$ to invert the reduced operator in (43). The RB QOI is then evaluated with the cost of $O(N^u)$ from (44). Therefore, the Online operation count to evaluate $\mu \to Q_i^{\mathrm{r},u}(\mu), 1 \le i \le n^{\mathrm{Q}}$ is completely independent of $\mathcal{N}^u$ and $\mathcal{N}^\theta$.

3.2.2. Reduced order model for the stress field

We first recall that the "exact" FE stress field $\sigma^{\mathrm{h}}(\mu) := D(\mu) : \epsilon(u^{\mathrm{h}}(\mu)) - D(\mu) : \epsilon_0(\theta^{\mathrm{h}}(\mu))$, satisfying the equilibrium in the FE sense, i.e.,

$$\begin{aligned}
&-\int_\Omega \sigma^{\mathrm{h}}(\mu) : \epsilon(v_2)\,d\Omega + \int_\Omega b(\mu)\cdot v_2\,d\Omega + \int_{\Gamma^t} t(\mu)\cdot v_2\,d\Gamma = 0,\\
&\forall v_2 \in \mathcal{U}^{\mathrm{h},0}(\Omega).
\end{aligned} \tag{45}$$

The space of stresses satisfying the parametrized equilibrium (45) in the FE sense is denoted by $\mathcal{S}^{\mathrm{h,Ad}}(\Omega;\mu)$. The construction of the stress surrogate relies on the separation of the FE stress field into two parts:

$$\sigma^{\mathrm{h}}(\mu) = \sigma^{\mathrm{h},0}(\mu) + \sigma^{\mathrm{h,p}}(\mu), \quad \forall \mu \in \mathcal{D}. \tag{46}$$

The first part $\sigma^{\mathrm{h},0}(\mu)$ belongs to the space $\mathcal{S}^{\mathrm{h},0}(\Omega)$ of stress fields satisfying the following homogeneous equilibrium conditions

$$\int_\Omega \sigma^{\mathrm{h},0}(\mu) : \epsilon(v_2)\,d\Omega = 0, \quad \forall v_2 \in \mathcal{U}^{\mathrm{h},0}(\Omega), \mu \in \mathcal{D}, \tag{47}$$

while the second part $\sigma^{\mathrm{h,p}}(\mu)$ belongs to $\mathcal{S}^{\mathrm{h,Ad}}(\Omega;\mu)$ and therefore satisfies the equation

$$\begin{aligned}
&-\int_\Omega \sigma^{\mathrm{h,p}}(\mu) : \epsilon(v_2)\,d\Omega + \int_\Omega b(\mu)\cdot v_2\,d\Omega + \int_{\Gamma^t} t(\mu)\cdot v_2\,d\Gamma = 0,\\
&\forall v_2 \in \mathcal{U}^{\mathrm{h},0}(\Omega).
\end{aligned} \tag{48}$$

Here, (46) is to be understood as follows: for given a valid equilibrated stress $\sigma^{\mathrm{h,p}}(\mu)$, the complementary part $\sigma^{\mathrm{h},0}(\mu)$ can be formally calculated from the knowledge of the exact FE stress $\sigma^{\mathrm{h}}(\mu)$. The stress field $\sigma^{\mathrm{h,p}}(\mu) \in \mathcal{S}^{\mathrm{h,Ad}}(\Omega;\mu)$ is explicitly defined as a function of the parametrized body forces and surface tractions, while the complementary part $\sigma^{\mathrm{h},0}(\mu)$ is approximated by its projection in a reduced vector space. Using a standard technique as described in section 3.2.2 of [26] and with the assumption of affine forms for body force $b(\mu)$ and surface traction $t(\mu)$, the particular stress field $\sigma^{\mathrm{h,p}}(\mu)$ can have the following affine form

$$\sigma^{\mathrm{h,p}}(\mu) = \sum_{i=1}^{\widetilde{n}^{\sigma,\mathrm{p}}} \widetilde{\gamma}_i^{\sigma,\mathrm{p}}(\mu)\sigma_i^{\mathrm{p}}, \quad \forall \mu \in \mathcal{D} \tag{49}$$

where $\widetilde{\gamma}_i^{\sigma,\mathrm{p}}(\mu)$ is the same with (38) in Ref. [26].

We introduce the nested parameter sets $S_{N^\sigma}^\sigma = \left\{\mu_1^\sigma \in \mathcal{D}, \ldots, \mu_{N^\sigma}^\sigma \in \mathcal{D}\right\}, 1 \le N^\sigma \le N_{\max}^\sigma$, and associated nested Lagrange RB spaces $\mathcal{S}_{N^\sigma}^{\mathrm{r},0}(\Omega) = \mathrm{span}\left\{\phi_m^\sigma, 1 \le m \le N^\sigma\right\}, 1 \le N^\sigma \le N_{\max}^\sigma$, where $\phi_m^\sigma \in \mathcal{S}_{N^\sigma}^{\mathrm{r},0}(\Omega), 1 \le m \le N_{\max}^\sigma$ are mutually orthonormal RB basis functions with respect to a particular norm using a Gram–Schmidt process. Details on how to construct efficiently the sets $S_{N^\sigma}^\sigma$ and $\mathcal{S}_{N^\sigma}^{\mathrm{r},0}(\Omega)$ are discussed in (3.2.5).

We first recall the definition of the RB stress field which is post-processed from the RB displacement and temperature fields $\sigma^{\mathrm{r}}(\mu) := D(\mu) : \epsilon(u^{\mathrm{r}}(\mu)) - D(\mu) : \epsilon_0(\theta^{\mathrm{r}}(\mu))$. To fully exploit the ROM efficacy, we propose to construct the surrogate stress field $\widehat{\sigma}(\mu)$ as

$$\sigma^{\mathrm{r}}(\mu) \approx \widehat{\sigma}(\mu) = \sigma^{\mathrm{r},0}(\mu) + \sigma^{\mathrm{h,p}}(\mu), \quad \forall \mu \in \mathcal{D}, \quad \text{where} \quad \sigma^{\mathrm{r},0}(\mu) = \sum_{i=1}^{N^\sigma}\alpha_i^\sigma(\mu)\phi_i^\sigma, \tag{50}$$

where $\alpha_i^\sigma(\mu) \in \mathbb{R}^{N^\sigma}$ are (unknown) generalized coefficients to be obtained by the projection.

Notice that this construction is slightly different from the original one proposed in Refs. [26,33] with $\sigma^{\mathrm{h}}(\mu) \approx \widehat{\sigma}(\mu)$. The reason for this modification is that the computation of $\sigma^{\mathrm{h}}(\mu)$ in this work includes additionally the term $\theta^{\mathrm{h}}(\mu)$, thus if we use $\sigma^{\mathrm{h}}(\mu) \approx \widehat{\sigma}(\mu)$, the online computation of $\widehat{\sigma}(\mu)$ would invoke $\theta^{\mathrm{h}}(\mu)$ for every input μ. In other words, in this case, the online computation cost would still depend on $\mathcal{N}^\theta$ and hence is expensive. This will be clear in the following derivation.

The generalized coefficients are required to satisfy the optimum property

$$\widehat{\sigma}(\mu) = \arg\min_{\sigma^\star \in \mathcal{S}^{\mathrm{r}}(\Omega;\mu)} \left\|\sigma^\star - \sigma^{\mathrm{r}}(\mu)\right\|_{C(\mu)}, \tag{51}$$

where the admissible space for reduced stress field is defined by $\mathcal{S}^{\mathrm{r}}(\Omega;\mu) = \{\sigma^\star \in \mathcal{S}(\Omega) \mid \sigma^\star = \sum_{i=1}^{N^\sigma}\alpha_i^\star\phi_i^\sigma + \sigma^{\mathrm{h,p}}(\mu), \forall \alpha^\star \in \mathbb{R}^{N^\sigma}\}$; $\|\cdot\|_{C(\mu)}$ is the so-called energy norm for the stress fields as defined in

Proposition 3.2.

Using the constitutive relation (5), the optimization problem (51) can be recast in the following variational form: find $\widehat{\sigma}(\mu) \in \mathcal{S}^{\mathrm{r}}(\Omega;\mu)$ such that

$$-\int_{\Omega} \widehat{\sigma}(\mu) : C(\mu) : \sigma^{\star}\, d\Omega + \int_{\Omega} \epsilon\left(u^{\mathrm{r}}(\mu)\right) : \sigma^{\star}\, d\Omega - \int_{\Omega} \epsilon_0\left(\theta^{\mathrm{r}}(\mu)\right) : \sigma^{\star}\, d\Omega = 0, \quad \forall \sigma^{\star} \in \mathcal{S}^{\mathrm{r},0}(\Omega), \tag{52}$$

where $\mathcal{S}^{\mathrm{r},0}(\Omega) = \{\sigma^{\star} \in \mathcal{S}(\Omega) \mid \sigma^{\star} = \sum_{i=1}^{N^{\sigma}} \alpha_i^{\star} \phi_i^{\sigma}, \forall \alpha^{\star} \in \mathbb{R}^{N^{\sigma}}\}$. Now, substituting (50) and (40) into (52) and noting (47), we obtain the following variational form to compute the stress field $\sigma^{\mathrm{r},0}(\mu)$:

$$\int_{\Omega} \sigma^{\mathrm{r},0}(\mu) : C(\mu) : \sigma^{\star}\, d\Omega = \int_{\Omega} \epsilon\left(\cancelto{0}{u^{\mathrm{r},0}(\mu)} + u^{\mathrm{h,p}}(\mu)\right) : \sigma^{\star}\, d\Omega - \int_{\Omega} \epsilon_0\left(\theta^{\mathrm{r}}(\mu)\right) : \sigma^{\star}\, d\Omega - \int_{\Omega} \sigma^{\mathrm{h,p}}(\mu) : C(\mu) : \sigma^{\star}\, d\Omega, \qquad \forall \sigma^{\star} \in \mathcal{S}^{\mathrm{r},0}(\Omega). \tag{53}$$

Offline-Online computational procedures for the dual ROM Thanks to the *affine* properties of $u^{\mathrm{h,p}}(\mu)$ eq. (39) and $\sigma^{\mathrm{h,p}}(\mu)$ Eq. (49), we see that Eq. (53) can also be decomposed into Offline-Online computational procedures if the operator $C(\mu)$ is also *affine*, which we will assume:

$$C(x,\mu) = \sum_{i=1}^{n^{\mathrm{C}}} \gamma_i^{\mathrm{C}}(\mu) \overline{C}_i(x), \quad \forall \mu \in D, x \in \Omega. \tag{54}$$

Invoking (39), (49), (54) and the expanded expression of the RB temperature field $\theta^{\mathrm{r}}(\mu) = \sum_{i=1}^{N^{\theta}} \alpha_i^{\theta}(\mu)\phi_i^{\theta} + \sum_{i=1}^{n^{\theta,\mathrm{w}}} \gamma_i^{\theta,\mathrm{w}}(\mu)\psi_i^{\theta}$, Eq. (53) can then be written as

$$\begin{aligned}
&\sum_{i=1}^{N^{\sigma}} \sum_{k=1}^{n^{\mathrm{C}}} \gamma_k^{\mathrm{C}}(\mu) \left(\int_{\Omega} \boldsymbol{\phi}_i^{\sigma} : \overline{\mathbf{C}}_k : \boldsymbol{\phi}_j^{\sigma}\, \mathbf{d\Omega} \right) \alpha_i^{\sigma}(\mu) \\
&= \sum_{k=1}^{n^{u,\mathrm{w}}} \gamma_k^{u,\mathrm{w}}(\mu) \left(\int_{\Omega} \boldsymbol{\epsilon}(\boldsymbol{\psi}_k^{u}) : \boldsymbol{\phi}_j^{\sigma}\, \mathbf{d\Omega} \right) - \sum_{i=1}^{N^{\theta}} \alpha_i^{\theta}(\mu) \int_{\Omega} \boldsymbol{\epsilon}_0\left(\boldsymbol{\phi}_i^{\theta}\right) : \boldsymbol{\phi}_j^{\sigma}\, \mathbf{d\Omega} \\
&\quad - \sum_{i=1}^{n^{\theta,\mathrm{w}}} \gamma_i^{\theta,\mathrm{w}}(\mu) \int_{\Omega} \boldsymbol{\epsilon}_0\left(\boldsymbol{\psi}_i^{\theta}\right) : \boldsymbol{\phi}_j^{\sigma}\, \mathbf{d\Omega} - \sum_{k=1}^{\widetilde{n}_{\mathrm{p}}} \sum_{l=1}^{n^{\mathrm{C}}} \widetilde{\gamma}_k^{\mathrm{p}}(\mu) \gamma_l^{\mathrm{C}}(\mu) \\
&\quad \times \left(\int_{\Omega} \boldsymbol{\sigma}_k^{\mathrm{p}} : \overline{\mathbf{C}}_l : \boldsymbol{\phi}_j^{\sigma}\, \mathbf{d\Omega} \right), \quad 1 \le j \le N^{\sigma}.
\end{aligned} \tag{55}$$

From the above decomposition, the computational procedures are now clear: an expensive μ-independent Offline stage performed only *once* and *many* cheap Online computations for any input parameter value $\mu \in D$. In particular, in the Offline stage the affine terms $\sigma_i^{\mathrm{p}}, 1 \le i \le \widetilde{n}^{\sigma,\mathrm{p}}$ (49), the RB basis functions $\{\phi_n^{\sigma}, 1 \le n \le N^{\sigma} \le N_{\max}^{\sigma}\}$ (50) and all the *parameter-independent* terms (bold typeface in (55)) will be computed and stored. In the Online stage, for any given μ, all the *parameter-dependent* functions (normal typeface in (55)) are evaluated, the reduced system (55) is assembled and solved to find the RB coefficients $\alpha_n^{\sigma}(\mu), 1 \le n \le N^{\sigma}$. The system matrix is very small, with a size $(N^{\sigma} \times N^{\sigma})$ completely independent of the FE space dimension $\mathcal{N}^{\sigma}$ (Here, $\mathcal{N}^{\sigma}$ denotes the dimension of the FE stress field.). The Online operation count is $O\left(n^{\mathrm{C}} N^{\sigma 2}\right)$ to assemble the system and $O\left(N^{\sigma 3}\right)$ to invert the matrix in (55). Therefore, the Online operation count to evaluate $\mu \to \alpha^{\sigma}(\mu)$ is also independent of $\mathcal{N}^{u}$ and $\mathcal{N}^{\theta}$.

3.2.3. Constitutive relation error for the elasticity

In this section, we derive a new CRE approximation for the elasticity equation by extending the technique developed originally in Ref. [26] as follows.

Proposition 3.2. *Let $e_{\theta}(\mu) = \theta^{\mathrm{h}}(\mu) - \theta^{\mathrm{r}}(\mu)$, $e_u(\mu) = u^{\mathrm{h}}(\mu) - u^{\mathrm{r}}(\mu)$ and $e_{\sigma}(\mu) = \sigma^{\mathrm{h}}(\mu) - \widehat{\sigma}(\mu)$ be the RB errors for the temperature, displacement and stress fields, respectively. We consider the energy norms $\|\theta^{\star}\|_{D(\mu)} = \left(\int_{\Omega} \epsilon_0(\theta^{\star}) : D(\mu) : \epsilon_0(\theta^{\star}) d\Omega\right)^{1/2}$ for a temperature field $\theta^{\star} \in \Theta^{\mathrm{h},0}(\Omega)$, $\|u^{\star}\|_{D(\mu)} = \left(\int_{\Omega} \epsilon(u^{\star}) : D(\mu) : \epsilon(u^{\star}) d\Omega\right)^{1/2}$ for a displacement field $u^{\star} \in \mathcal{U}^{\mathrm{h},0}(\Omega)$, and $\|\sigma^{\star}\|_{C(\mu)} = \left(\int_{\Omega} \sigma^{\star} : C(\mu) : \sigma^{\star}\, d\Omega\right)^{1/2}$ for a stress field $\sigma^{\star} \in \mathcal{S}(\Omega)$. Then, by controlling appropriately the term $e_{\theta}(\mu)$, we can obtain the CRE estimator*

$$\Delta_u^{\mathrm{CRE}}(\mu)^2 := \|\sigma^{\mathrm{r}}(\mu) - \widehat{\sigma}(\mu)\|_{C(\mu)}^2 \approx \|e_u(\mu)\|_{D(\mu)}^2 + \|e_{\sigma}(\mu)\|_{C(\mu)}^2. \tag{56}$$

Proof. We sketch the proof as follows. By substituting the constitutive relation expressions for $\sigma^{\mathrm{h}}(\mu)$ and $\sigma^{\mathrm{r}}(\mu)$ from (5) into $\Delta_u^{\mathrm{CRE}}(\mu)$ and after some algebraic manipulations, we obtain

$$\begin{aligned}
\Delta_u^{\mathrm{CRE}}(\mu)^2 &= \|\sigma^{\mathrm{r}}(\mu) - \widehat{\sigma}(\mu)\|_{C(\mu)}^2 = \|\sigma^{\mathrm{r}}(\mu) - \sigma^{\mathrm{h}}(\mu) + \sigma^{\mathrm{h}}(\mu) - \widehat{\sigma}(\mu)\|_{C(\mu)}^2 \\
&= \|-D(\mu) : \epsilon(e_u(\mu)) + D(\mu) : \epsilon_0(e_{\theta}(\mu)) + e_{\sigma}(\mu)\|_{C(\mu)}^2 \\
&= \|e_u(\mu)\|_{D(\mu)}^2 + \|e_{\sigma}(\mu)\|_{C(\mu)}^2 - 2\int_{\Omega} \epsilon(e_u(\mu)) : e_{\sigma}(\mu)\, d\Omega \\
&\quad + \|e_{\theta}(\mu)\|_{D(\mu)}^2 - 2\int_{\Omega} \epsilon_0(e_{\theta}(\mu)) : D(\mu) : \epsilon(e_u(\mu))\, d\Omega \\
&\quad + 2\int_{\Omega} \epsilon_0(e_{\theta}(\mu)) : e_{\sigma}(\mu)\, d\Omega.
\end{aligned} \tag{57}$$

The above expression can be rewritten as

$$\Delta_u^{\mathrm{CRE}}(\mu)^2 = \|e_u(\mu)\|_{D(\mu)}^2 + \|e_{\sigma}(\mu)\|_{C(\mu)}^2 + T + S, \tag{58}$$

where

$$\begin{cases}
T = -2\displaystyle\int_{\Omega} \epsilon\left(e_u(\mu)\right) : e_{\sigma}(\mu) d\Omega \\
S = \|e_{\theta}(\mu)\|_{D(\mu)}^2 - 2\displaystyle\int_{\Omega} \epsilon_0\left(e_{\theta}(\mu)\right) : D(\mu) : \epsilon\left(e_u(\mu)\right) d\Omega \\
\qquad + 2\displaystyle\int_{\Omega} \epsilon_0\left(e_{\theta}(\mu)\right) : e_{\sigma}(\mu) d\Omega.
\end{cases} \tag{59}$$

We observe that the term $T = 0$ due to (47) as $e_u(\mu) = u^{\mathrm{h},0}(\mu) - u^{\mathrm{r},0}(\mu) \in \mathcal{U}^{\mathrm{h},0}(\Omega)$ and $e_{\sigma}(\mu) = \sigma^{\mathrm{h},0}(\mu) - \sigma^{\mathrm{r},0}(\mu) \in \mathcal{S}^{\mathrm{h},0}(\Omega)$ (see for examples [26,33]). The term S depends on $e_{\theta}(\mu)$ whose magnitude can be completely controlled by its *a posteriori* CRE upper bound, i.e., $\|e_{\theta}(\mu)\|_{k(\mu)} \le \Delta_{\theta}^{\mathrm{CRE}}(\mu), \forall \mu \in \mathcal{D}$ (31). Hence, we can control *appropriately* the magnitude of term S (through $e_{\theta}(\mu)$ or indirectly through $\Delta_{\theta}^{\mathrm{CRE}}(\mu)$) such that

$$S\left(e_{\theta}(\mu)\right) \ll \|e_u(\mu)\|_{D(\mu)}^2 + \|e_{\sigma}(\mu)\|_{C(\mu)}^2. \tag{60}$$

From the above observations, the terms T and S can be eliminated from (58) which concludes the proof. □

Similar to the computation of $\Delta_{\theta}^{\mathrm{CRE}}(\mu)$ in (3.1.3), the computation of $\Delta_u^{\mathrm{CRE}}(\mu)$ is also very efficient with completely decomposed Offline-Online procedures. The technique, which is very similar to the one presented in Appendix B of [26], is detailed in Appendix A. The key point to note is that the cost to compute $\Delta_u^{\mathrm{CRE}}(\mu)$ (in the online stage) is completely independent of $\mathcal{N}^{u}$, $\mathcal{N}^{\sigma}$, and $\mathcal{N}^{\theta}$. It only depends on N^{θ}, N^{u}, and N^{σ}. We define the effectivities of CRE bound for both displacement and stress fields as

$$\eta_u^{\mathrm{CRE}}(\mu) = \frac{\Delta^{\mathrm{CRE}}(\mu)}{\|u^{\mathrm{h}}(\mu) - u^{\mathrm{r}}(\mu)\|_{D(\mu)}}, \quad \text{and} \quad \eta_{\sigma}^{\mathrm{CRE}}(\mu) = \frac{\Delta^{\mathrm{CRE}}(\mu)}{\|\sigma^{\mathrm{h}}(\mu) - \sigma^{\mathrm{r}}(\mu)\|_{C(\mu)}}, \tag{61}$$

respectively.

3.2.4. Goal-oriented error bound approximations for the elasticity equation

Similar to section 3.1.4, duality technique is employed to bound engineering QoIs. We first pursue this approach to derive the goal-oriented error approximation for the elasticity equation.

For each one of the QoIs, we define the FE dual (or adjoint) problem

$$a^{uu}\left(z_i^{\mathrm{h},0}(\mu), v_2; \mu\right) = \ell_i^u\left(v_2; \mu\right), \quad \forall v_2 \in \mathcal{U}^{\mathrm{h},0}(\Omega), \quad 1 \le i \le n^{\mathrm{Q}}, \tag{62}$$

where $z_i^{\mathrm{h},0}(\mu) \in \mathcal{U}^{\mathrm{h},0}, 1 \le i \le n^{\mathrm{Q}}$ is the FE dual displacement field corresponding to the output functional ℓ_i^u, which is required to satisfy homogeneous Dirichlet boundary conditions.

We solve this problem approximately by the projection-based ROM obtained by the reduced Galerkin formulation: find $z_i^{\mathrm{r},0}(\mu) \in \mathcal{U}^{\mathrm{h},0}(\Omega)$ such that

$$a^{uu}\left(z_i^{\mathrm{r},0}(\mu), v_2; \mu\right) = \ell_i^u\left(v_2; \mu\right), \quad \forall v_2 \in \mathcal{U}_{z,i}^{\mathrm{r},0}(\Omega), \quad 1 \le i \le n^{\mathrm{Q}}, \tag{63}$$

where $\mathcal{U}_{z,i}^{\mathrm{r},0}(\Omega) \subset \mathcal{U}^{\mathrm{h},0}(\Omega)$ is the reduced basis space for the dual displacement field associated with the output functional ℓ_i^u; and generally $\mathcal{U}_{z,i}^{\mathrm{r},0}(\Omega) \ne \mathcal{U}_{N^u}^{\mathrm{r},0}(\Omega)$, $1 \le i \le n^{\mathrm{Q}}$. For consistency, we also define the sets of RB basis functions for dual displacements $\{\phi_n^{z,i}, 1 \le n \le N^{z,i}\}$, and that for dual stresses $\{\phi_m^{\widetilde{\sigma},i}, 1 \le m \le N^{\widetilde{\sigma},i}\}$, $1 \le i \le n^{\mathrm{Q}}$ for the i-th QoI, respectively.

Using the classical technique in Ref. [36], we obtain the following expression

$$\begin{aligned} Q_i^{\mathrm{h},u}(\mu) - Q_i^{\mathrm{r},u}(\mu) = \ell_i^u(e_u(\mu)) &= a^{uu}\left(z_i^{\mathrm{h},0}(\mu), e_u(\mu); \mu\right), \\ &= a^{uu}\left(e_{z,i}(\mu), e_u(\mu); \mu\right) \\ &\quad + a^{uu}\left(z_i^{\mathrm{r},0}(\mu), e_u(\mu); \mu\right), \quad 1 \le i \le n^{\mathrm{Q}} \end{aligned} \tag{64}$$

where $e_{z,i}(\mu) := z_i^{\mathrm{h}}(\mu) - z_i^{\mathrm{r}}(\mu)$ is the true error for the dual variables.

Applying Cauchy–Schwarz inequality to separate the errors in primal and dual problems, and substituting the CRE as a computable bound for exact errors in energy norm, we obtain

$$Q_i^{\mathrm{r},u,\mathrm{low}}(\mu) \le Q_i^{\mathrm{h},u}(\mu) \le Q_i^{\mathrm{r},u,\mathrm{up}}(\mu), \tag{65}$$

where $\begin{cases} Q_i^{\mathrm{r},u,\mathrm{low}}(\mu) = Q_i^{\mathrm{r},u}(\mu) - \Delta_u^{\mathrm{CRE}}(\mu)\Delta_{z,i}^{\mathrm{CRE}}(\mu) \\ \qquad\qquad - \Delta_u^{\mathrm{CRE}}(\mu)\, \|z_i^{\mathrm{r},0}(\mu)\|_{D(\mu)} \\ Q_i^{\mathrm{r},u,\mathrm{up}}(\mu) = Q_i^{\mathrm{r},u}(\mu) + \Delta_u^{\mathrm{CRE}}(\mu)\Delta_{z,i}^{\mathrm{CRE}}(\mu) \\ \qquad\qquad + \Delta_u^{\mathrm{CRE}}(\mu)\, \|z_i^{\mathrm{r},0}(\mu)\|_{D(\mu)} \end{cases}, \quad 1 \le i \le n^{\mathrm{Q}}.$

We notice from this expression that the "uncertainty gap": $\mathtt{gap}_i(\mu) = Q_i^{\mathrm{r},u,\mathrm{up}}(\mu) - Q_i^{\mathrm{r},u,\mathrm{low}}(\mu) = O\left(\Delta_u^{\mathrm{CRE}}(\mu)\left(\Delta_{z,i}^{\mathrm{CRE}}(\mu) + \|z_i^{\mathrm{r},0}(\mu)\|_{D(\mu)}\right)\right) \approx O\left(c\Delta_u^{\mathrm{CRE}}(\mu)\right)$, where c is an arbitrary constant as usually $\Delta_{z,i}^{\mathrm{CRE}}(\mu) \ll \|z_i^{\mathrm{r},0}(\mu)\|_{D(\mu)}$. In other words, the uncertainty gap $\mathtt{gap}_i(\mu)$ now depends linearly with $\Delta_u^{\mathrm{CRE}}(\mu)$ rather than quadratic dependence as in classical derivation [25,36,37,42–44] due to the ROM approximation $\theta^{\mathrm{h}}(\mu) \approx \theta^{\mathrm{r}}(\mu)$ in $\widehat{f}^u(v_2; \mu)$ in (41).

Due to this reason, we follow the primal-only approach which is simpler and also has linearly dependence of "uncertainty gap" on the CRE estimator. Following classical and standard derivations such as in Ref. [25], we can easily have

$$\begin{aligned} \left|Q_i^{\mathrm{h},u}(\mu) - Q_i^{\mathrm{r},u}(\mu)\right| &= \left|\ell_i^u(e_u(\mu))\right| \\ &\le \|\ell_i^u\|_{(\mathcal{U}^{\mathrm{h},0}(\Omega))'}\, \|e_u(\mu)\|_{D(\mu)} \\ &\le \|\ell_i^u\|_{(\mathcal{U}^{\mathrm{h},0}(\Omega))'} \Delta_u^{\mathrm{CRE}}(\mu), \quad 1 \le i \le n^{\mathrm{Q}}, \end{aligned} \tag{66}$$

where X' denotes the dual space to X. From which, we obtain the following goal-oriented bounds

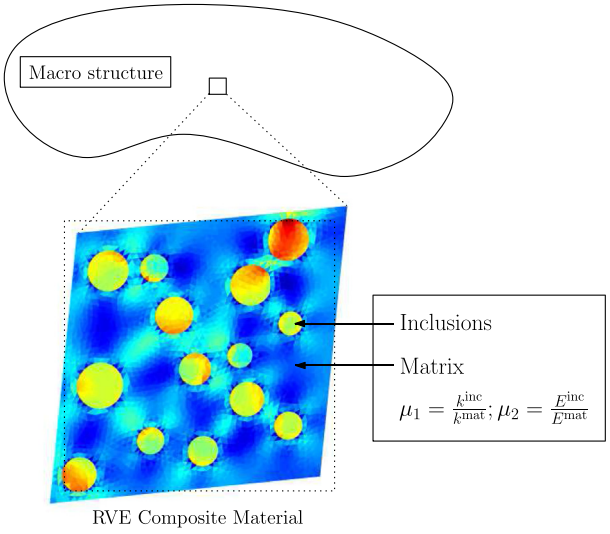

Fig. 1. Schematic representation of the computational homogenization framework for composite materials. The heat conductive contrast and elastic contrast of the particulate composite are parametrized.

$$Q_i^{\mathrm{r},u,\mathrm{low}}(\mu) \le Q_i^{\mathrm{h},u}(\mu) \le Q_i^{\mathrm{r},u,\mathrm{up}}(\mu), \tag{67}$$

where $\begin{cases} Q_i^{\mathrm{r},u,\mathrm{low}}(\mu) = Q_i^{\mathrm{r},u}(\mu) - \|\ell_i^u\|_{(\mathcal{U}^{\mathrm{h},0}(\Omega))'}\Delta_u^{\mathrm{CRE}}(\mu) \\ Q_i^{\mathrm{r},u,\mathrm{up}}(\mu) = Q_i^{\mathrm{r},u}(\mu) + \|\ell_i^u\|_{(\mathcal{U}^{\mathrm{h},0}(\Omega))'}\Delta_u^{\mathrm{CRE}}(\mu) \end{cases}, \quad 1 \le i \le n^{\mathrm{Q}}.$

3.2.5. Two-field, CRE-based greedy sampling for the elasticity equation

Principle: As similar to the heat equation, with the available CRE estimator (56), it is natural to set the minimization of the maximum CRE over the parameter domain as our target for the construction of the projection subspaces. Again, this minimization problem is not directly solvable, and we will make use of a greedy algorithm. This greedy algorithm is quite similar to the one presented in section 3.1.5 or the one developed originally in Ref. [26]. In addition, as derived in Proposition 3.2, the CRE displacement error estimator ($\Delta_u^{\mathrm{CRE}}(\mu)$) requires some *proper control* of the CRE temperature error estimator ($\Delta_\theta^{\mathrm{CRE}}(\mu)$). For this purpose, we propose a new control procedure (so-called "procedure to select N^θ") within the greedy

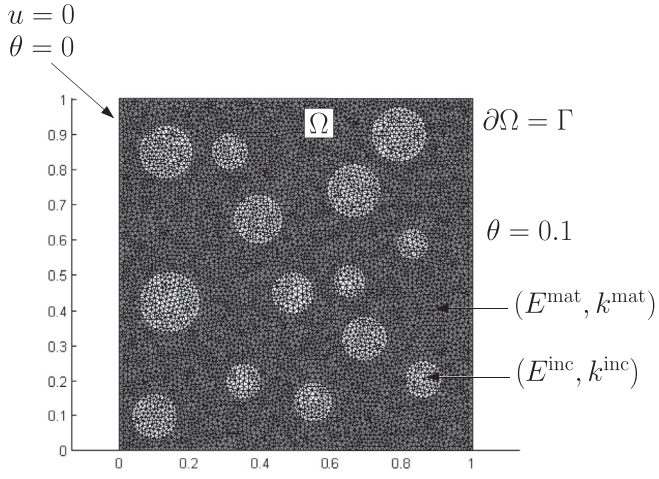

Fig. 2. FE discretization of the parametrized SVE.

algorithm. The main idea of this procedure is to choose adaptively and automatically the RB dimension of the temperature field (N^θ) so that the CRE expression (56) is valid as this is crucial for this approach.

The greedy algorithm proceeds iteratively by assuming the existence of projection subspaces for both displacement and stress fields and performing a rank-one correction in such a way that the maximum of the CRE over the parameter domain is approximately minimized. As the CRE is an *approximated* bound for both RB displacement and stress errors, the algorithm can be stopped whenever the CRE is sufficiently low over the entire parameter domain.

The rank-one update is performed as follows. First, we identify the point of the parameter domain where the CRE is at its largest. Then, a simple test on enrichment to identify which one of the enrichments would result in the largest decrease in the CRE at this particular parameter point will be performed. Finally, we enrich either the displacement or the stress ROM by adding the corresponding solution (after orthonormalization) to the corresponding existing reduced basis. (For interested readers, the convergence of greedy algorithm for reduced basis method was proved in Ref. [45].)

Greedy algorithm: The two-field greedy sampling algorithm is presented in Algorithm 1[2]

The input parameter ϵ^{tol} can be set either directly or through a maximum RB dimension $N^u_{\max}$. A training sample $\Xi_{\text{train}} \subset \mathcal{D}$ is a discrete set representing a very fine sample of $n_{\text{train}} = |\Xi_{\text{train}}|$ points in the parameter domain. And ϵ^{CRE} and Ξ^{st} are the parameters for the selection procedure `selectNtheta`. There are two sets of RB basis functions to be built: the RB displacement set ($\mathcal{Z}_{N^u}$) and the RB stress set ($\widetilde{\mathcal{Z}}_{N^\sigma}$). The two-field greedy algorithm starts with arbitrarily chosen parameters $\mu^u_1, \mu^\sigma_1 \in \Xi_{\text{train}}$ to construct $\mathcal{Z}_1 = \{\phi^u_1\}$ and $\widetilde{\mathcal{Z}}_1 = \{\phi^\sigma_1\}$, respectively (lines 1–2). We now analyse each greedy iteration in detail as follows.

We first perform the selection procedure to choose a proper N^θ based on the current sets $\mathcal{Z}_{N^u}$ and $\widetilde{\mathcal{Z}}_{N^\sigma}$ (line 4). We then compute the CRE indicators $\Delta^{\text{CRE},u}_{N^u,N^\sigma,N^\theta}(\mu), \forall \mu \in \Xi_{\text{train}}$ based on the current RB displacement and stress spaces, i.e., $\mathcal{U}^{\text{r},0}_{N^u}(\Omega) = \text{span}\{\phi^u_n, 1 \le n \le N^u\}$ and $\mathcal{S}^{\text{r},0}_{N^\sigma}(\Omega) = \text{span}\{\phi^\sigma_m, 1 \le m \le N^\sigma\}$ (line 5). The "worst" parameter point $\mu^\star$ which induces the maximum error indicator thus can be found (line 6). We then perform two following tests at $\mu^\star$. First, we compute the CRE indicator $\Delta^{\text{CRE}}_{N^u+1,N^\sigma,N^\theta}(\mu^\star)$ after enriching the current RB displacement space with $\phi^u(\mu^\star)$. Second, we compute the CRE indicator $\Delta^{\text{CRE}}_{N^u,N^\sigma+1,N^\theta}(\mu^\star)$ after enriching the current RB stress space with $\phi^\sigma(\mu^\star)$ (line 7). These two CRE indicators are then compared with each other, and the actual enrichment is decided based on this comparison. If $\Delta^{\text{CRE}}_{N^u+1,N^\sigma,N^\theta}(\mu^\star) < \Delta^{\text{CRE}}_{N^u,N^\sigma+1,N^\theta}(\mu^\star)$, this implies that the "testing" displacement enrichment helps to decrease the CRE error indicator at $\mu^\star$ more than the "testing" stress enrichment does; and hence "actual" displacement enrichment will be performed (lines 9–10). In a completely opposite way, the fact $\Delta^{\text{CRE}}_{N^u+1,N^\sigma,N^\theta}(\mu^\star) \ge \Delta^{\text{CRE}}_{N^u,N^\sigma+1,N^\theta}(\mu^\star)$ implies that the "testing" stress enrichment reduces the CRE indicator at $\mu^\star$ more than the "testing" displacement enrichment does; and hence "actual" stress enrichment will be performed (lines 12–13). The iteration of this algorithm continues until it satisfies the stopping criterion (line 3). Lastly, we use two functions `GSdisp` and `GSstress` to construct next RB basis functions for displacement and stress fields using Gram–Schmidt orthogonalization process, respectively. The function `selectNtheta` is discussed in next two paragraphs.

Algorithm 1 Two-field greedy sampling strategy.

INPUT: Ξ_{train}, ϵ^{tol} (or $N^u_{\max}$); Ξ^{st}, ϵ^{CRE}

OUTPUT: $\mathcal{Z}_{N^u} = \{\phi^u_n, 1 \le n \le N^u\}$; $\widetilde{\mathcal{Z}}_{N^\sigma} = \{\phi^\sigma_m, 1 \le m \le N^\sigma\}$

$\phi^u_1 = \frac{u^{\text{h},0}(\mu_1)}{\|u^{\text{h},0}(\mu_1)\|_{D(\mu_0)}}$; $\mathcal{Z}_1 = \{\phi^u_1\}$; $N^u = 1$;

$\phi^\sigma_1 = \frac{\sigma^{\text{h},0}(\widetilde{\mu}_1)}{\|\sigma^{\text{h},0}(\widetilde{\mu}_1)\|_{C(\mu_0)}}$; $\widetilde{\mathcal{Z}}_1 = \{\phi^\sigma_1\}$; $N^\sigma = 1$;

While $\Delta^{\text{CRE,max}} > \epsilon^{\text{tol}}$ **do**

- $N^\theta = \texttt{selectNtheta}\left(\epsilon^{\text{CRE}}, \Xi^{\text{st}}, \mathcal{Z}_{N^u}, \widetilde{\mathcal{Z}}_{N^\sigma}\right)$;
- Compute $\alpha^\theta(\mu)$, $\alpha^u(\mu)$, $\alpha^\sigma(\mu)$ and $\Delta^{\text{CRE},u}_{N^u,N^\sigma,N^\theta}(\mu)$, $\forall \mu \in \Xi_{\text{train}}$;
- Set: $\Delta^{\text{CRE,max}} = \max_{\mu \in \Xi_{\text{train}}} \Delta^{\text{CRE},u}_{N^u,N^\sigma,N^\theta}(\mu)$; $\mu^\star = \arg\max_{\mu \in \Xi_{\text{train}}} \Delta^{\text{CRE},u}_{N^u,N^\sigma,N^\theta}(\mu)$;
- Test: compute $\Delta^{\text{CRE},u}_{N^u,N^\sigma+1,N^\theta}(\mu^\star)$ and $\Delta^{\text{CRE},u}_{N^u+1,N^\sigma,N^\theta}(\mu^\star)$;

if $\Delta^{\text{CRE},u}_{N^u+1,N^\sigma,N^\theta}(\mu^\star) < \Delta^{\text{CRE},u}_{N^u,N^\sigma+1,N^\theta}(\mu^\star)$ **then**

$\phi^u_{N^u+1} = \texttt{GSdisp}\left(u^{\text{h}}(\mu^\star) - u^{\text{h,p}}(\mu^\star), \mathcal{Z}_{N^u}\right)$;

$\mathcal{Z}_{N^u+1} \leftarrow \mathcal{Z}_{N^u} \cup \phi^u_{N^u+1}$; $N^u \leftarrow N^u + 1$;

else

$\phi^\sigma_{N^\sigma+1} = \texttt{GSstress}\left(\sigma^{\text{h}}(\mu^\star) - \sigma^{\text{h,p}}(\mu^\star), \widetilde{\mathcal{Z}}_{N^\sigma}\right)$;

$\widetilde{\mathcal{Z}}_{N^\sigma+1} \leftarrow \widetilde{\mathcal{Z}}_{N^\sigma} \cup \phi^\sigma_{N^\sigma+1}$; $N^\sigma \leftarrow N^\sigma + 1$;

end if

end While

$$\texttt{GSdisp}: \phi^u_{N^u+1} \leftarrow u^{h,0}(\mu^\star) - \sum_{n=1}^{N^u} \left(u^{h,0}(\mu^\star), \phi^u_n\right)_{D(\mu_0)} \phi^u_n;$$

$$\phi^u_{N^u+1} \leftarrow \frac{\phi^u_{N^u+1}}{\|\phi^u_{N^u+1}\|_{D(\mu_0)}}.$$

$$\texttt{GSstress}: \phi^\sigma_{N^\sigma+1} \leftarrow \sigma^{h,0}(\mu^\star) - \sum_{m=1}^{N^\sigma} \left(\sigma^{h,0}(\mu^\star), \phi^\sigma_m\right)_{C(\mu_0)} \phi^\sigma_m;$$

$$\phi^\sigma_{N^\sigma+1} \leftarrow \frac{\phi^\sigma_{N^\sigma+1}}{\|\phi^\sigma_{N^\sigma+1}\|_{C(\mu_0)}}.$$

The basic idea of this proposed algorithm is that we use only one single greedy loop to build simultaneously two RB spaces ($\mathcal{U}^{\text{r},0}_{N^u}(\Omega)$ and $\mathcal{S}^{\text{r},0}_{N^\sigma}(\Omega)$) in an optimal way. At one greedy iteration, the particular set of RB basis functions is chosen for "actual" enrichment depending on the performance of its "testing" enrichment set on $\mu^\star$: which "testing" set decreases $\Delta^{\text{CRE}}_u(\mu^\star)$ the most will be chosen.

Finally, the efficient offline-online computational procedures for the TF-greedy sampling algorithm are detailed as follows. We consider one TF-greedy iteration in more details. With the reduced spaces $\mathcal{Z}_{N^u}$, $\widetilde{\mathcal{Z}}_{N^\sigma}$ and associated offline terms available from the previous iteration, we can perform an exhaustive search over the training sample Ξ_{train} to compute $\Delta^{\text{CRE},u}_{N^u,N^\sigma,N^\theta}(\mu)$ from Eq. (83) (line 5 in Algorithm 1); from which, the "worst" parameter point $\mu^\star$ can be extracted (line 6 in Algorithm 1). At $\mu^\star$, we solve the full order Eqs. (5), (14) and (15) to compute $\Delta^{\text{CRE},u}_{N^u+1,N^\sigma,N^\theta}(\mu^\star)$ and $\Delta^{\text{CRE},u}_{N^u,N^\sigma+1,N^\theta}(\mu^\star)$ (line 7 in Algorithm 1). The enrichment of the field is determined via the comparison of these two error measures. If the displacement field is enriched, $u^{\text{h},0}(\mu^\star)$ is added to the set $\mathcal{Z}_{N^u}$, a Gram–Schmidt orthogonalization is performed and N^u is updated (lines 9–10 in Algorithm 1). Correspondingly, all the offline terms associated with the RB displacement basis functions (i.e., ϕ^u) in (41) and the CRE in (86)–(109) are all

[2] Note that in this algorithm, we will write $\Delta^{\text{CRE}}_u(\mu)$ as $\Delta^{\text{CRE},u}_{N^u,N^\sigma,N^\theta}(\mu)$ to reflect the fact that this term depends on N^u, N^σ and N^θ – the number of RB basis functions for displacement, stress and temperature fields, respectively.

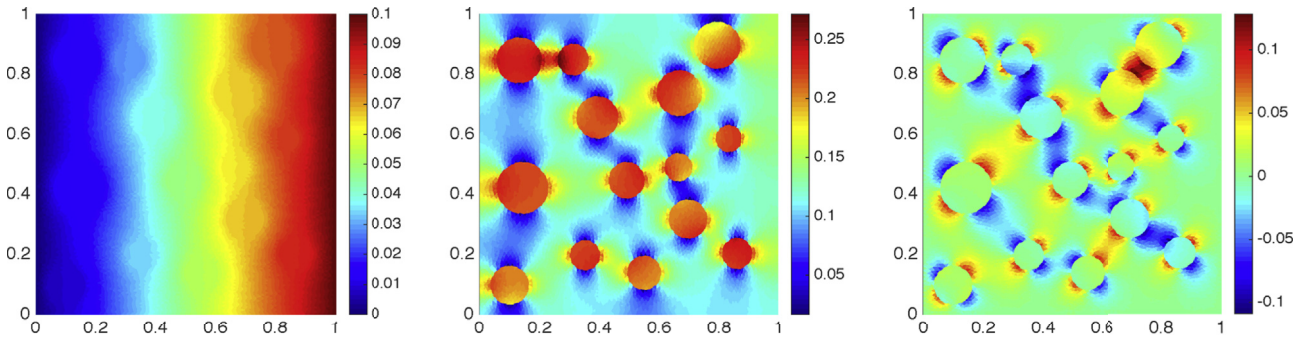

Fig. 3. Solution visualization with $\mu^{\text{test}} = (10, 0.1)$.

computed/updated and stored. In the other case, if the stress field is enriched, $\sigma^{\text{h},0}(\mu^\star)$ is added to the set $\widetilde{\mathcal{Z}}_{N^\sigma}$, a Gram–Schmidt process is also performed and N^σ is updated accordingly (lines 12–13 in Algorithm 1). At last, all the offline terms associated with the RB stress basis functions (i.e., ϕ^σ) in (53) and the CRE in (86)–(109) are all updated and stored.

Procedure to select N^θ: As shown in Proposition 3.2, controlling the term S (through $e_\theta(\mu)$) such that (60) holds true is the key idea to obtain the *a posteriori* CRE estimator (56). The most feasible way to control $e_\theta(\mu) = \theta^{\text{h}}(\mu) - \theta^{\text{r}}(\mu)$ is by choosing *adaptively* N^θ which is the number of RB basis vectors for the temperature field of the heat diffusion equation. In particular, we want to choose N^θ sufficiently big so that $\Delta_\theta^{\text{CRE}}(\mu)$ is sufficiently small, and hence $e_\theta(\mu)$ will be small too because $\Delta_\theta^{\text{CRE}}(\mu) \geq \|e_\theta(\mu)\|_{k(\mu)}, \forall \mu$ from (31). For this purpose, we propose the following criterion to select N^θ: choose N^θ (sufficiently big) such that

$$\frac{\sqrt{|S|}}{\Delta_u^{\text{CRE}}(\mu)} := \frac{\sqrt{\left|\Delta_u^{\text{CRE}}(\mu)^2 - \left(\|e_u(\mu)\|_{D(\mu)}^2 + \|e_\sigma(\mu)\|_{C(\mu)}^2\right)\right|}}{\Delta_u^{\text{CRE}}(\mu)} \leq \epsilon^{\text{CRE}},$$
$$\forall \mu \in \Xi^{\text{st}}, \tag{68}$$

where $\Xi^{\text{st}} \subset \mathcal{D}$ is a given (coarse) subset of input parameters μ and ϵ^{CRE} is a prescribed error tolerance.

Essentially, (68) implies that the normalized residual of Eq. (58) is smaller than some prescribed tolerance over a given (coarse) subset of the parameter domain $\mathcal{D}$. Thus if we prescribe some small values for ϵ^{CRE} (e.g., 1%, 5%), Eq. (60) and ultimately (56) will hold true. The `selectNtheta` function is described as follows

`selectNtheta`: $N^\theta = 1$;
While 1
• Check (68) $\forall \mu \in \Xi^{\text{st}}$;
If exist any μ not satisfied (68) and $N^\theta < N_{\max}^\theta$ **then**
$N^\theta \leftarrow N^\theta + 1$;
end if
If $N^\theta == N_{\max}^\theta$ or (68) is satisfied for all $\mu \in \Xi^{\text{st}}$ **then**
exit while loop;
end if
end while

In practice, N^θ takes the smallest possible value such that (68) is satisfied with all $\mu \in \Xi^{\text{st}}$. The iterative procedure starts with $N^\theta = 1$ and keeps increasing to $N_{\max}^\theta$ whenever there exists any μ not satisfied (68). Otherwise, the procedure stops at one specific value of $N^\theta \left(1 \leq N^\theta \leq N_{\max}^\theta\right)$ if all $\mu \in \Xi^{\text{st}}$ satisfy (68). This is a simple yet effective criterion to choose *appropriately* N^θ such that the approximation sign "$\approx$" in (56) is as close to the equal sign "$=$" as possible. We use the following notation to denote this algorithm: $N^\theta = \texttt{selectNtheta}\left(\epsilon^{\text{CRE}}, \Xi^{\text{st}}, \mathcal{Z}_{N^u}, \widetilde{\mathcal{Z}}_{N^\sigma}\right)$.

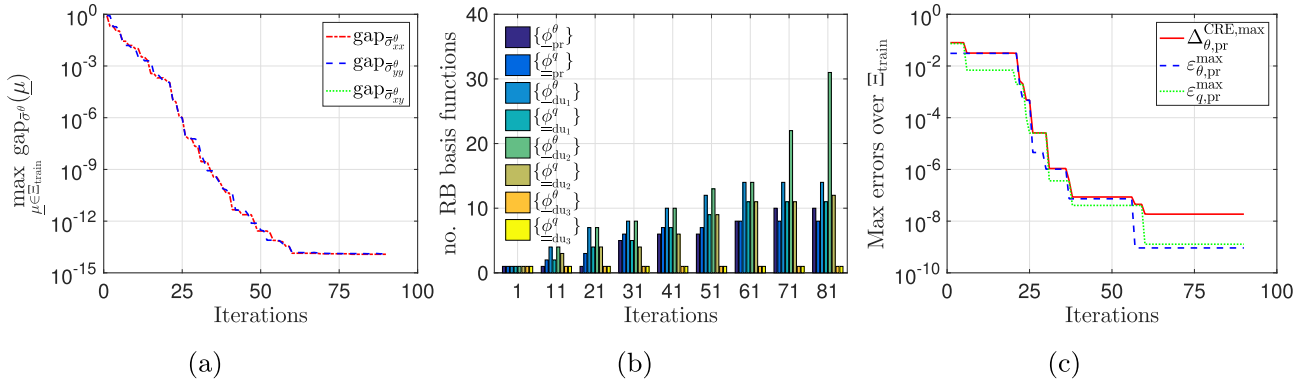

Fig. 4. (a) Maximum of $\texttt{gap}_{\overline{\sigma}^\theta}$, (b) number of RB basis functions, and (c) maximum of CRE error $\Delta_\theta^{CRE,\max}$, temperature RB error $\epsilon_\theta^{\max}$ and flux RB error $\epsilon_q^{\max}$ over Ξ_{train} as functions of GO-greedy iterations.

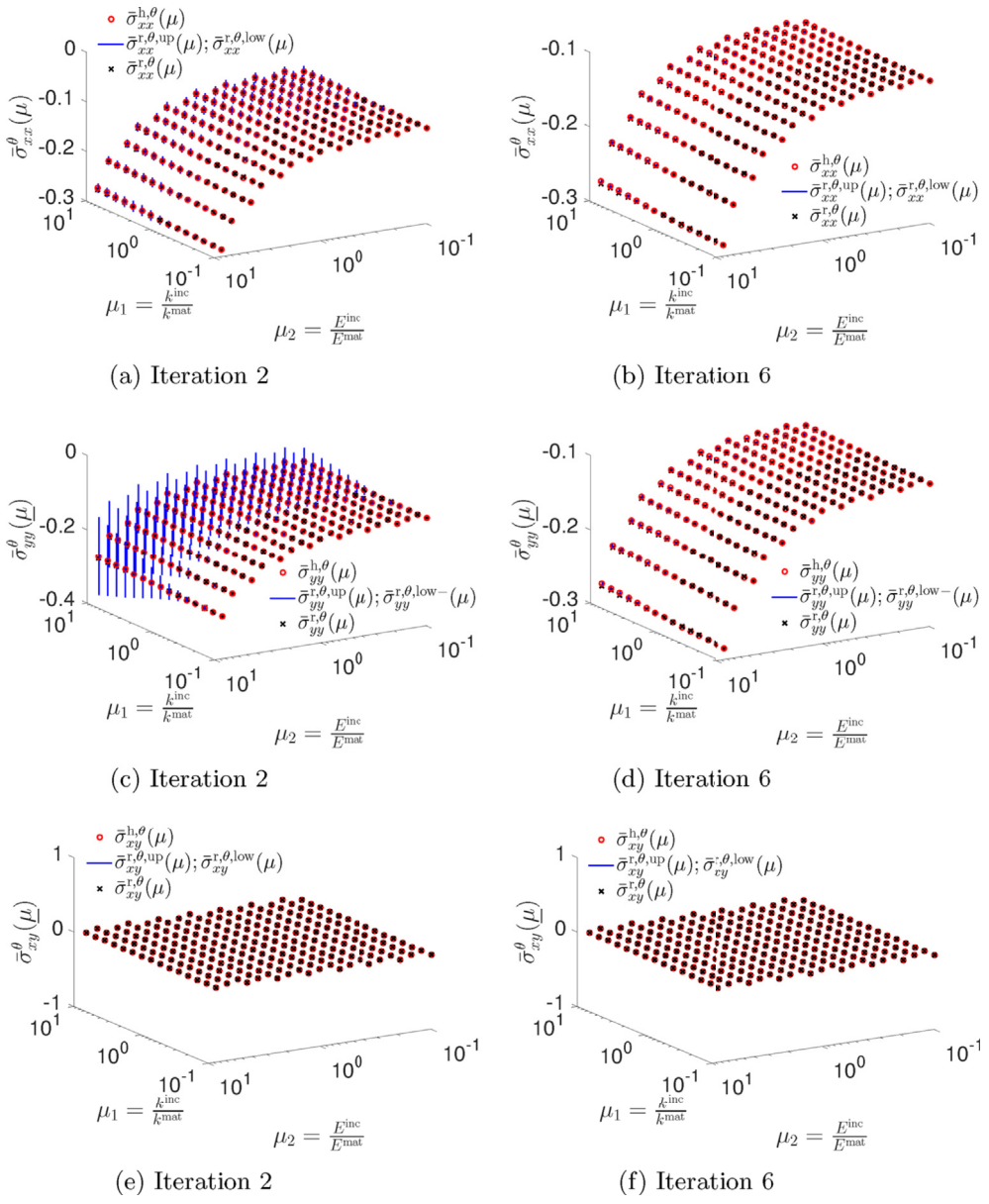

Fig. 5. Virtual charts of 3 QoIs: $\overline{\sigma}^{\theta}_{xx}(\mu)$ (first row), $\overline{\sigma}^{\theta}_{yy}(\mu)$ (second row) and $\overline{\sigma}^{\theta}_{xy}(\mu)$ (third row) with respect to the variations of material heterogeneity at various Greedy iterations for thermal equation.

Remark 3.3.

1. *From* section 3.2.3, *we see that* (60) *(and hence the approximation* (56)*) is violated when the magnitude of* $\|e_u(\mu)\|_{D(\mu)}$ *and* $\|e_\sigma(\mu)\|_{C(\mu)}$ *are close to that of* $\|e_\theta(\mu)\|_{D(\mu)}$. *In other words, the value of the CRE estimator* (56) *is limited by the value of* $\|e_\theta(\mu)\|_{D(\mu)}$ *and ultimately by* ϵ^{CRE}.
2. *In general, due to the way we solve the coupled thermoelasticity problem, i.e., solve the heat equation first and then pass the approximated RB temperature field to the elastic equation to solve for the displacement field, the ROM approximation accuracy of the elastic equation could not be better than that of the heat equation. This is the key point of this proposed work.*
3. *There is a situation in which all* μ *points in* Ξ^{st} *do not validate the criterion* (68) *for a given* ϵ^{CRE}. *In this case,* N^θ *is simply set to* $N^\theta_{\max}$ *as this is the best possible value of* N^θ. *We note that the CRE estimator* $(\Delta^{\text{CRE}}(\mu))$ *becomes an error approximation for both* $\|e_u(\mu)\|_{D(\mu)}$ *and* $\|e_\sigma(\mu)\|_{C(\mu)}$ *rather than a strict upper bound as before. Hence, it may approximate even better these two true errors.*

4. Upper and lower bounds of the effective coefficient of thermal expansion

The FE effective coefficient of thermal expansion (CTE) can be computed numerically as [46].

$$\alpha^{\text{h,eff}}(\mu) = -\frac{1}{\Delta T} C^{\text{h,eff}}(\mu)\langle\sigma^{\text{h}}(\mu)\rangle, \tag{69}$$

where $C^{\text{h,eff}}(\mu) = D^{\text{h,eff}}(\mu)^{-1}$ is the FE effective compliance tensor, and $\langle\sigma^{\text{h}}(\mu)\rangle = \frac{1}{|\Omega|}\int_\Omega \sigma^{\text{h}}(\mu)d\Omega$ is the FE average stress. Here, the components of $\langle\sigma^{\text{h}}(\mu)\rangle$ can be computed as follows: for a 2D problem, $1 \le i,j \le 2$,

$$Q^{\text{h}}_{ij}(\mu) = \Sigma_{ij}\langle\sigma^{\text{h}}(\mu)\rangle = \frac{1}{|\Omega|}\int_\Omega \Sigma_{ij} : \sigma^{\text{h}}(\mu)\, d\Omega$$

$$= \frac{1}{|\Omega|}\int_\Omega \Sigma_{ij} : D(\mu) : \epsilon\left(u^{\text{h}}(\mu)\right) d\Omega$$

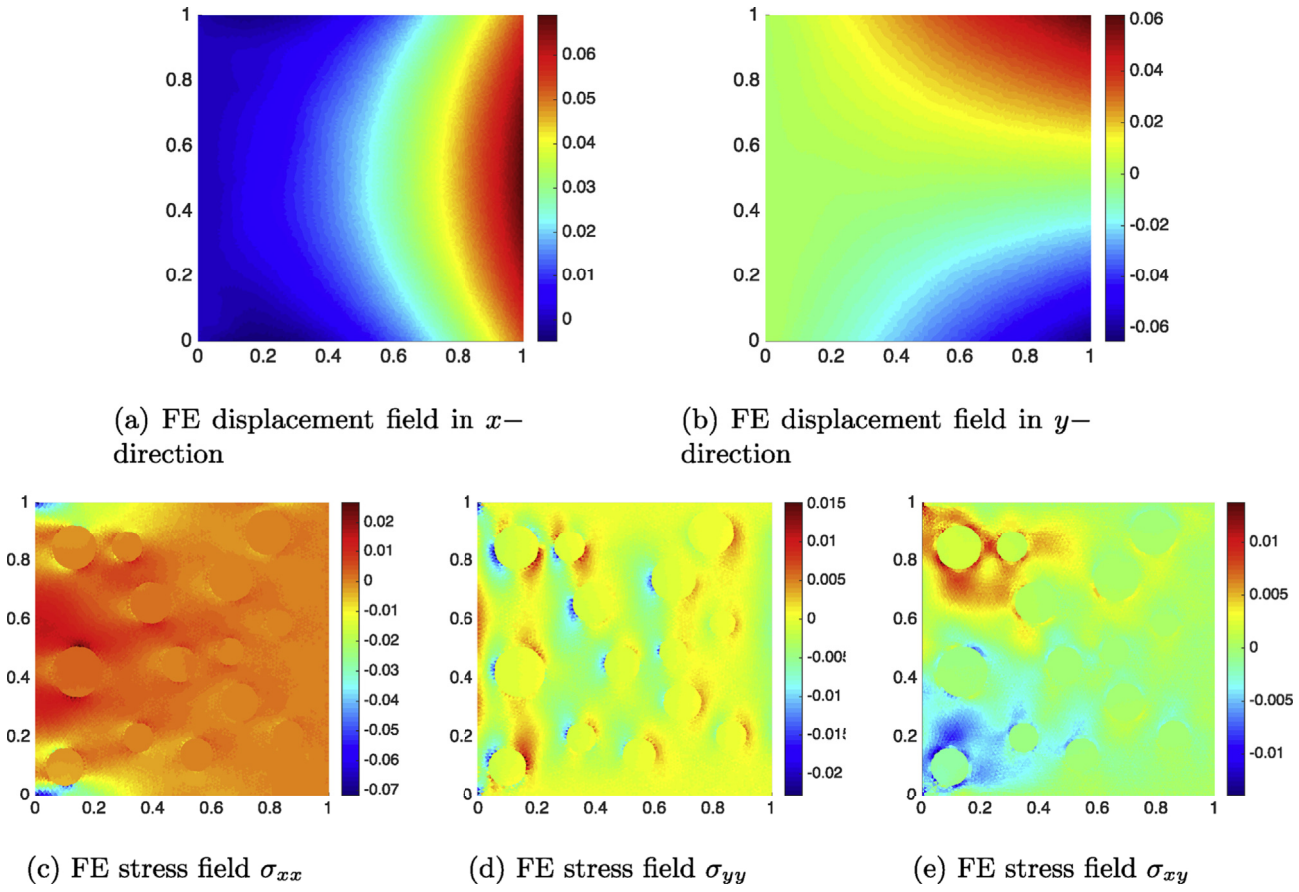

(a) FE displacement field in $x-$ direction

(b) FE displacement field in $y-$ direction

(c) FE stress field σ_{xx}

(d) FE stress field σ_{yy}

(e) FE stress field σ_{xy}

Fig. 6. Solution visualization with $\mu^{\text{test}} = (10, 0.1)$.

$$-\frac{1}{|\Omega|}\int_{\Omega} \Sigma_{ij} : D(\mu) : \epsilon_0\left(\theta^{\text{h}}(\mu)\right) d\Omega = Q_{ij}^{\text{h},u}(\mu) + Q_{ij}^{\text{h},\theta}(\mu), \tag{70}$$

which is one specific FE QoI as defined in (16).

The RB approximation for the effective CTE is

$$\alpha^{\text{r,eff}}(\mu) = -\frac{1}{\Delta T} C^{\text{r,eff}}(\mu)\langle\sigma^{\text{r}}(\mu)\rangle, \tag{71}$$

where $C^{\text{r,eff}}(\mu) = D^{\text{r,eff}}(\mu)^{-1}$ can be computed very efficiently from our previous work [26], and $\langle\sigma^{\text{r}}(\mu)\rangle$ is a vector of several RB QoI as defined in (21) and (42).

Since each ij-component of the term $\langle\sigma^{\text{h}}(\mu)\rangle = \overline{\sigma}_{ij}^{\text{h}}(\mu)$ is one specific FE QoI, it can be bounded from above and below as

$$\overline{\sigma}_{ij}^{\text{r,low}}(\mu) \le \overline{\sigma}_{ij}^{\text{h}}(\mu) \le \overline{\sigma}_{ij}^{\text{r,up}}(\mu), \tag{72}$$

where

$$\begin{cases} \overline{\sigma}_{ij}^{\text{r,low}}(\mu) = Q_{ij}^{\text{r},u,\text{low}}(\mu) + Q_{ij}^{\text{r},\theta,\text{low}}(\mu) \\ \overline{\sigma}_{ij}^{\text{r,up}}(\mu) = Q_{ij}^{\text{r},u,\text{up}}(\mu) + Q_{ij}^{\text{r},\theta,\text{up}}(\mu) \end{cases}, \quad 1 \le i,j \le 2,$$

from (35) and (67).

Now, if we can approximate sufficiently well $C^{\text{h,eff}}(\mu) \approx C^{\text{r,eff}}(\mu) = c_{ij}^{\text{r}}(\mu)$ (thanks to the computations of $G^{\text{eff}}(\mu)$ and $\lambda^{\text{eff}}(\mu)$ from our previous work [26]) and define

$$\begin{cases} Q_{ij}^{\text{r,up}}(\mu) = \max\left\{-\frac{c_{ij}^{\text{r}}(\mu)}{\Delta T}\overline{\sigma}_{ij}^{\text{r,low}}(\mu), -\frac{c_{ij}^{\text{r}}(\mu)}{\Delta T}\overline{\sigma}_{ij}^{\text{r,up}}(\mu)\right\} \\ Q_{ij}^{\text{r,low}}(\mu) = \min\left\{-\frac{c_{ij}^{\text{r}}(\mu)}{\Delta T}\overline{\sigma}_{ij}^{\text{r,low}}(\mu), -\frac{c_{ij}^{\text{r}}(\mu)}{\Delta T}\overline{\sigma}_{ij}^{\text{r,up}}(\mu)\right\} \end{cases}, \tag{73}$$

we obtain the bounds for the k-component of the FE effective CTE as

$$\boxed{Q_{ij}^{\text{r,low}}(\mu) \le \alpha_k^{\text{h,eff}}(\mu) \le Q_{ij}^{\text{r,up}}(\mu),} \quad 1 \le k \le \frac{d(d+1)}{2}, \tag{74}$$

where the indices are $(i,j,k) = (1,1,1)$, $(1,2,2)$ and $(2,2,3)$, respectively.

Note that the key point of this derivation is that we need to approximate sufficiently well $C^{\text{h,eff}}(\mu) \approx C^{\text{r,eff}}(\mu)$ (i.e., this associated error reaches machine errors) such that the error $\left(\alpha^{\text{h,eff}}(\mu) - \alpha^{\text{r,eff}}(\mu)\right)$ now depends *only* on $\left(\langle\sigma^{\text{h}}(\mu)\rangle - \langle\sigma^{\text{r}}(\mu)\rangle\right)$, not $\left(C^{\text{h,eff}}(\mu) - C^{\text{r,eff}}(\mu)\right)$.

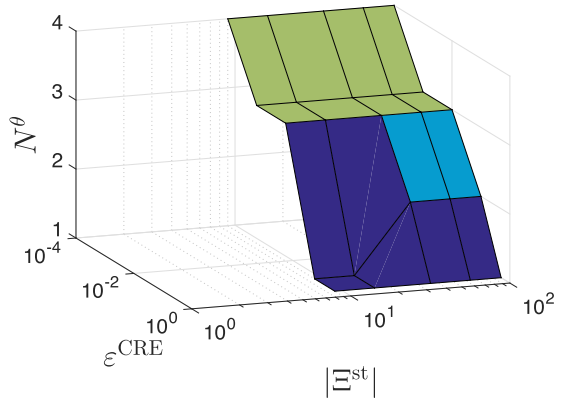

Fig. 7. Effects of the prescribed tolerance ϵ^{CRE} and the size $|\Xi^{\text{st}}|$ on the number of temperature RB basis functions N^θ using our proposed `selectNtheta` algorithm with fixed $\mathcal{Z}_2$ and $\widetilde{\mathcal{Z}}_2$.

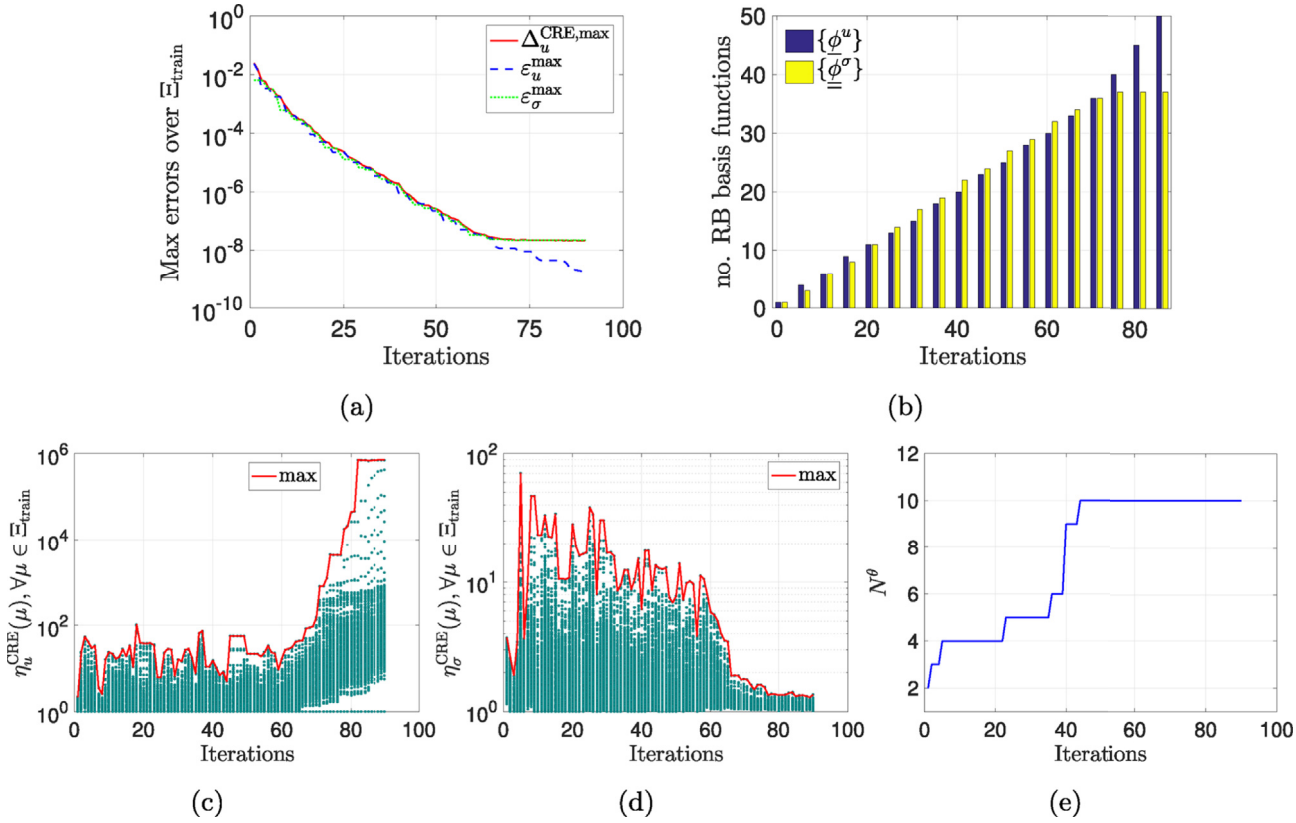

Fig. 8. (a) Maximum of CRE error $\Delta_u^{CRE,\max}$, displacement RB error $\epsilon_u^{\max}$ and stress RB error $\epsilon_\sigma^{\max}$ over Ξ_{train}, (b) sizes of sets $\mathcal{Z}_{N^u}$ and $\widetilde{\mathcal{Z}}_{N^\sigma}$, (c) displacement effectivity $\eta_u^{\text{CRE}}(\mu)$, (d) stress effectivity $\eta_\sigma^{\text{CRE}}(\mu)$, and (e) number of temperature RB basis functions N^θ as functions of TF-greedy iterations (setting $\epsilon^{\text{CRE}} = 0.01$ and $|\Xi^{\text{st}}| = 36$).

5. Numerical study

We apply the TF-RBM algorithm to the metamodelling of computational models of thermoelastic heterogeneous materials, under 2D plane strain assumption. The heterogeneous material of interest is made of two isotropic linear thermoelastic phases possessing distinct heat/elastic properties: circular inclusions and surrounding matrix. The positions and diameters of the inclusions are distributed randomly. The aim is to determine the so-called "overall" (or "effective") CTE as a function of some characteristics $\mu \in \mathcal{D}$ of the material heterogeneities. In other words, we build a virtual chart of the overall homogenized properties for the class of composite materials under investigation (see Fig. 1).

We consider a 2D statistical volume element (SVE) model under plane strain assumption in Fig. 2. The domain Ω is a unit square which is defined by $\Omega = [0,1] \times [0,1]$. The model is composed of two distinct material phases: the circular inclusions characterized by Young's modulus E^{inc} and thermal conductivity k^{inc}; and the surrounding matrix characterized by Young's modulus E^{mat} and thermal conductivity k^{mat}. Both phases are assumed to have elastic and isotropic behaviour. The random distribution of positions and diameters of the inclusions is performed via the package [47,48]. For the heat conduction problem, the Dirichlet boundary conditions include $\theta = 0$ and $\theta = 0.1$ on the left and right edges, and no heat source nor surface flux, respectively (see Fig. 2). For the elastic problem, there are no body force nor surface traction; and the left edge is fixed as a homogeneous Dirichlet boundary condition $u = 0$. In other words, the model deformation is caused only by thermal load. The SVE boundary value problems are parametrized by the material parameters $\mu = (\mu_1, \mu_2) = \left(\frac{k^{\text{inc}}}{k^{\text{mat}}}, \frac{E^{\text{inc}}}{E^{\text{mat}}}\right) \in \mathcal{D} \equiv [0.1, 10] \times [0.1, 10]$, where $E^{\text{mat}} = 1$ and the heat conductivity $k_{xx}^{\text{mat}} = k_{yy}^{\text{mat}} = 1$. The (very fine) FE mesh consists of 7693 nodes and 15114 linear triangular elements as shown in Fig. 2.

The ultimate goal is to build the virtual charts of the effective CTE as functions of thermal and elastic contrasts. As shown in (69), the computation of effective CTE invokes the computation of effective compliance tensor $C^{\text{h,eff}}(\mu)$ and the average stress tensor $\langle \sigma^{\text{h}}(\mu) \rangle$. The computation of average stress tensor which implements all the proposed theory in this paper will be detailed in section 5.1.

Regarding the computation of effective compliance tensor, $C^{\text{h,eff}}(\mu) = D^{\text{h,eff}}(\mu)^{-1}$, where $D^{\text{h,eff}}(\mu)$ is the effective stiffness tensor which can be found via two effective Lamé constants $E^{\text{h,eff}}(\mu)$ and $\nu^{\text{h,eff}}(\mu)$ (or $\lambda^{\text{h,eff}}(\mu)$ and $G^{\text{h,eff}}(\mu)$), respectively. Following [46] (Eq. (26)), $D^{\text{h,eff}}(\mu)$ is calculated at the reference temperature θ^{ref}, thus taking into account only the *elastic* effects and ignoring the *thermal* ones. Consequently, considering only the elastic equation with the elastic contrast (μ_2) as the only input parameter is sufficient to calculate $D^{\text{h,eff}}(\mu)$. For convenience and compatibility, we adopt the approach in our previous work [26] to compute these effective Lamé constants and ultimately the effective compliance tensor $C^{\text{h,eff}}(\mu)$. This part is detailed in section 5.2.

5.1. Computation of average stress tensor

The "truth" FE SVE problems read: find $\theta^{\text{h,0}}(\mu) \in \Theta^{\text{h,0}}(\Omega)$ and $u^{\text{h,0}}(\mu) \in \mathcal{U}^{\text{h,0}}(\Omega)$ such that

$$\int_\Omega k(\mu) \cdot \nabla \theta^{\text{h,0}}(\mu) \cdot v_1 \, d\Omega = -\int_\Omega k(\mu) \cdot \nabla \theta^{\text{h,p}}(\mu) \cdot v_1 \, d\Omega, \quad \forall v_1 \in \Theta^{\text{h,0}}(\Omega), \tag{75a}$$

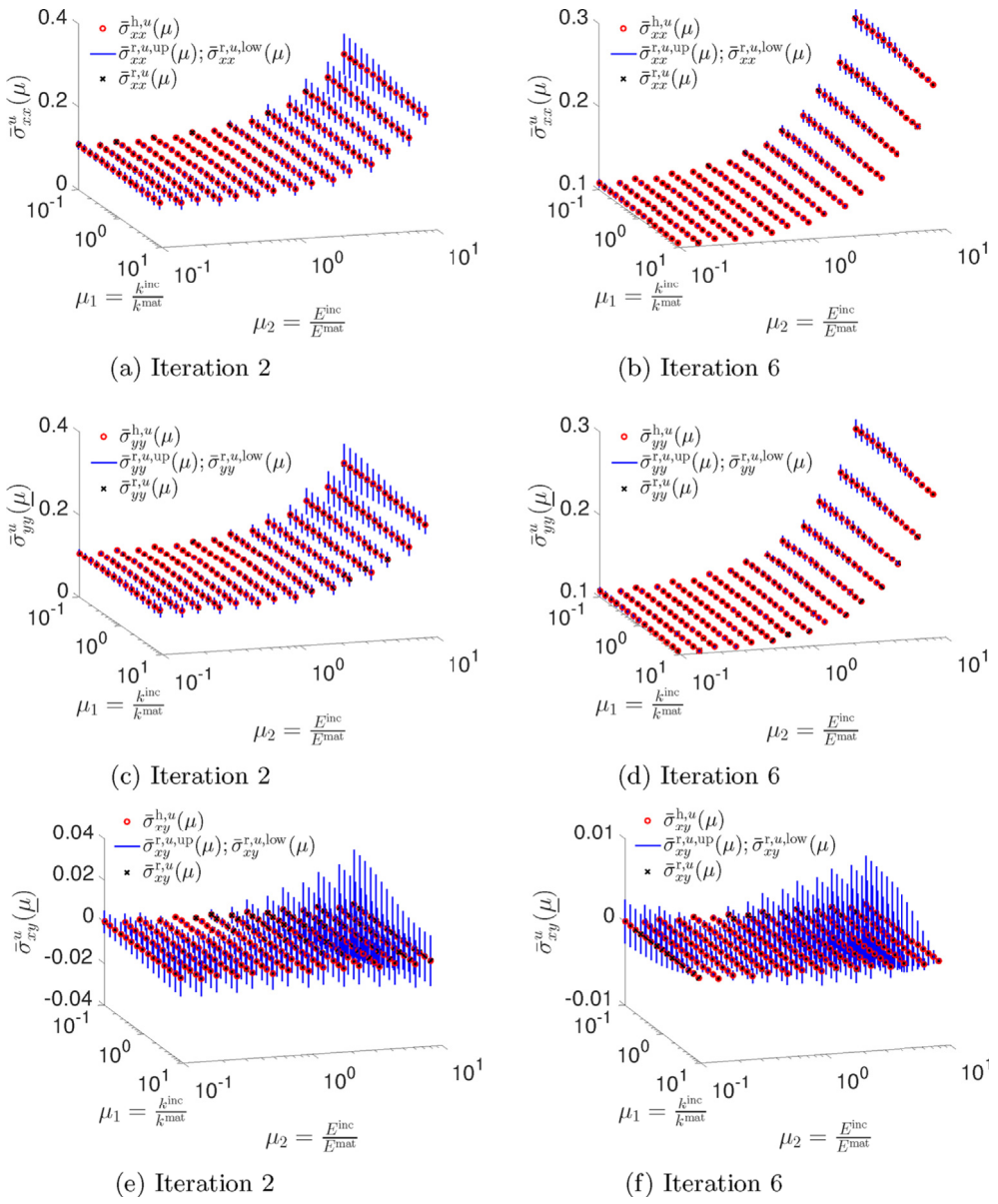

Fig. 9. Virtual charts of 3 QoIs: $\overline{\sigma}^{u}_{xx}(\mu)$ (first row), $\overline{\sigma}^{u}_{yy}(\mu)$ (second row) and $\overline{\sigma}^{u}_{xy}(\mu)$ (third row) with respect to the variations of material heterogeneity at various Greedy iterations for thermal equation.

$$
\begin{aligned}
&\int_\Omega \epsilon\left(u^{\mathrm{h},0}(\mu)\right) : D(\mu) : \epsilon\left(v_2\right)\, d\Omega \\
&= \int_\Omega \epsilon_0\left(\theta^{\mathrm{h}}(\mu)\right) : D(\mu) : \epsilon\left(v_2\right)\, d\Omega, \quad \forall v_2 \in \mathcal{V}^{\mathrm{h},0}(\Omega), \\
&= \int_\Omega \epsilon_0\left(\theta^{\mathrm{h},0}(\mu)\right) : D(\mu) : \epsilon\left(v_2\right)\, d\Omega \\
&\quad + \int_\Omega \epsilon_0\left(\theta^{\mathrm{h,p}}(\mu)\right) : D(\mu) : \epsilon\left(v_2\right)\, d\Omega,
\end{aligned} \tag{75b}
$$

where $\theta^{\mathrm{h,p}}(x,\mu) = 0.1, \forall \mu \in D, x \in \Gamma^{\theta}$ and $u^{\mathrm{h,p}}(\mu) = 0$ are known temperature/displacement fields as described above; $\theta^{\mathrm{h},0}(\mu)$ and $u^{\mathrm{h},0}(\mu)$ are the unknown temperature/displacement fields which will be approximated using RB method.

The computation of effective CTE will need all components of the average stress, i.e., $\langle \sigma^{\mathrm{h}}(\mu)\rangle = \overline{\sigma}^{\mathrm{h}}_{k}(\mu), 1 \le k \le \frac{d(d+1)}{2} = 3$ with $d = 2$ for our specific problem. Therefore, three QoIs from $\langle \sigma^{\mathrm{h}}(\mu)\rangle$ include $Q^{\mathrm{h}}_{xx}(\mu)$, $Q^{\mathrm{h}}_{yy}(\mu)$ and $Q^{\mathrm{h}}_{xy}(\mu)$ defined as

$$
\begin{aligned}
Q^{\mathrm{h}}_{ij}(\mu) &= \Sigma_{ij}\langle \sigma^{\mathrm{h}}(\mu)\rangle = \frac{1}{|\Omega|}\int_\Omega \Sigma_{ij} : \sigma^{\mathrm{h}}(\mu)\, d\Omega \\
&= \frac{1}{|\Omega|}\int_\Omega \Sigma_{ij} : D(\mu) : \epsilon\left(u^{\mathrm{h}}(\mu)\right) d\Omega \\
&\quad - \frac{1}{|\Omega|}\int_\Omega \Sigma_{ij} : D(\mu) : \epsilon_0\left(\theta^{\mathrm{h}}(\mu)\right) d\Omega \\
&= \overline{\sigma}^{\mathrm{h},u}_{ij}(\mu) + \overline{\sigma}^{\mathrm{h},\theta}_{ij}(\mu), \\
&= Q^{\mathrm{h},u}_{ij}(\mu) + Q^{\mathrm{h},\theta}_{ij}(\mu), \quad 1 \le i,j \le 2,
\end{aligned} \tag{76}
$$

where $\Sigma_{xx} = [0,0,1]^T$, $\Sigma_{yy} = [0,1,0]^T$ and $\Sigma_{xy} = [0,0,1]^T$ are field extractors to compute the x-, y- and xy-components of $\langle \sigma^{\mathrm{h}}(\mu)\rangle$, respectively. Note also that all QoIs $\overline{\sigma}^{\mathrm{h},u}_{ij}(\mu)$ and $\overline{\sigma}^{\mathrm{h},\theta}_{ij}(\mu)$ are noncompliant outputs, respectively.

The affine representation of heat conductivity and Hooke's elasticity tensor over the parameter domain reads

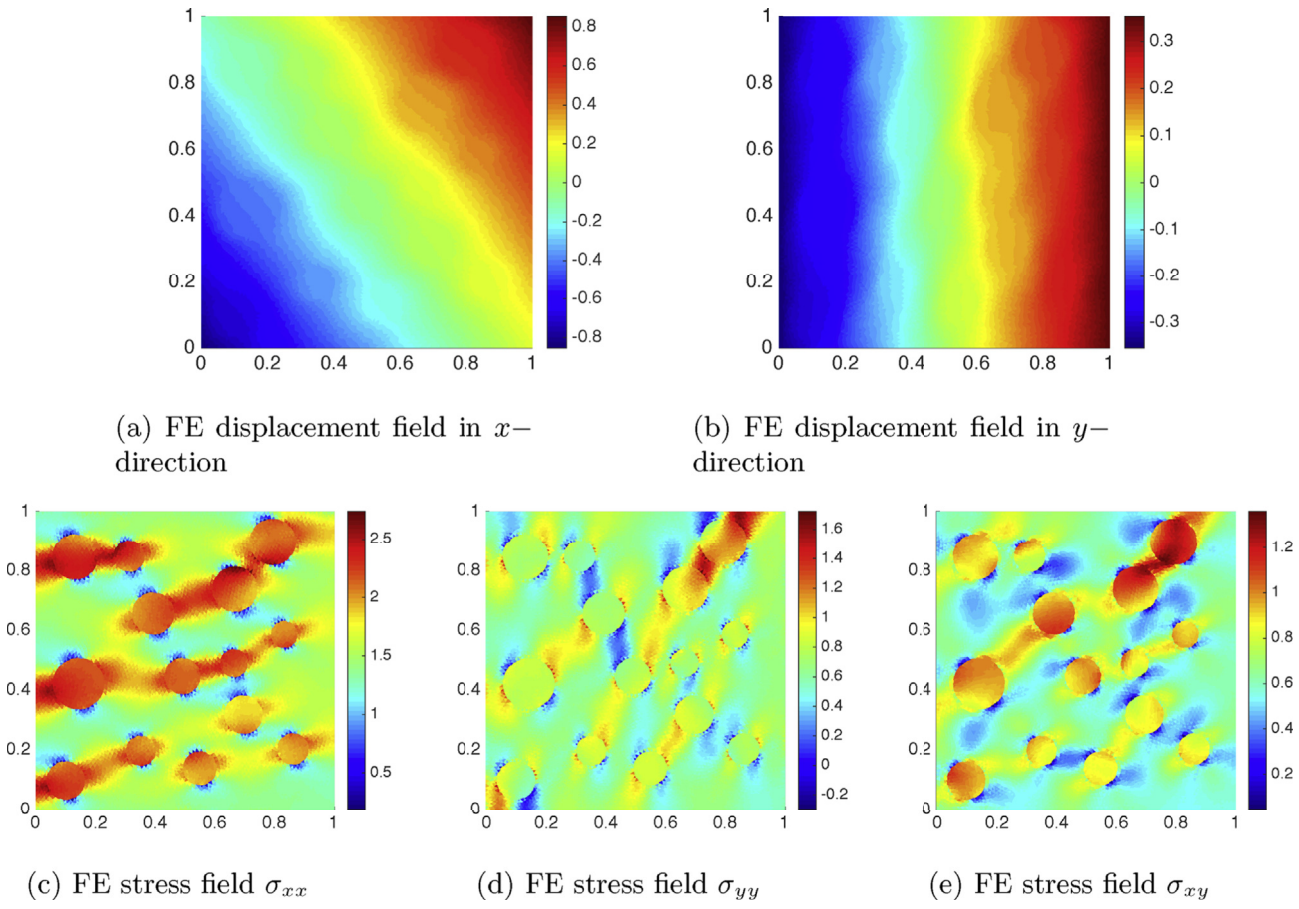

Fig. 10. Effective compliance tensor problem: solution visualization with $\mu^{\text{test}} = (10, 0.1)$.

$$
\begin{aligned}
k(x,\mu) &= k^{\text{mat}} + (\mu_1 - 1) H^{\text{inc}}(x) k^{\text{mat}}, \quad \forall \mu \in \mathcal{D}, x \in \Omega, \\
D(x,\mu) &= D^{\text{mat}} + (\mu_2 - 1) H^{\text{inc}}(x) D^{\text{mat}}, \quad \forall \mu \in \mathcal{D}, x \in \Omega.
\end{aligned} \tag{77}
$$

Here, $H^{\text{inc}}(x)$ is the indicator function of the inclusion phase. Namely, it is equal to 1 for a point located in an inclusion and 0 elsewhere. The tensors of the matrix phase k^{mat} and D^{mat} are defined by (4) and (5) with $k^{\text{mat}} = \begin{bmatrix} k_{xx}^{\text{mat}} & 0 \\ 0 & k_{yy}^{\text{mat}} \end{bmatrix}$, $k_{xx}^{\text{mat}} = k_{yy}^{\text{mat}} = 1$, $E^{\text{mat}} = 1$, $\nu^{\text{mat}} = \nu^{\text{inc}} = 0.3$, respectively.

The affine representation for the inverse of the above tensors over the parameter domain become

$$
\begin{aligned}
l(x,\mu) &= l^{\text{mat}} + \left(\frac{1}{\mu_1} - 1\right) H^{\text{inc}}(x)\, l^{\text{mat}}, \quad \forall \mu \in \mathcal{D}, x \in \Omega, \\
C(x,\mu) &= C^{\text{mat}} + \left(\frac{1}{\mu_2} - 1\right) H^{\text{inc}}(x)\, C^{\text{mat}}, \quad \forall \mu \in \mathcal{D}, x \in \Omega,
\end{aligned} \tag{78}
$$

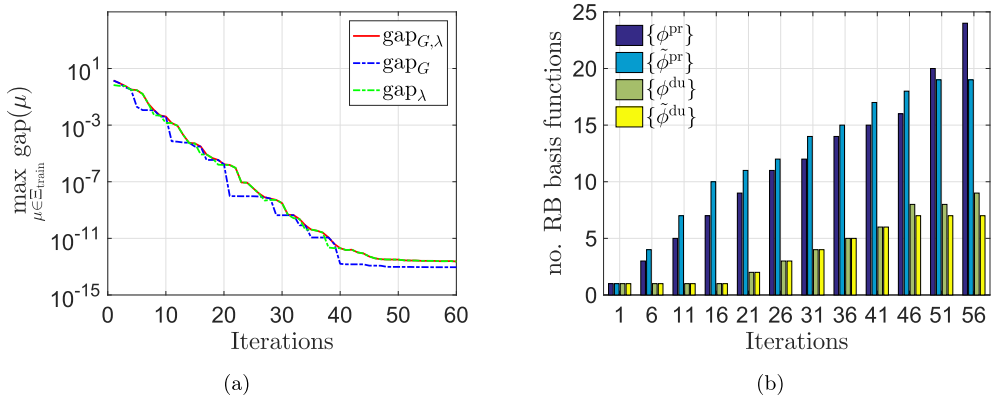

Fig. 11. Effective compliance tensor problem: (a) Maximum of $\texttt{gap}_{G,\lambda}$, $\texttt{gap}_G$ and $\texttt{gap}_\lambda$ over Ξ_{train}, and (b) sizes of the sets $\mathcal{Z}^{\text{pr}}$, $\tilde{\mathcal{Z}}^{\text{pr}}$, $\mathcal{Z}^{\text{du}}$ and $\tilde{\mathcal{Z}}^{\text{du}}$ as functions of GO-greedy iterations (only first 56 iterations are shown in (b)).

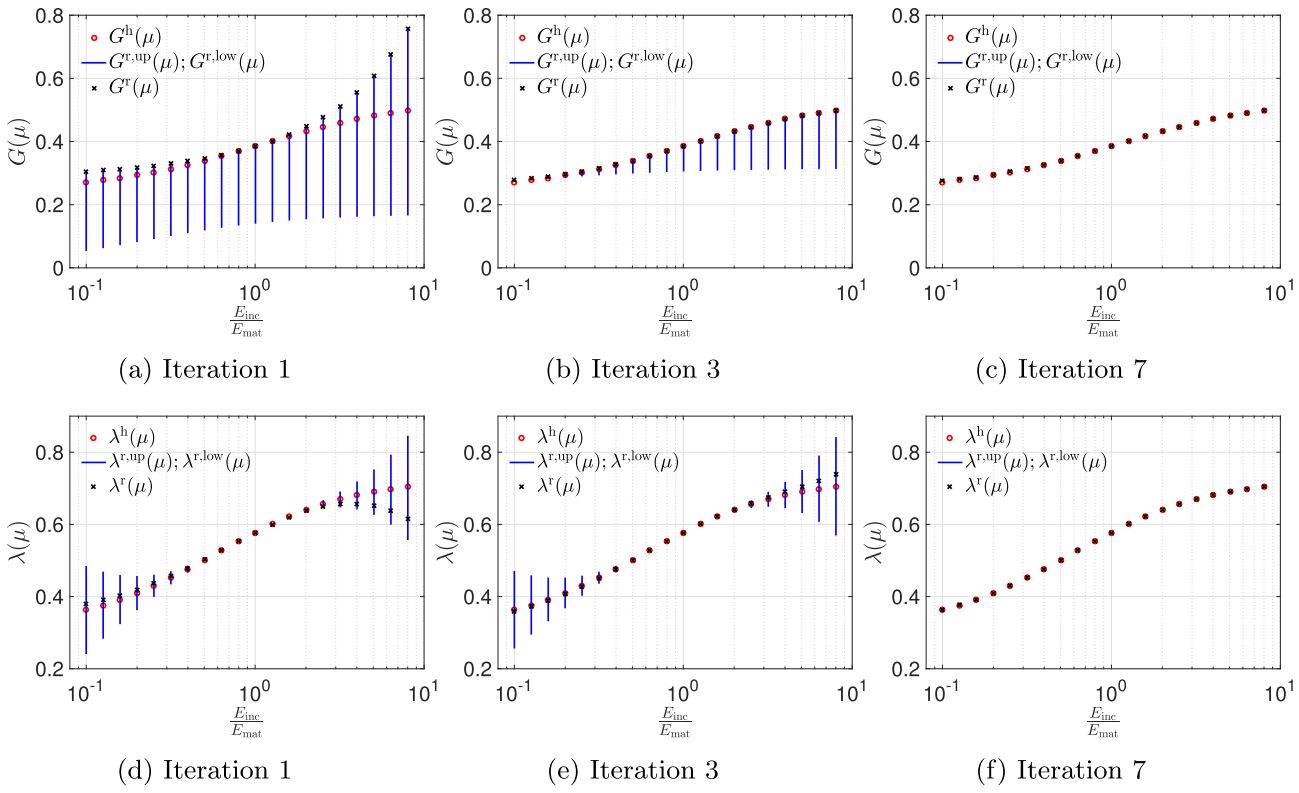

Fig. 12. Effective compliance tensor problem: Virtual charts of $G^{\text{eff}}(\mu)$ (first row) and $\lambda^{\text{eff}}(\mu)$ (second row) with respect to the variations of material heterogeneity after first 7 GO-greedy iterations.

where l^{mat} and C^{mat} are the heat and elastic compliance tensors of the matrix phase.

In order to implement all sampling strategies (described in section 5 of [26], section 3.1.5 and section 3.2.5), we first create the training sample set Ξ_{train}. In particular, the parameter domain $D \equiv [0.1, 10] \times [0.1, 10]$ is divided by a logarithmically equidistant distribution along two axes μ_1 and μ_2 with 900 $(= 30 \times 30)$ sample "points" $\mu = (\mu_1, \mu_2)$.

In the following, the treatment of heat Eq. (75a) and associated QoIs $\overline{\sigma}_{ij}^{\text{h},\theta}(\mu)$ in (76) is detailed in section 5.1.1; while that of elastic Eq. (75b) with QoIs $\overline{\sigma}_{ij}^{\text{h},u}(\mu)$ in Eq. (76) is described in section 5.1.2, respectively.

5.1.1. FE and GO-RBM approximations for the heat equation

a) Here, we have three noncompliant QoIs $\overline{\sigma}_{xx}^{\text{h},\theta}(\mu)$, $\overline{\sigma}_{yy}^{\text{h},\theta}(\mu)$ and $\overline{\sigma}_{xy}^{\text{h},\theta}(\mu)$ with three corresponding dual problems. The primal problem has primal temperature and primal flux fields, while each dual problem will also have its own dual temperature and dual flux fields. Thus, there are totally eight sets of RB basis vectors that need to be built. For reference, the FE primal temperature and FE primal flux fields are shown in Fig. 3.

b) We implement the GO-greedy sampling strategy (section 3.1.5 and section 5.2 of [26]) to build simultaneously these eight sets. The convergent results are shown in Fig. 4. We show the maximum of three uncertainty gaps $\texttt{gap}^{\max}_{\overline{\sigma}^{\theta}_{xx}}$, $\texttt{gap}^{\max}_{\overline{\sigma}^{\theta}_{yy}}$ and $\texttt{gap}^{\max}_{\overline{\sigma}^{\theta}_{xy}}$ and the evolution of the temperature and flux reduced basis functions in Fig. 4a and b, respectively. In Fig. 4c, we show the value of the maximum of primal CRE $\Delta^{\text{CRE,max}}_{\theta,\text{pr}} = \max_{\mu\in\Xi_{\text{train}}} \Delta^{\text{CRE}}_{\theta,\text{pr}}(\mu)$, the primal temperature error $\epsilon^{\max}_{\theta,\text{pr}} = \max_{\mu\in\Xi_{\text{train}}} \|e_{\theta,\text{pr}}(\mu)\|_{k(\mu)}$ and primal flux error $\epsilon^{\max}_{q,\text{pr}} = \max_{\mu\in\Xi_{\text{train}}} \|e_{q,\text{pr}}(\mu)\|_{l(\mu)}$ over Ξ_{train} as a function of the greedy iteration number.

The GO-RBM algorithm converges both in QoI gaps and solution errors in energy norms. Due to the way of excitation via Dirichlet boundary conditions for our particular problem, the xy-component of QoIs are zeros, i.e., $\overline{\sigma}_{xy}^{\text{h},\theta}(\mu) = \overline{\sigma}_{xy}^{\text{h},u}(\mu) = 0$. This is reflected in Fig. 4a and b, where $\texttt{gap}^{\max}_{\overline{\sigma}^{\theta}_{xy}} = 0$; $\{\phi^{\theta}_{\text{du}_3}\}$, $\{\phi^{q}_{\text{du}_3}\}$ each has only one "initial" RB basis vector during the whole Greedy algorithm. Lastly, Fig. 4b and c show that the maximum number of RB basis functions for temperature field will be $N^{\theta,\text{pr}}_{\max} = 10$ at greedy iterations 60–80. These information will be used in the TF-RBM approximation of the elastic equation afterwards.

c) Finally, we show the virtual charts of 3 QoIs $\overline{\sigma}^{\theta}_{ij}(\mu), 1 \le i,j \le 2$ as functions of material heterogeneity at various Greedy iterations on Fig. 5.

5.1.2. FE and TF-RBM approximations for the elastic equation

a) With the available results from section 5.1.1, we now proceed to approximate the elastic equation with three QoIs $\overline{\sigma}_{xx}^{\text{h},u}(\mu)$, $\overline{\sigma}_{yy}^{\text{h},u}(\mu)$ and $\overline{\sigma}_{xy}^{\text{h},u}(\mu)$. Note that there is no dual problem to solve as explained in section 3.2.4. For reference, the FE primal displacement and FE primal stress fields are shown in Fig. 6.

b) Regarding the proposed algorithm `selectNtheta` described in section 3.2.5, there are two control parameters which are a prescribed tolerance ϵ^{CRE} and a coarse discretized subset Ξ^{st} of D. The effects of these two parameters on N^{θ} is investigated parametrically as follows. In particular, we fix $\mathcal{Z}_2 = \{\phi^{u}_i, 1 \le i \le 2\}$, $\widetilde{\mathcal{Z}}_2 = \{\phi^{\sigma}_j, 1 \le j \le 2\}$ and let $\epsilon^{\text{CRE}} \in \{0.5, 0.1, 0.01, 0.001, 0.0001\}$ and $|\Xi^{\text{st}}| \in \{9, 16, 36, 64, 100\}$; then run `selectNtheta` algorithm to find N^{θ} corresponding with each pair of $(\epsilon^{\text{CRE}}, |\Xi^{\text{st}}|)$ in the above sets. The final result is shown in Fig. 7. We observe from Fig. 7 that N^{θ} is sensitive to the change of ϵ^{CRE} and less sensitive

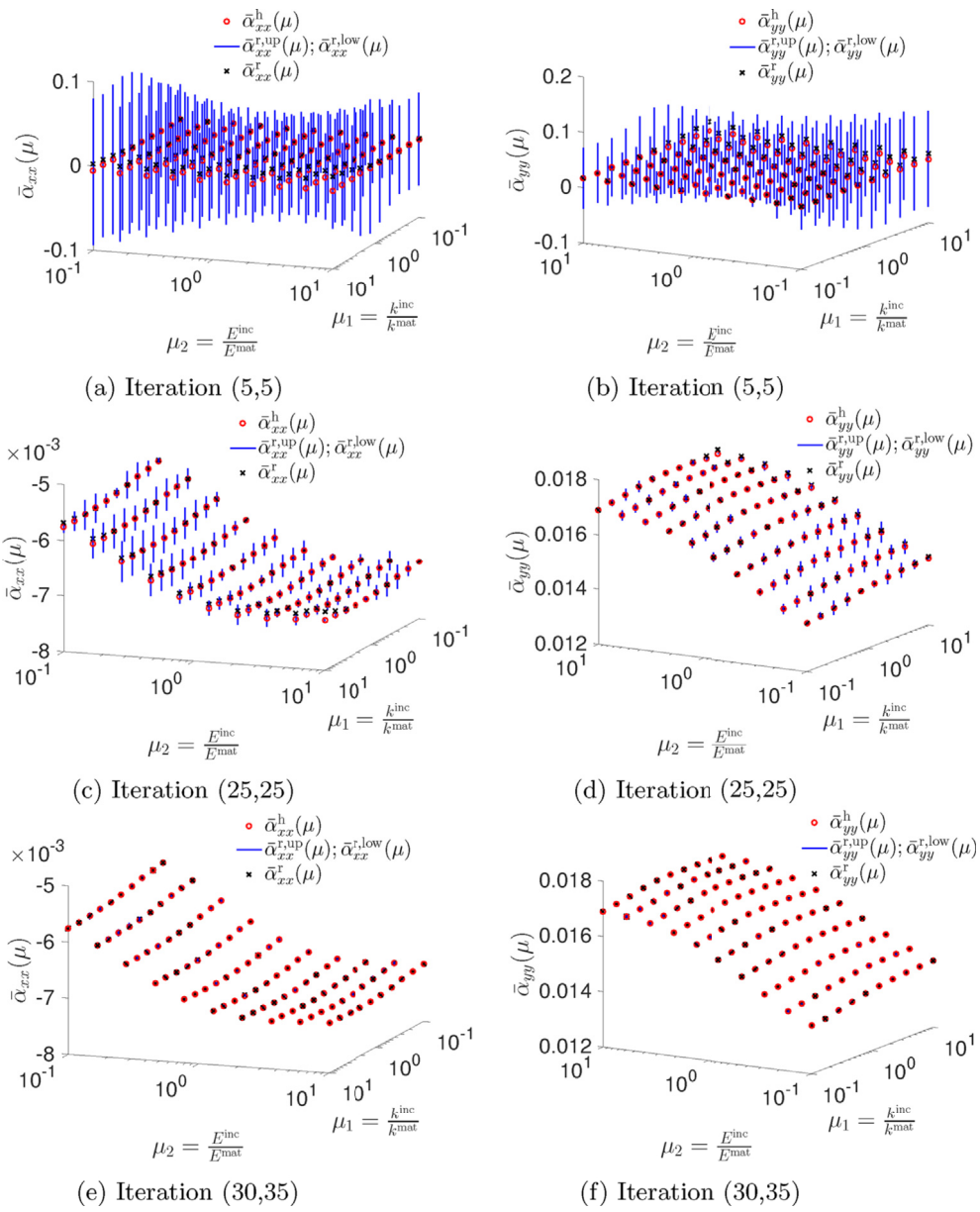

Fig. 13. Virtual charts of the *xx*-component (first column) and *yy*-component (second column) of effective CTE, $\overline{\alpha}_{xx}(\mu)$ and $\overline{\alpha}_{yy}(\mu)$, with respect to the variations of material heterogeneity at various combinations of the number of Greedy iterations for thermal and elastic equations.

to that of $|\Xi^{\text{st}}|$. The general rule would be: N^{θ} will increase with a decrease in ϵ^{CRE} and vice versa; and N^{θ} might be less sensitive to $|\Xi^{\text{st}}|$. This is reasonable as we need more temperature RB basis functions to make the approximation sign in (56) closer to the equal sign.

c) From the above analysis, we use the "modest" setting $(\epsilon^{\text{CRE}}, |\Xi^{\text{st}}|) = (0.01, 36)$ to implement the two-field greedy algorithm. The convergent results are presented in Fig. 8. Fig. 8a shows the maximum values of CRE $\Delta_u^{\text{CRE,max}} = \max_{\mu\in\Xi_{\text{train}}} \Delta_u^{\text{CRE}}(\mu)$, the displacement error $\epsilon_u^{\text{max}} = \max_{\mu\in\Xi_{\text{train}}} \|e_u(\mu)\|_{D(\mu)}$ and stress error $\epsilon_\sigma^{\text{max}} = \max_{\mu\in\Xi_{\text{train}}} \|e_\sigma(\mu)\|_{C(\mu)}$ over Ξ_{train} as a function of the greedy iteration number. Fig. 8b shows the evolution of the displacement/stress reduced basis; Fig. 8c and d report all displacement and stress effectivities for all $\mu \in \Xi_{\text{train}}$; while 8e presents the history of number of temperature RB basis functions found by the `selectNtheta` algorithm as functions of the greedy iterations, respectively.

We observe that the TF-RBM converges well both in stress and displacement fields, and the `selectNtheta` algorithm did choose adaptively $N^{\theta,\text{pr}}$ for the CRE equality of the elastic equation (Fig. 8e). This is reflected clearly in Fig. 8c and d that our CRE upper bound is strict and rigorous.

d) Finally, we show the virtual charts of 3 QoIs $\overline{\sigma}_{ij}^{u}(\mu), 1 \le i,j \le 2$ as functions of material heterogeneity at various Greedy iterations in Fig. 9. We observe that the goal-oriented bounds derived in (67) indeed work very well (i.e., strictly upper/lower bounds). This is because the approximation sign in (56) is very close to the equal one thanks to the good performance of the proposed `selectNtheta` algorithm in c) above.

Table 1
Comparison of CPU-time for FE and RB[a] analyses of problem 2 ($t_{\text{FEM}} = 0.6501$sec).

Greedy iter. (thermal)	Greedy iter. (elastic)	$\max_{\mu\in\Xi_{\text{train}}} \frac{\lvert\overline{\sigma}^{\text{h}}_{xx}(\mu)-\overline{\sigma}^{\text{r}}_{xx}(\mu)\rvert}{\lvert\overline{\sigma}^{\text{h}}_{xx}(\mu)\rvert}$	Speedup = $\frac{t_{\text{FEM}}}{t_{\text{RB(online)}}}$
20	20	2.4124×10^{0}	247
25	25	2.1003×10^{-2}	242
28	28	6.3747×10^{-4}	241
30	30	2.0382×10^{-4}	241
40	38	1.7793×10^{-4}	240
60	40	5.2011×10^{-5}	232
60	50	1.4621×10^{-5}	229

[a] The number of Greedy iterations to evaluate the RB effective compliance tensor is fixed at 45.

5.2. Computation of the effective compliance tensor

5.2.1. FE approximations for effective compliance tensor

We now turn back to the computation of the effective compliance tensor $C^{\text{h,eff}}(\mu)$. The specific model problem is elaborated in Ref. [26] (section 6.1), here we recall briefly the main equations and results. The model problem as shown in Fig. 2 with the elastic contrast as the only parameter is considered. There are no body force nor surface traction–the only load applying to the model is via parametrized Dirichlet boundary conditions. The SVE boundary value problem is parametrized by the material parameters μ^{m} and the load parameters μ^{l} as: $\mu = (\mu^{\text{m}}, \mu^{\text{l}}) \equiv \left(\mu^{\text{m}}, \mu^{\text{l}}_1, \mu^{\text{l}}_2, \mu^{\text{l}}_3\right) \equiv (\mu_1, \mu_2, \mu_3, \mu_4)$. The material heterogeneities are only parametrized by the elastic contrast $\mu^{\text{m}} \equiv \mu_1 = \frac{E^{\text{inc}}}{E^{\text{mat}}}$. The load parameters μ^{l} are constituted by the independent components of the effective strain tensor ϵ^{M}, where $\epsilon^{\text{M}} \in \mathbb{R}^2\times\mathbb{R}^2$ and $\epsilon^{\text{M}} = \epsilon^{\text{M}^T}$. More precisely, we define $\mu^{\text{l}}_1 \equiv \mu_2 = \epsilon^{\text{M}}_{11}$, $\mu^{\text{l}}_2 \equiv \mu_3 = \epsilon^{\text{M}}_{22}$ and $\mu^{\text{l}}_3 \equiv \mu_4 = \epsilon^{\text{M}}_{12}$. The affine representation of the Dirichlet boundary conditions is thus defined as

$$
\begin{aligned}
w(x,\mu) &= \epsilon^{\text{M}}(\mu^{\text{l}})(x-\overline{x}) \\
&= \left(\begin{pmatrix}1 & 0\\ 0 & 0\end{pmatrix}\mu_2 + \begin{pmatrix}0 & 0\\ 0 & 1\end{pmatrix}\mu_3 + \begin{pmatrix}0 & 1\\ 1 & 0\end{pmatrix}\mu_4\right)(x-\overline{x}), \\
&\forall \mu \in \mathcal{D}, x \in \partial\Omega^{\text{w}},
\end{aligned}
\tag{79}
$$

with $\overline{x}$ being the barycenter of Ω (i.e., $\int_\Omega (x-\overline{x})\,d\Omega = 0$).

The "truth" FE SVE problem reads: find $u^{\text{h},0}(\mu) \in \mathcal{U}^{\text{h},0}(\Omega)$ such that

$$
\begin{aligned}
\int_\Omega \epsilon\left(u^{\text{h},0}(\mu)\right) : D(\mu) : \epsilon(v)\,d\Omega &= -\int_\Omega \epsilon\left(u^{\text{h,p}}(\mu)\right) : D(\mu) : \epsilon(v)\,d\Omega, \\
&= \widehat{f}(v), \quad \forall v \in \mathcal{U}^{\text{h},0}(\Omega),
\end{aligned}
\tag{80}
$$

where $u^{\text{h,p}}(x,\mu) = w(x,\mu), \forall \mu \in \mathcal{D}, x \in \partial\Omega^{\text{w}}$ is a known displacement field as described above, and $u^{\text{h},0}(\mu)$ is the unknown displacement field approximated using the RB method. The "truth" effective Lamé constants $G^{\text{M,h}}(\mu^{\text{m}}) \equiv G^{\text{h}}(\mu)$ and $\lambda^{\text{M,h}}(\mu^{\text{m}}) \equiv \lambda^{\text{h}}(\mu)$ are computed as (see Chapter 7 of [49])

$$
G^{\text{h}}(\mu) = \ell^G\left(u^{\text{h}}(\mu)\right) = \frac{1}{|\Omega|}\int_\Omega \Sigma_G : D(\mu) : \epsilon(u^{\text{h}}(\mu))\,d\Omega, \tag{81a}
$$

$$
\lambda^{\text{h}}(\mu) = \ell^\lambda\left(u^{\text{h}}(\mu)\right) = \frac{1}{|\Omega|}\int_\Omega \Sigma_\lambda : D(\mu) : \epsilon(u^{\text{h}}(\mu))\,d\Omega, \tag{81b}
$$

where Σ_G and Σ_λ are field extractors such that $\ell^G(v) = -\frac{1}{|\Omega|}\widehat{f}(v)$ and $\ell^\lambda(v) \neq \widehat{f}(v)$. Hence, $G^{\text{h}}(\mu)$ and $\lambda^{\text{h}}(\mu)$ are compliant and noncompliant outputs, respectively.

We now note that by solving {(80), (81)}, setting $\mu \equiv \mu^G = \left(\mu_1, 0, 0, \frac{1}{2}\right)$, $\Sigma_G = \begin{pmatrix}0 & \frac{1}{2}\\ \frac{1}{2} & 0\end{pmatrix}$ renders $G^{\text{h}}(\mu)$; while setting $\mu \equiv \mu^\lambda = \left(\mu_1, 1, 0, \frac{1}{\sqrt{2}}\right)$, $\Sigma_\lambda = \begin{pmatrix}1 & -\frac{1}{\sqrt{2}}\\ -\frac{1}{\sqrt{2}} & 0\end{pmatrix}$ renders $\lambda^{\text{h}}(\mu)$, respectively. Therefore, the only "actual" parameter of this problem is $\mu_1 = \frac{E^{\text{inc}}}{E^{\text{mat}}} \in \mathcal{D} \equiv [0.1, 10]$; and note that each μ_1 provides correspondingly one μ^G and one μ^λ as described above. The (very fine) FE mesh consists of 7693 nodes and 15114 linear triangular elements as shown in Fig. 2. The FE space to approximate the 2D homogenization problem is of dimension $\mathcal{N} = 14846$. The reference parameter used in this work is chosen as $\mu_0 = (1,0,0,0)$; $Q_a = 2$, $n_{\text{w}} = 3$, $n_{\text{c}} = 2$, and $\widetilde{n}_{\text{p}} = 0$ as there is no body force nor surface traction applied to the model (Note that the dual problem will have $\widetilde{n}_{\text{p}} \neq 0$ as there is an applied body force which comes from the primal output $\ell^\lambda(v)$.). We show the FE displacement field and the corresponding FE stress field in Fig. 10 with $\mu^{\lambda,\text{test}} = (5,1,0,\frac{1}{\sqrt{2}})$, respectively.

To implement the GO-greedy sampling strategy (section 5.2 of [26]), we first create the training sample set Ξ_{train}. In particular, the range $\mathcal{D} \equiv [0.1, 10]$ is divided by a logarithmically equidistant distribution with 500 sample points μ^{m}; and each μ^{m} provides correspondingly one μ^G and one μ^λ. Hence, the training sample set Ξ_{train} contains a total of 1000 sample parameter values which are 500 pairs (μ^G, μ^λ) logarithmically equidistant distributed.

5.2.2. RB approximations for effective compliance tensor

The QoI gaps of the homogenization problem are defined as

$$
\texttt{gap}_G \equiv \texttt{gap}(\mu^G) = \frac{2\left|G^{\text{r,up}}(\mu^G) - G^{\text{r,low}}(\mu^G)\right|}{\left|G^{\text{r,up}}(\mu^G)\right| + \left|G^{\text{r,low}}(\mu^G)\right|}, \tag{82a}
$$

$$
\texttt{gap}_\lambda \equiv \texttt{gap}(\mu^\lambda) = \frac{2\left|\lambda^{\text{r,up}}(\mu^\lambda) - \lambda^{\text{r,low}}(\mu^\lambda)\right|}{\left|\lambda^{\text{r,up}}(\mu^\lambda)\right| + \left|\lambda^{\text{r,low}}(\mu^\lambda)\right|}, \tag{82b}
$$

where $G^{\text{r,up}}(\mu)$, $G^{\text{r,low}}(\mu)$, $\lambda^{\text{r,up}}(\mu)$ and $\lambda^{\text{r,low}}(\mu)$ have the same roles as $Q^{\text{r,u,up}}(\mu)$ and $Q^{\text{r,u,low}}(\mu)$ in (67) for compliant and noncompliant QoIs, respectively. In addition, there is a dual equation associated with $\lambda^{\text{h}}(\mu)$, and no dual equation associated with $G^{\text{h}}(\mu)$ due to this reason.

We now implement the GO greedy sampling strategy (section 5.2 of [26]). The results are shown in Fig. 11. In particular, we present the maximum of gaps $\texttt{gap}^{\max}_{G,\lambda} = \max_{\mu\in\Xi_{\text{train}}}\{\texttt{gap}_G, \texttt{gap}_\lambda\}$ together with $\texttt{gap}^{\max}_G = \max_{\mu^G\in\Xi_{\text{train}}}\texttt{gap}_G$ and $\texttt{gap}^{\max}_\lambda = \max_{\mu^\lambda\in\Xi_{\text{train}}}\texttt{gap}_\lambda$ in Fig. 11a. In addition, Fig. 11b shows the sizes of $\mathcal{Z}^{\text{pr}}$, $\widetilde{\mathcal{Z}}^{\text{pr}}$, $\mathcal{Z}^{\text{du}}$ and $\widetilde{\mathcal{Z}}^{\text{du}}$ as functions of GO-greedy iterations (first 56 iterations), respectively. It is observed from Fig. 11a that the GO-greedy strategy converges in a goal-oriented manner: the strategy only enriches necessary RB basis functions (primal/dual displacement/stress) to minimize the QoI gaps. Fig. 11b shows that the primal displacement/stress RB basis functions are enriched more frequently than the dual ones. This is because $\mathcal{Z}^{\text{pr}}$

and $\widetilde{\mathcal{Z}}^{\mathrm{pr}}$ help to improve both gaps, i.e., $\{\mathtt{gap}_G, \mathtt{gap}_\lambda\}$; while $\mathcal{Z}^{\mathrm{du}}$ and $\widetilde{\mathcal{Z}}^{\mathrm{du}}$ contributes to the improvement of $\mathtt{gap}_\lambda$ only. Fig. 12 illustrates the virtual charts of $G^{\mathrm{eff}}(\mu)$ and $\lambda^{\mathrm{eff}}(\mu)$ as functions of the material heterogeneity $\mu^{\mathrm{m}} = \frac{E^{\mathrm{inc}}}{E^{\mathrm{mat}}}$ after first 7 GO-greedy iterations, respectively.

Finally, as we will use the ROM approximation $C^{\mathrm{h,eff}}(\mu) \approx C^{\mathrm{r,eff}}(\mu)$ in the computation of the bounds for the effective CTE (74), we will use the best possible approximation, i.e., with 45 iterations in Fig. 11a.

5.3. Computation of the effective CTE

Now all necessary ingredients are ready so that we can easily obtain the bounds for the effective CTE. Fig. 13 illustrates the virtual charts of the effective coefficients of thermal expansion in x- and y-directions, i.e., $\overline{\alpha}_{xx}(\mu)$ and $\overline{\alpha}_{yy}(\mu)$ as functions of material heterogeneity $\mu_1 = \frac{k^{\mathrm{inc}}}{k^{\mathrm{mat}}}$ and $\mu_2 = \frac{E^{\mathrm{inc}}}{E^{\mathrm{mat}}}$ using various combinations of the number of Greedy iterations of thermal and elastic equations, respectively. The bounds for $\overline{\alpha}^{\mathrm{h}}_{xx}(\mu)$ and $\overline{\alpha}^{\mathrm{h}}_{yy}(\mu)$ are derived in (74). We also note that the xy-component of the effective CTE, $\overline{\alpha}^{\mathrm{h}}_{xy}(\mu)$, is zero and hence is not shown here.

We report the "online" computational time for the computation $\mu \to \left\{\overline{\alpha}^{\mathrm{r}}_{xx}(\mu), \overline{\alpha}^{\mathrm{r,low/up}}_{xx}(\mu)\right\}$ and compare it with that of FE computation $\mu \to \overline{\alpha}^{\mathrm{h}}_{xx}(\mu)$. Notice that the yy-component is completely similar and hence we just use the xx-component as an illustration. Table 1 records the RB online computational time and associated maximum relative error for $\overline{\alpha}^{\mathrm{h}}_{xx}(\mu)$ over Ξ_{train} as a function of number of Greedy iterations for both thermal and elastic equations. The results show that we achieve the speedup of up to two orders of magnitude while still maintaining very high accuracy.

Finally, we comment on the convergence of the proposed greedy algorithm with the increase/decrease of number of particles for a given volume fraction of inclusions/matrix. In general, with an increasing/decreasing of number of particles, the Kolmogorov N-Width for the particular parametrized homogenization problem might increase/decrease correspondingly, the convergence rate of greedy algorithm thus might be slower/faster appropriately. This point was already mentioned in section 6.2.2 of [26]. However, the key point is that the greedy algorithm will eventually converge following the proof in Ref. [45].

6. Conclusion

A new reduced basis framework has been proposed for the metamodelling of parametrized one-way coupled thermoelasticity problems. While the CRE estimator for the thermal PDE is straightforward, that of the elastic PDE does not hold true due to the appearance of expansion terms. The first novel idea is to propose an adaptive algorithm to eliminate those terms, thus recover *approximately* the CRE equality for the elastic PDE. This CRE estimator is then used as an indication of accuracy of the ROM to (i) construct the projection spaces based on a greedy sampling of the parameter domain and (ii) certify the final ROM. The method requires the construction of separate ROMs for the primal (displacement) and flux (stress) fields. The second key idea is to extend this concept to the context of goal-oriented error estimation with many QoIs. The technique is applied to evaluate the effective CTE of heterogeneous composite materials. Numerical experiments show that the approach permits to construct ROMs that are directly certified in terms of input/output maps, and extremely efficient in terms of computational expense.

In our future work, we will develop more efficient sampling techniques to further reduce the computational cost while we can more strictly control the error from the ROM approximation. It can be done via developing more suitable objective function for the developed GO-greedy algorithm.

Appendix A. offline-online computational procedures for $\Delta^{\mathrm{CRE}}(\mu)$

We first expand (56) and noting the definition of $\|\cdot\|_{C(\mu)}$ (Proposition 3.2) as follows

$$\Delta^{\mathrm{CRE},u}_{N^u,N^\sigma,N^\theta}(\mu)^2 := \|\sigma^{\mathrm{r}}(\mu) - \widehat{\sigma}(\mu)\|^2_{C(\mu)} = \int_\Omega \left(\sigma^{\mathrm{r}}(\mu) - \widehat{\sigma}(\mu)\right) : C(\mu) : \left(\sigma^{\mathrm{r}}(\mu) - \widehat{\sigma}(\mu)\right) d\Omega = \int_\Omega \sigma^{\mathrm{r}}(\mu) : C(\mu) : \sigma^{\mathrm{r}}(\mu)\, d\Omega$$
$$+ \int_\Omega \widehat{\sigma}(\mu) : C(\mu) : \widehat{\sigma}(\mu)\, d\Omega - 2\int_\Omega \sigma^{\mathrm{r}}(\mu) : C(\mu) : \widehat{\sigma}(\mu)\, d\Omega = \mathbf{RR}(\mu) + \mathbf{HH}(\mu) - 2\mathbf{RH}(\mu). \tag{83}$$

Now, we expand $\sigma^{\mathrm{r}}(\mu)$ by using (5), (39) and (40) as

$$\sigma^{\mathrm{r}}(\mu) = D(\mu) : \epsilon\left(u^{\mathrm{r},0}(\mu) + u^{\mathrm{h,p}}(\mu)\right) - D(\mu) : \epsilon_0\left(\theta^{\mathrm{r},0}(\mu) + \theta^{\mathrm{h,p}}(\mu)\right)$$
$$= D(\mu) : \epsilon\left(\sum_{i=1}^{N^u} \alpha^u_i(\mu)\phi^u_i + \sum_{j=1}^{n^{u,\mathrm{w}}} \gamma^{u,\mathrm{w}}_j(\mu)\psi^u_j\right) - D(\mu) : \epsilon_0\left(\sum_{i=1}^{N^\theta} \alpha^\theta_i(\mu)\phi^\theta_i + \sum_{i=1}^{n^{\theta,\mathrm{w}}} \gamma^{\theta,\mathrm{w}}_i(\mu)\psi^\theta_i\right)$$
$$= D(\mu) : \epsilon\left(\sum_{i=1}^{N^u} \alpha^u_i(\mu)\phi^u_i\right) + D(\mu) : \epsilon\left(\sum_{j=1}^{n^{u,\mathrm{w}}} \gamma^{u,\mathrm{w}}_j(\mu)\psi^u_j\right) - D(\mu) : \epsilon_0\left(\sum_{i=1}^{N^\theta} \alpha^\theta_i(\mu)\phi^\theta_i\right) - D(\mu) : \epsilon_0\left(\sum_{i=1}^{n^{\theta,\mathrm{w}}} \gamma^{\theta,\mathrm{w}}_i(\mu)\psi^\theta_i\right)$$
$$= \mathbf{B}_1(\mu) + \mathbf{B}_2(\mu) - \mathbf{B}_3(\mu) - \mathbf{B}_4(\mu), \tag{84}$$

and $\widehat{\sigma}(\mu)$ by using (49) and (50) as

$$\widehat{\sigma}(\mu) = \sigma^{\mathrm{r},0}(\mu) + \sigma^{\mathrm{h,p}}(\mu) = \sum_{i=1}^{N^\sigma} \alpha^\sigma_i(\mu)\phi^\sigma_i + \sum_{j=1}^{\widetilde{n}_{\mathrm{p}}} \widetilde{\gamma}^{\mathrm{p}}_j(\mu)\sigma^{\mathrm{p}}_j = \mathbf{B}_5(\mu) + \mathbf{B}_6(\mu). \tag{85}$$

1. Using (84), the term $\mathbf{RR}(\mu)$ in (83) can be written as

$$\begin{aligned}\mathbf{RR}(\mu) &= \int_\Omega \sigma^{\mathrm{r}}(\mu) : C(\mu) : \sigma^{\mathrm{r}}(\mu)\, d\Omega \\ &= \int_\Omega \left(\mathbf{B}_1(\mu)+\mathbf{B}_2(\mu)-\mathbf{B}_3(\mu)-\mathbf{B}_4(\mu)\right) : C(\mu) : \left(\mathbf{B}_1(\mu)+\mathbf{B}_2(\mu)-\mathbf{B}_3(\mu)-\mathbf{B}_4(\mu)\right) d\Omega \\ &= \int_\Omega \mathbf{B}_1(\mu) : C(\mu) : \mathbf{B}_1(\mu)\, d\Omega + \int_\Omega \mathbf{B}_1(\mu) : C(\mu) : \mathbf{B}_2(\mu)\, d\Omega + \cdots + \int_\Omega \mathbf{B}_4(\mu) : C(\mu) : \mathbf{B}_4(\mu)\, d\Omega \\ &= \mathbf{RR}_{11}(\mu)+\mathbf{RR}_{12}(\mu)+\cdots+\mathbf{RR}_{44}(\mu) \\ &= \mathbf{RR}_{11}(\mu)+2\mathbf{RR}_{12}(\mu)-2\mathbf{RR}_{13}(\mu)-2\mathbf{RR}_{14}(\mu)+\mathbf{RR}_{22}(\mu)-2\mathbf{RR}_{23}(\mu)-2\mathbf{RR}_{24}(\mu)+\mathbf{RR}_{33}(\mu)+2\mathbf{RR}_{34}(\mu)+\mathbf{RR}_{44}(\mu). \end{aligned} \tag{86}$$

Let us take the term $\mathbf{RR}_{11}(\mu)$ as an example

$$\begin{aligned}\mathbf{RR}_{11}(\mu) &= \int_\Omega \left(D(\mu) : \epsilon\left(\sum_{i=1}^{N^u}\alpha_i^u(\mu)\phi_i^u\right)\right) : C(\mu) : \left(D(\mu) : \epsilon\left(\sum_{j=1}^{N^u}\alpha_j^u(\mu)\phi_j^u\right)\right) d\Omega \\ &= \int_\Omega \epsilon\left(\sum_{i=1}^{N^u}\alpha_i^u(\mu)\phi_i^u\right) : D(\mu) : \epsilon\left(\sum_{j=1}^{N^u}\alpha_j^u(\mu)\phi_j^u\right) d\Omega, \quad (\text{as } D(\mu) : C(\mu) = \mathbb{I}) \\ &= \sum_{i,j=1}^{N^u}\alpha_i^u(\mu)\left(\int_\Omega \epsilon(\phi_i^u) : D(\mu) : \epsilon(\phi_j^u)\, d\Omega\right)\alpha_j^u(\mu) = \sum_{i,j=1}^{N^u}\sum_{k=1}^{n^{\mathrm{D}}}\alpha_i^u(\mu)\alpha_j^u(\mu)\gamma_k^{\mathrm{D}}(\mu)\left(\int_\Omega \epsilon(\boldsymbol{\phi}_i^{\boldsymbol{u}}) : \overline{\boldsymbol{D}}_{\boldsymbol{k}} : \epsilon(\boldsymbol{\phi}_j^{\boldsymbol{u}})\, \boldsymbol{d\Omega}\right). \end{aligned} \tag{87}$$

We observe from the last line of (87) that the term inside the brackets (in bold typeface) is μ-independent and hence can be pre-computed and stored in the Offline stage; and then in the Online stage $\mathbf{RR}_{11}(\mu)$ can be estimated rapidly with the computational cost independent of $\mathcal{N}^u$ by assembling all remaining μ-dependent terms. Applying the same trick to other terms, we obtain the following results (note that all the offline terms will be in bold typeface):

$$\mathbf{RR}_{12}(\mu) = \sum_{i=1}^{N^u}\sum_{j=1}^{n^{u,\mathrm{w}}}\sum_{k=1}^{n^{\mathrm{D}}}\alpha_i^u(\mu)\gamma_j^{u,\mathrm{w}}(\mu)\gamma_k^{\mathrm{D}}(\mu)\left(\int_{\boldsymbol{\Omega}} \boldsymbol{\epsilon}(\boldsymbol{\phi}_{\boldsymbol{i}}^{\boldsymbol{u}}) : \overline{\boldsymbol{D}}_{\boldsymbol{k}} : \boldsymbol{\epsilon}(\boldsymbol{\psi}_{\boldsymbol{j}}^{\boldsymbol{u}})\, \boldsymbol{d\Omega}\right), \tag{88}$$

$$\mathbf{RR}_{13}(\mu) = \sum_{i=1}^{N^u}\sum_{j=1}^{N^\theta}\sum_{k=1}^{n^{\mathrm{D}}}\alpha_i^u(\mu)\alpha_j^\theta(\mu)\gamma_k^{\mathrm{D}}(\mu)\left(\int_{\boldsymbol{\Omega}} \boldsymbol{\epsilon}(\boldsymbol{\phi}_{\boldsymbol{i}}^{\boldsymbol{u}}) : \overline{\boldsymbol{D}}_{\boldsymbol{k}} : \boldsymbol{\epsilon}_{\mathbf{0}}(\boldsymbol{\phi}_{\boldsymbol{j}}^{\boldsymbol{\theta}})\, \boldsymbol{d\Omega}\right), \tag{89}$$

$$\mathbf{RR}_{14}(\mu) = \sum_{i=1}^{N^u}\sum_{j=1}^{n^{\theta,\mathrm{w}}}\sum_{k=1}^{n^{\mathrm{D}}}\alpha_i^u(\mu)\gamma_j^{\theta,\mathrm{w}}(\mu)\gamma_k^{\mathrm{D}}(\mu)\left(\int_{\boldsymbol{\Omega}} \boldsymbol{\epsilon}(\boldsymbol{\phi}_{\boldsymbol{i}}^{\boldsymbol{u}}) : \overline{\boldsymbol{D}}_{\boldsymbol{k}} : \boldsymbol{\epsilon}_{\mathbf{0}}(\boldsymbol{\psi}_{\boldsymbol{j}}^{\boldsymbol{\theta}})\, \boldsymbol{d\Omega}\right), \tag{90}$$

$$\mathbf{RR}_{22}(\mu) = \sum_{i=1}^{n^{u,\mathrm{w}}}\sum_{j=1}^{n^{u,\mathrm{w}}}\sum_{k=1}^{n^{\mathrm{D}}}\gamma_i^{u,\mathrm{w}}(\mu)\gamma_j^{u,\mathrm{w}}(\mu)\gamma_k^{\mathrm{D}}(\mu)\left(\int_{\boldsymbol{\Omega}} \boldsymbol{\epsilon}(\boldsymbol{\psi}_{\boldsymbol{i}}^{\boldsymbol{u}}) : \overline{\boldsymbol{D}}_{\boldsymbol{k}} : \boldsymbol{\epsilon}(\boldsymbol{\psi}_{\boldsymbol{j}}^{\boldsymbol{u}})\, \boldsymbol{d\Omega}\right), \tag{91}$$

$$\mathbf{RR}_{23}(\mu) = \sum_{i=1}^{n^{u,\mathrm{w}}}\sum_{j=1}^{N^\theta}\sum_{k=1}^{n^{\mathrm{D}}}\gamma_i^{u,\mathrm{w}}(\mu)\alpha_j^\theta(\mu)\gamma_k^{\mathrm{D}}(\mu)\left(\int_{\boldsymbol{\Omega}} \boldsymbol{\epsilon}(\boldsymbol{\psi}_{\boldsymbol{i}}^{\boldsymbol{u}}) : \overline{\boldsymbol{D}}_{\boldsymbol{k}} : \boldsymbol{\epsilon}_{\mathbf{0}}(\boldsymbol{\phi}_{\boldsymbol{j}}^{\boldsymbol{\theta}})\, \boldsymbol{d\Omega}\right), \tag{92}$$

$$\mathbf{RR}_{24}(\mu) = \sum_{i=1}^{n^{u,\mathrm{w}}}\sum_{j=1}^{n^{\theta,\mathrm{w}}}\sum_{k=1}^{n^{\mathrm{D}}}\gamma_i^{u,\mathrm{w}}(\mu)\gamma_j^{\theta,\mathrm{w}}(\mu)\gamma_k^{\mathrm{D}}(\mu)\left(\int_{\boldsymbol{\Omega}} \boldsymbol{\epsilon}(\boldsymbol{\psi}_{\boldsymbol{i}}^{\boldsymbol{u}}) : \overline{\boldsymbol{D}}_{\boldsymbol{k}} : \boldsymbol{\epsilon}_{\mathbf{0}}(\boldsymbol{\psi}_{\boldsymbol{j}}^{\boldsymbol{\theta}})\, \boldsymbol{d\Omega}\right), \tag{93}$$

$$\mathbf{RR}_{33}(\mu) = \sum_{i=1}^{N^\theta}\sum_{j=1}^{N^\theta}\sum_{k=1}^{n^{\mathrm{D}}}\alpha_i^\theta(\mu)\alpha_j^\theta(\mu)\gamma_k^{\mathrm{D}}(\mu)\left(\int_{\boldsymbol{\Omega}} \boldsymbol{\epsilon}_{\mathbf{0}}(\boldsymbol{\phi}_{\boldsymbol{i}}^{\boldsymbol{\theta}}) : \overline{\boldsymbol{D}}_{\boldsymbol{k}} : \boldsymbol{\epsilon}_{\mathbf{0}}(\boldsymbol{\phi}_{\boldsymbol{j}}^{\boldsymbol{\theta}})\, \boldsymbol{d\Omega}\right), \tag{94}$$

$$\mathbf{RR}_{34}(\mu) = \sum_{i=1}^{N^\theta}\sum_{j=1}^{n^{\theta,\mathrm{w}}}\sum_{k=1}^{n^{\mathrm{D}}}\alpha_i^\theta(\mu)\gamma_j^{\theta,\mathrm{w}}(\mu)\gamma_k^{\mathrm{D}}(\mu)\left(\int_{\boldsymbol{\Omega}} \boldsymbol{\epsilon}_{\mathbf{0}}(\boldsymbol{\phi}_{\boldsymbol{i}}^{\boldsymbol{\theta}}) : \overline{\boldsymbol{D}}_{\boldsymbol{k}} : \boldsymbol{\epsilon}_{\mathbf{0}}(\boldsymbol{\psi}_{\boldsymbol{j}}^{\boldsymbol{\theta}})\, \boldsymbol{d\Omega}\right), \tag{95}$$

and

$$\mathbf{RR}_{44}(\mu) = \sum_{i=1}^{n^{\theta,\mathrm{w}}}\sum_{j=1}^{n^{\theta,\mathrm{w}}}\sum_{k=1}^{n^{\mathrm{D}}}\gamma_i^{\theta,\mathrm{w}}(\mu)\gamma_j^{\theta,\mathrm{w}}(\mu)\gamma_k^{\mathrm{D}}(\mu)\left(\int_{\boldsymbol{\Omega}} \boldsymbol{\epsilon}_{\mathbf{0}}(\boldsymbol{\psi}_{\boldsymbol{i}}^{\boldsymbol{\theta}}) : \overline{\boldsymbol{D}}_{\boldsymbol{k}} : \boldsymbol{\epsilon}_{\mathbf{0}}(\boldsymbol{\psi}_{\boldsymbol{j}}^{\boldsymbol{\theta}})\, \boldsymbol{d\Omega}\right). \tag{96}$$

We note that for all the terms related to $\epsilon_0(\bullet)$, $\epsilon_0(\bullet) \overset{\text{def}}{=} \epsilon_0(\bullet - \theta^{\mathrm{ref}})$, where θ^{ref} is the reference temperature for which thermal strains are zero (see for instance Eq. (1.9) of [28] or Eq. (8.23) in Ref. [29]). In our derivations, we choose $\theta^{\mathrm{ref}} = 0$ for simplicity, but its extension for the general case $\theta^{\mathrm{ref}} \neq 0$ is really straightforward since the term $\epsilon_0(\theta^{\mathrm{ref}})$ is treated as an additional constant.

2. Similarly, using (85), the term $\mathbf{HH}(\mu)$ in (83) can be written as

$$\begin{aligned}\mathbf{HH}(\mu) &= \int_\Omega \widehat{\sigma}(\mu) : C(\mu) : \widehat{\sigma}(\mu)\, d\Omega = \int_\Omega \big(\mathbf{B}_5(\mu) + \mathbf{B}_6(\mu)\big) : C(\mu) : \big(\mathbf{B}_5(\mu) + \mathbf{B}_6(\mu)\big)\, d\Omega \\ &= \int_\Omega \mathbf{B}_5(\mu) : C(\mu) : \mathbf{B}_5(\mu)\, d\Omega + 2\int_\Omega \mathbf{B}_5(\mu) : C(\mu) : \mathbf{B}_6(\mu)\, d\Omega + \int_\Omega \mathbf{B}_6(\mu) : C(\mu) : \mathbf{B}_6(\mu)\, d\Omega \\ &= \mathbf{HH}_{55}(\mu) + 2\mathbf{HH}_{56}(\mu) + \mathbf{HH}_{66}(\mu). \end{aligned} \tag{97}$$

Using the same method as above: substituting the expressions for $\mathbf{B}_5(\mu)$ and $\mathbf{B}_6(\mu)$ (from (85)), expanding and assembling the μ-independent terms, we finally obtain

$$\mathbf{HH}_{55}(\mu) = \sum_{i=1}^{N^\sigma}\sum_{j=1}^{N^\sigma}\sum_{k=1}^{n^{\mathrm{C}}} \alpha_i^\sigma(\mu)\alpha_j^\sigma(\mu)\gamma_k^{\mathrm{C}}(\mu)\left(\int_\Omega \boldsymbol{\phi}_i^\sigma : \overline{\boldsymbol{C}}_k : \boldsymbol{\phi}_j^\sigma\, d\Omega\right), \tag{98}$$

$$\mathbf{HH}_{56}(\mu) = \sum_{i=1}^{N^\sigma}\sum_{j=1}^{\widetilde{n}_{\mathrm{p}}}\sum_{k=1}^{n^{\mathrm{C}}} \alpha_i^\sigma(\mu)\widetilde{\gamma}_j^{\mathrm{p}}(\mu)\gamma_k^{\mathrm{C}}(\mu)\left(\int_\Omega \boldsymbol{\phi}_i^\sigma : \overline{\boldsymbol{C}}_k : \boldsymbol{\sigma}_j^{\mathrm{p}}\, d\Omega\right), \tag{99}$$

$$\mathbf{HH}_{66}(\mu) = \sum_{i=1}^{\widetilde{n}_{\mathrm{p}}}\sum_{j=1}^{\widetilde{n}_{\mathrm{p}}}\sum_{k=1}^{n^{\mathrm{C}}} \widetilde{\gamma}_i^{\mathrm{p}}(\mu)\widetilde{\gamma}_j^{\mathrm{p}}(\mu)\gamma_k^{\mathrm{C}}(\mu)\left(\int_\Omega \boldsymbol{\sigma}_i^{\mathrm{p}} : \overline{\boldsymbol{C}}_k : \boldsymbol{\sigma}_j^{\mathrm{p}}\, d\Omega\right). \tag{100}$$

3. Finally, for the term $\mathbf{RH}(\mu)$ in (105), we also have

$$\begin{aligned}\mathbf{RH}(\mu) &= \int_\Omega \sigma^{\mathrm{r}}(\mu) : C(\mu) : \widehat{\sigma}(\mu)\, d\Omega \\ &= \int_\Omega \big(\mathbf{B}_1(\mu) + \mathbf{B}_2(\mu) - \mathbf{B}_3(\mu) - \mathbf{B}_4(\mu)\big) : C(\mu) : \big(\mathbf{B}_5(\mu) + \mathbf{B}_6(\mu)\big)\, d\Omega \\ &= \int_\Omega \mathbf{B}_1(\mu) : C(\mu) : \mathbf{B}_5(\mu)\, d\Omega + \int_\Omega \mathbf{B}_1(\mu) : C(\mu) : \mathbf{B}_6(\mu)\, d\Omega + \cdots - \int_\Omega \mathbf{B}_4(\mu) : C(\mu) : \mathbf{B}_6(\mu)\, d\Omega \\ &= \mathbf{RH}_{15}(\mu) + \mathbf{RH}_{16}(\mu) + \mathbf{RH}_{25}(\mu) + \mathbf{RH}_{26}(\mu) - \mathbf{RH}_{35}(\mu) - \mathbf{RH}_{36}(\mu) - \mathbf{RH}_{45}(\mu) - \mathbf{RH}_{46}(\mu), \end{aligned} \tag{101}$$

where

$$\mathbf{RH}_{15}(\mu) = \sum_{i=1}^{N^u}\sum_{j=1}^{N^\sigma} \alpha_i^u(\mu)\alpha_j^\sigma(\mu)\left(\int_\Omega \epsilon(\boldsymbol{\phi}_i^u) : \boldsymbol{\phi}_j^\sigma\, d\Omega\right), \tag{102}$$

$$\mathbf{RH}_{16}(\mu) = \sum_{i=1}^{N^u}\sum_{j=1}^{\widetilde{n}_{\mathrm{p}}} \alpha_i^u(\mu)\widetilde{\gamma}_j^{\mathrm{p}}(\mu)\left(\int_\Omega \epsilon(\boldsymbol{\phi}_i^u) : \boldsymbol{\sigma}_j^{\mathrm{p}}\, d\Omega\right), \tag{103}$$

$$\mathbf{RH}_{25}(\mu) = \sum_{i=1}^{n^{u,\mathrm{w}}}\sum_{j=1}^{N^\sigma} \gamma_i^{u,\mathrm{w}}(\mu)\alpha_j^\sigma(\mu)\left(\int_\Omega \epsilon(\boldsymbol{\psi}_i^u) : \boldsymbol{\phi}_j^\sigma\, d\Omega\right), \tag{104}$$

$$\mathbf{RH}_{26}(\mu) = \sum_{i=1}^{n^{u,\mathrm{w}}}\sum_{j=1}^{\widetilde{n}_{\mathrm{p}}} \gamma_i^{u,\mathrm{w}}(\mu)\widetilde{\gamma}_j^{\mathrm{p}}(\mu)\left(\int_\Omega \epsilon(\boldsymbol{\psi}_i^u) : \boldsymbol{\sigma}_j^{\mathrm{p}}\, d\Omega\right), \tag{105}$$

$$\mathbf{RH}_{35}(\mu) = \sum_{i=1}^{N^\theta}\sum_{j=1}^{N^\sigma} \alpha_i^\theta(\mu)\alpha_j^\sigma(\mu)\left(\int_\Omega \epsilon_{\mathbf{0}}(\boldsymbol{\phi}_i^\theta) : \boldsymbol{\phi}_j^\sigma\, d\Omega\right), \tag{106}$$

$$\mathbf{RH}_{36}(\mu) = \sum_{i=1}^{N^\theta}\sum_{j=1}^{\widetilde{n}_{\mathrm{p}}} \alpha_i^\theta(\mu)\widetilde{\gamma}_j^{\mathrm{p}}(\mu)\left(\int_\Omega \epsilon_{\mathbf{0}}(\boldsymbol{\phi}_i^\theta) : \boldsymbol{\sigma}_j^{\mathrm{p}}\, d\Omega\right), \tag{107}$$

$$\mathbf{RH}_{45}(\mu) = \sum_{i=1}^{n^{\theta,\mathrm{w}}}\sum_{j=1}^{N^\sigma} \gamma_i^{\theta,\mathrm{w}}(\mu)\alpha_j^\sigma(\mu)\left(\int_\Omega \epsilon_{\mathbf{0}}(\boldsymbol{\psi}_i^\theta) : \boldsymbol{\phi}_j^\sigma\, d\Omega\right), \tag{108}$$

$$\mathbf{RH}_{46}(\mu) = \sum_{i=1}^{n^{\theta,\mathrm{w}}}\sum_{j=1}^{\widetilde{n}_{\mathrm{p}}} \gamma_i^{\theta,\mathrm{w}}(\mu)\widetilde{\gamma}_j^{\mathrm{p}}(\mu)\left(\int_\Omega \epsilon_{\mathbf{0}}(\boldsymbol{\psi}_i^\theta) : \boldsymbol{\sigma}_j^{\mathrm{p}}\, d\Omega\right). \tag{109}$$

In summary, there are 4 types of terms that need to be pre-computed offline as follows.

- 5 terms relates to $\{\phi^u\}$: the bold terms of $\mathbf{RR}_{11}(\mu)$, $\mathbf{RR}_{12}(\mu)$, $\mathbf{RR}_{13}(\mu)$, $\mathbf{RR}_{14}(\mu)$ and $\mathbf{RH}_{16}(\mu)$.
- 5 terms relates to $\{\phi^\sigma\}$: the bold terms of $\mathbf{HH}_{55}(\mu)$, $\mathbf{HH}_{56}(\mu)$, $\mathbf{RH}_{25}(\mu)$, $\mathbf{RH}_{35}(\mu)$ and $\mathbf{RH}_{45}(\mu)$.
- 1 term relates to both $\{\phi^u\}$ and $\{\phi^\sigma\}$: the bold term of $\mathbf{RH}_{15}(\mu)$.
- 10 independent terms which do not depend on either $\{\phi^u\}$ or $\{\phi^\sigma\}$, and thus can be computed *independently*: $\mathbf{RR}_{22}(\mu)$, $\mathbf{RR}_{23}(\mu)$, $\mathbf{RR}_{24}(\mu)$, $\mathbf{RR}_{33}(\mu)$, $\mathbf{RR}_{34}(\mu)$, $\mathbf{RR}_{44}(\mu)$, $\mathbf{HH}_{66}(\mu)$, $\mathbf{RH}_{26}(\mu)$, $\mathbf{RH}_{36}(\mu)$ and $\mathbf{RH}_{46}(\mu)$, respectively.

The above analysis demonstrates that the *a posteriori* CRE error estimator defined in (56) also accepts a very efficient Offline-Online computational strategy. In the Offline stage, the terms $\{\psi_i^u, 1 \le i \le n^{u,\mathrm{w}}\}$, $\{\sigma_k^{\mathrm{p}}, 1 \le k \le \widetilde{n}_{\mathrm{p}}\}$ and the RB basis functions $\{\phi_n^u, 1 \le n \le N^u\}$, $\{\phi_m^\sigma, 1 \le m \le N^\sigma\}$ are computed first; then all the offline terms (bold typeface in brackets) in (86)–(109) are computed and stored. In the Online stage, for any given μ, we first solve (39) to get $\alpha_n^\theta(\mu), 1 \le n \le N^\theta$; solve (43) to get $\alpha_n^u(\mu), 1 \le n \le N^u$; then solve (55) to obtain $\alpha_m^\sigma(\mu), 1 \le m \le N^\sigma$; and finally assemble all the remaining terms to compute $\Delta^{\mathrm{CRE}}(\mu)$ from (83).

For any given μ, the Online operation count at this stage includes (excluding the Online counts described in section 3.2.1 and section 3.2.2): $O\left(n^{\mathrm{D}}(N^{u2} + N^u N^\theta + N^{\theta 2})\right)$ operations to assemble and compute $\mathbf{RR}(\mu)$ in (86), $O\left(n^{\mathrm{C}} N^{\sigma 2}\right)$ operations to assemble and compute $\mathbf{HH}(\mu)$ in (97), and $O\left(N^u N^\sigma + N^\theta N^\sigma\right)$ operations to assemble and compute $\mathbf{RH}(\mu)$ in (101)[3] Therefore, the Online operation count to evaluate $\mu \to \Delta^{\mathrm{CRE}}(\mu)$ is also independent of $\mathcal{N}^u$.

Appendix B. Supplementary data

Supplementary data related to this article can be found at https://doi.org/10.1016/j.finel.2017.12.004.

References

[1] T. Reis, T. Stykel, A Survey on Model Reduction of Coupled Systems, in: Model Order Reduction: Theory, Research Aspects and Applications, Springer, 2008, pp. 133–155.
[2] P. Benner, L. Feng, Model Order Reduction for Coupled Problems, Max Planck Institute Magdeburg Preprints, 2015.
[3] W.C. Hurty, Vibrations of structural systems by component mode synthesis, J. Eng. Mech. Div. 86 (4) (1960) 51–70.
[4] M.C. Bampton, R.R. Craig Jr., Coupling of substructures for dynamic analyses, AIAA J. 6 (7) (1968) 1313–1319.
[5] P. Koutsovasilis, M. Beitelschmidt, Comparison of model reduction techniques for large mechanical systems, Multibody Syst. Dyn. 20 (2) (2008) 111–128.
[6] T. Reis, T. Stykel, Stability analysis and model order reduction of coupled systems, Math. Comput. Model. Dyn. Syst. 13 (5) (2007) 413–436.
[7] N. Lang, J. Saak, P. Benner, Model order reduction for systems with moving loads, at-Automatisierungstechnik, 62 (7) (2014) 512–522.
[8] A. Vandendorpe, P. Van Dooren, Model reduction of interconnected systems, in: Model Order Reduction: Theory, Research Aspects and Applications, Springer, 2008, pp. 305–321.
[9] Y.-L. Jiang, C.-Y. Chen, H.-B. Chen, Model-order reduction of coupled DAE systems via ϵ-embedding technique and Krylov subspace method, J. Frankl. Inst. 349 (10) (2012) 3027–3045.
[10] G.S. Pau, Reduced basis method for simulation of nanodevices, Phys. Rev. B 78 (15) (2008) 155425.
[11] I. Martini, G. Rozza, B. Haasdonk, Reduced basis approximation and a-posteriori error estimation for the coupled Stokes-Darcy system, Adv. Comput. Math. (2014) 1–27.
[12] M. Hinze, M. Kunkel, A. Steinbrecher, T. Stykel, Model order reduction of coupled circuit-device systems, Int. J. Numer. Model. Electron. Netw. Devices Fields 25 (4) (2012) 362–377.
[13] O. Lass, S. Volkwein, POD Galerkin schemes for nonlinear elliptic-parabolic systems, SIAM J. Sci. Comput. 35 (3) (2013) A1271–A1298.
[14] T. Henneron, S. Clenet, Proper generalized decomposition method applied to solve 3-d magnetoquasi-static field problems coupling with external electric circuits, magnetics, IEEE Trans. 51 (6) (2015) 1–10.
[15] J.P. Carter, J.R. Booker, Finite element analysis of coupled thermoelasticity, Comput. Struct. 31 (1) (1989) 73–80.
[16] E. Serra, M. Bonaldi, A finite element formulation for thermoelastic damping analysis, Int. J. Numer. methods Eng. 78 (6) (2009) 671–691.
[17] K. Willcox, J. Peraire, Balanced model reduction via the proper orthogonal decomposition, AIAA J. 40 (11) (2002).
[18] K. Kunisch, S. Volkwein, Galerkin proper orthogonal decomposition methods for a general equation in fluid dynamics, SIAM J. Numer. Anal. 40 (2) (2003) 492–515.
[19] K. Carlberg, C. Farhat, J. Cortial, D. Amsallem, The GNAT method for nonlinear model reduction: effective implementation and application to computational fluid dynamics and turbulent flows, J. Comput. Phys. 242 (2013) 623–647.
[20] D. Amsallem, U. Hetmaniuk, Error estimates for Galerkin reduced-order models of the semi-discrete wave equation, ESAIM Math. Model. Numer. Anal. 48 (01) (2014).
[21] D. Ryckelynck, F. Chinesta, E. Cueto, A. Ammar, On the a priori model reduction: overview and recent developments, Archiv. Comput. Methods Eng. State Art Rev. 13 (1) (2006) 91–128.
[22] D. Ryckelynck, Hyper-reduction of mechanical models involving internal variables, Int. J. Numer. Methods Eng. 77 (1) (2008) 75–89.
[23] P. Ladevèze, L. Chamoin, On the verification of model reduction methods based on the proper generalized decomposition, Comput. Methods Appl. Mech. Eng. 200 (23) (2011) 2032–2047.
[24] M.A. Grepl, Y. Maday, N.C. Nguyen, A.T. Patera, Efficient reduced-basis treatment of nonaffine and nonlinear partial differential equations, ESAIM Math. Model. Numer. Anal. 41 (03) (2007) 575–605.
[25] G. Rozza, D. Huynh, A.T. Patera, Reduced basis approximation and a posteriori error estimation for affinely parametrized elliptic coercive partial differential equations, Archiv. Comput. Methods Eng. 15 (3) (2008) 229–275.
[26] K. Hoang, P. Kerfriden, S. Bordas, A fast, certified and "tuning free" two-field reduced basis method for the metamodelling of affinely-parametrised elasticity problems, Comput. Methods Appl. Mech. Eng. 298 (2016) 121–158.
[27] P. Nachtergaele, D. Rixen, A. Steenhoek, Efficient weakly coupled projection basis for the reduction of thermo-mechanical models, J. Comput. Appl. Math. 234 (7) (2010) 2272–2278.
[28] O.C. Zienkiewicz, R.L. Taylor, The Finite Element Method for Solid and Structural Mechanics, Butterworth-heinemann, 2005.
[29] S.S. Rao, The Finite Element Method in Engineering, Butterworth-heinemann, 2005.
[30] A. Tabarraei, J.-H. Song, H. Waisman, A two-scale strong discontinuity approach for evolution of shear bands under dynamic impact loads, Int. J. Multiscale Comput. Eng. 11 (6) (2013).
[31] C. McAuliffe, H. Waisman, Mesh insensitive formulation for initiation and growth of shear bands using mixed finite elements, Comput. Mech. 51 (5) (2013) 807–823.
[32] M.D. Gunzburger, J.S. Peterson, J.N. Shadid, Reduced-order modeling of time-dependent PDEs with multiple parameters in the boundary data, Comput. Methods Appl. Mech. Eng. 196 (4) (2007) 1030–1047.
[33] P. Kerfriden, J.-J. Ródenas, S.-A. Bordas, Certification of projection-based reduced order modelling in computational homogenisation by the constitutive relation error, Int. J. Numer. Methods Eng. 97 (6) (2014) 395–422.
[34] K.C. Hoang, B.C. Khoo, G.R. Liu, N.C. Nguyen, A.T. Patera, Rapid identification of material properties of the interface tissue in dental implant systems using reduced basis method, Inverse Problems Sci. Eng. 21 (8) (2013) 1310–1334.
[35] K.C. Hoang, P. Kerfriden, B. Khoo, S.P.A. Bordas, An efficient goal-oriented sampling strategy using reduced basis method for parametrized elastodynamic problems, Numer. Methods Partial Differ. Equ. 31 (2) (2015) 575–608.
[36] J.T. Oden, S. Prudhomme, Goal-oriented error estimation and adaptivity for the finite element method, Comput. Math. Appl. 41 (5) (2001) 735–756.
[37] R. Becker, R. Rannacher, An optimal control approach to a posteriori error estimation in finite element methods, Acta Numer. 2001 10 (2001) 1–102.
[38] M. Meyer, H. Matthies, Efficient model reduction in non-linear dynamics using the Karhunen-Loeve expansion and dual-weighted-residual methods, Comput. Mech. 31 (1) (2003) 179–191.
[39] T. Bui-Thanh, K. Willcox, O. Ghattas, B. van Bloemen Waanders, Goal-oriented, model-constrained optimization for reduction of large-scale systems, J. Comput. Phys. 224 (2) (2007) 880–896.
[40] A. Janon, M. Nodet, C. Prieur, Goal-oriented Error Estimation for Reduced Basis Method, with Application to Certified Sensitivity Analysis, 2013. arXiv preprint arXiv:1303.6618.
[41] K. Hoang, Y. Fu, J. Song, An hp-proper orthogonal decomposition–moving least squares approach for molecular dynamics simulation, Comput. Methods Appl. Mech. Eng. 298 (2016) 548–575.
[42] P. Ladevèze, Upper error bounds on calculated outputs of interest for linear and nonlinear structural problems, Comptes Rendus Mécanique 334 (7) (2006) 399–407.
[43] E. Stein, M. Rüter, Finite Element Methods for Elasticity with Error-controlled Discretization and Model Adaptivity, Encyclopedia of Computational Mechanics, 2007.
[44] P. Dıez, N. Parés, A. Huerta, Error Estimation and Quality Control, Encyclopedia of Aerospace Engineering, 2010.
[45] A. Buffa, Y. Maday, A.T. Patera, C. Prud'homme, G. Turinici, A priori convergence of the greedy algorithm for the parametrized reduced basis method, ESAIM Math. Model. Numer. Anal. 46 (3) (2012) 595–603.
[46] C. Karch, Micromechanical analysis of thermal expansion coefficients, Model. Numer. Simul. Mater. Sci. 4 (03) (2014) 104.
[47] M. Tschopp, G. Wilks, J. Spowart, Multi-scale characterization of orthotropic microstructures, Model. Simul. Mater. Sci. Eng. 16 (6) (2008) 065009.
[48] G. Wilks, M. Tschopp, J. Spowart, Multi-scale characterization of inhomogeneous morphologically textured microstructures, Mater. Sci. Eng. A 527 (4) (2010) 883–889.
[49] S. Nemat-Nasser, M. Hori, Micromechanics: Overall Properties of Heterogeneous Materials, vol. 2, Elsevier Amsterdam, 1999.

[3] For all model problems considered in section 5, usually $N^\theta, N^u, N^\sigma \gg n^{\mathrm{D}}, n^{\mathrm{C}}, n^{u,\mathrm{w}}, n^{\theta,\mathrm{w}}, \widetilde{n}_{\mathrm{p}}$ the online computational cost thus depends mostly on the terms having N^θ, N^u and N^σ.